PB-242 830

RAINFALL-RUNOFF RELATIONS ON URBAN AND RURAL AREAS

Ernest F. Brater, et al

Michigan University

Prepared for:

National Environmental Research Center

May 1975

DISTRIBUTED BY:

NTIS

National Technical Information Service
U. S. DEPARTMENT OF COMMERCE

191067

EPA-670/2-75-046
May 1975

PB242830

Environmental Protection Technology Series

Reproduced by
NATIONAL TECHNICAL
INFORMATION SERVICE
US Department of Commerce
Springfield, VA. 22151

TECHNICAL REPORT DATA
(Please read Instructions on the reverse before completing)

1. REPORT NO.	2.	PB 242 830
EPA-670/2-75-046		

4. TITLE AND SUBTITLE
RAINFALL-RUNOFF RELATIONS ON URBAN AND RURAL AREAS

5. REPORT DATE
May 1975; Issuing Date

6. PERFORMING ORGANIZATION CODE

7. AUTHOR(S)
Ernest F. Brater and James D. Sherrill

8. PERFORMING ORGANIZATION REPORT NO.

9. PERFORMING ORGANIZATION NAME AND ADDRESS
Department of Civil Engineering
University of Michigan
Ann Arbor, Michigan 48104

10. PROGRAM ELEMENT NO.
1BB034; ROAP 21AT3; TASK 008

11. CONTRACT/GRANT NO.
11040 DRS

12. SPONSORING AGENCY NAME AND ADDRESS
National Environmental Research Center
Office of Research and Development
U.S. Environmental Protection Agency
Cincinnati, Ohio 45268

13. TYPE OF REPORT AND PERIOD COVERED
Final

14. SPONSORING AGENCY CODE

15. SUPPLEMENTARY NOTES

16. ABSTRACT
A procedure was developed for estimating the frequency of storm runoff of various magnitudes from rainfall and/or snowmelt on small drainage basins in various stages of urbanization. The study was based primarily on the analysis of storm runoff events on real basins varying in size from 0.02 to 734 sq mi. The method is based on applying unit hydrographs to precipitations of various frequencies after deducting infiltration and retention. A concurrent study with an analytical drainage basin model provided additional understanding of the effects of some parameters. The unit hydrograph-infiltration capacity concept was selected as the most accurate practical method for predicting storm runoff. It was found that the form of the unit hydrograph could be related to drainage basin size and degree of urbanization as measured by population density. Other characteristics of the drainage basin are much less important. The form of the unit hydrograph stays relatively constant for various durations and magnitudes of input as long as the duration of input is smaller than a critical time which can also be related to the size and population density of the basin. As the population increased from rural to highly urbanized, peak discharges for the same runoff became as much as ten times greater. Infiltration capacity was found to vary seasonally. The prediction of flood frequency by this procedure is fully operable for Southeastern Michigan. For application to other areas some hydrograph analysis must be made.

PRICES SUBJECT TO CHANGE

17. KEY WORDS AND DOCUMENT ANALYSIS

a. DESCRIPTORS	b. IDENTIFIERS/OPEN ENDED TERMS	c. COSATI Field/Group
*Watersheds *Mathematical models *Runoff *Urban areas *Surface water runoff Rural areas	Unit hydrograph Southeastern Michigan Hydrograph analysis Infiltration/retention Infiltration capacity	13B

18. DISTRIBUTION STATEMENT	19. SECURITY CLASS (This Report)	21. NO. OF PAGES
RELEASE TO PUBLIC	UNCLASSIFIED	108
	20. SECURITY CLASS (This page) UNCLASSIFIED	22. PRICE $5.25/2.25

EPA Form 2220-1 (9-73)

☆ U.S. GOVERNMENT PRINTING OFFICE: 1975-657-593/5384 Region No. 5-11

EPA-670/2-75-046
May 1975

RAINFALL-RUNOFF RELATIONS ON URBAN AND RURAL AREAS

By

Ernest F. Brater
James D. Sherrill
University of Michigan
Ann Arbor, Michigan 48104

Grant No. R-800941 (11040 DRS)
Program Element No. 1BB034

Project Officer

David J. Cesareo
Storm and Combined Sewer Section (Edison, N.J.)
Advanced Waste Treatment Research Laboratory
National Environmental Research Center
Cincinnati, Ohio 45268

NATIONAL ENVIRONMENTAL RESEARCH CENTER
OFFICE OF RESEARCH AND DEVELOPMENT
U.S. ENVIRONMENTAL PROTECTION AGENCY
CINCINNATI, OHIO 45268

REVIEW NOTICE

The National Environmental Research Center--Cincinnati has reviewed this report and approved its publication. Approval does not signify that the contents necessarily reflect the views and policies of the U.S. Environmental Protection Agency, nor does mention of trade names or commercial products constitute endorsement or recommendation for use.

FOREWORD

Man and his environment must be protected from the adverse effects of pesticides, radiation, noise and other forms of pollution, and the unwise management of solid waste. Efforts to protect the environment require a focus that recognizes the interplay between the components of our physical environment--air, water, and land. The National Environmental Research Centers provide this multidisciplinary focus through programs engaged in

- studies on the effects of environmental contaminants on man and the biosphere, and
- a search for ways to prevent contamination and to recycle valuable resources.

As part of these activities, the study described here investigated the factors which control the relationship between storm rainfall, snow melt, and the resulting storm runoff, including the effects of urbanization on the runoff process.

A. W. Breidenbach, Ph.D.
Director
National Environmental
Research Center, Cincinnati

ABSTRACT

A procedure was developed for estimating the frequency of storm runoff of various magnitudes from rainfall and/or snowmelt on small drainage basins in various stages of urbanization. The study was based primarily on the analysis of storm runoff events on real basins varying in size from 0.02 to 734 sq mi. The method is based on applying unit hydrographs to precipitations of various frequencies after deducting infiltration and retention. A concurrent study with an analytical drainage basin model provided additional understanding of the effects of some parameters. The unit hydrograph-infiltration capacity concept was selected as the most accurate practical method for predicting storm runoff. It was found that the form of the unit hydrograph could be related to drainage basin size and degree of urbanization as measured by population density. Other characteristics of the drainage basin are much less important. The form of the unit hydrograph stays relatively constant for various durations and magnitudes of input as long as the duration of input is smaller than a critical time which can also be related to the size and population density of the basin. As the population increased from rural to highly urbanized peak discharges for the same runoff became as much as ten times greater. Infiltration capacity was found to vary seasonally. The prediction of flood frequency by this procedure is fully operable for Southeastern Michigan. For application to other areas some hydrograph analysis must be made.

This report was submitted in fulfillment of Project Number R-800941 (formerly 11040 DRS), by The University of Michigan, under the (partial) sponsorship of the Environmental Protection Agency. Work was completed as of July 1973.

CONTENTS

		Page
Review Notice		ii
Foreword		iii
Abstract		iv
List of Figures		vi
List of Tables		viii
Acknowledgments		ix
Sections		
I	Conclusions	1
II	Recommendations	4
III	Introduction	6
IV	The State-of-the-Art	7
V	Collecting Data	10
VI	Hydrograph Analysis	19
VII	Infiltration Capacity	32
VIII	Unit Hydrographs	38
IX	Mathematical Model	69
X	Frequency Studies	71
XI	Time-Intensity Rainfall Patterns	76
XII	Predicting Flood Magnitudes and Frequencies	85
XIII	References	94

LIST OF FIGURES

No.		Page
1	Typical hyetographs and hydrographs.	11
2	Complex hyetograph and hydrograph.	20
3	Relation between slope and discharge on ground water depletion curve.	22
4	Relation between slope and discharge on ground water depletion curve.	23
5	Surface runoff vs. precipitation.	26
6	Surface runoff vs. precipitation.	27
7	Surface runoff vs. precipitation.	28
8	Seasonal variation of infiltration capacity.	33
9	Five unit hydrographs from the same basin.	39
10	Reproduction of a complex hydrograph.	41
11	Definition sketch.	42
12	Unit hydrograph peaks vs. area (original data).	48
13	Unit hydrograph peaks vs. area with uniform slopes.	49
14	Unit hydrograph peaks vs. population density.	50
15	Significant period of rise vs. area.	51
16	Significant period of rise vs. area with uniform density.	52

LIST OF FIGURES (Concluded)

No.		Page
17	Significant period of rise vs. population density.	53
18	Period of rise vs. area.	54
19	Period of rise vs. area with uniform slope.	55
20	Period of rise vs. population density.	56
21	Unit hydrograph peak vs. area-design curves.	62
22	Significant period of rise vs. area-design curves.	63
23	Period of rise vs. area-design curves.	64
24	Width at 75 percent of peak vs. area-design curves.	65
25	Width at 50 percent of peak vs. area-design curves.	66
26	Width at 25 percent of peak vs. area-design curves.	67
27	Width of base vs. area-design curves.	68
28	The effect of snowmelt on frequency.	73
29	The effect of length of record on frequency.	74
30	Final seasonal frequency curves.	75
31	Precipitation-duration expressed as percent of 24-hr rainfall.	77
32	Intensity-duration expressed as percent of 24-hr rainfall.	78
33	Typical seasonal hyetographs expressed as percent of 24-hr rainfall.	82
34	Area-depth curves.	84
35	Synthesized and observed unit hydrographs for Red Run.	87
36	Predicted and observed flood frequencies for Red Run.	92

TABLES

No.		Page
1	Flood Runoff Data	12
2	Computations of Surface Runoff and Unit Hydrograph Ordinates for Rain of Spril 1, 1959, on Plum Brook	36
3	Computation of Infiltration Capacity	37
4	Unit Hydrograph Parameters	43
5	Legend for Figures 12-20	47
6	Equations and Statistical Parameters for Lines on Figures 12, 13, 15, 16, 18, and 19	57
7	Maximum Rainfall for Various Durations	79
8	Hyetograph Ordinates in Percent of 24-Hour Rainfall per Hour	83
9	Twenty-Four Hour Rains of Various Frequencies	86
10	Computation of Volume of Surface Runoff for a 50-Year Winter Rain	89
11	Computation of Composite Hydrograph for 50-Year Winter Rain	91

ACKNOWLEDGMENTS

The financial support of the Environmental Protection Agency is gratefully acknowledged. The assistance of Messrs. Robert M. Buckley and David J. Cesareo, Project Officers, has been most appreciated.

The project was initiated in 1964 by means of a small grant from the University of Michigan Graduate School. In 1965 a grant was obtained from the National Institutes of Health. This grant was continued to this time under the sponsorship of FWQA and EPA. During the period 1966-1971 additional support was provided by the Michigan Department of State Highways and the U.S. Bureau of Public Roads.

Many graduate students worked on the project. Their services made the project possible. Particular acknowledgment is made to Dr. Suresh K. Sangal who not only worked on the project but contributed greatly to the research through his Ph.D. dissertation.

SECTION I

CONCLUSIONS

The unit hydrograph-infiltration capacity method has been developed by this research program to the point where it provides very satisfactory estimates of peak discharge and if needed entire flood hydrographs, of various frequencies for drainage basins of all sizes and all degrees of urbanization. The procedure consists of forming runoff hydrographs of various frequencies by applying the unit hydrograph for that basin size and population density to the precipitation excess. The precipitation excess is precipitation plus snowmelt of a selected frequency minus retention and infiltration on the permeable portions of basins and minus retention on the impermeable portions. The methods described in this report provide the most accurate method of determining required capacities of storm sewers, culverts, bridges and other flood carrying structures known to the writers.

The specific conclusions are summarized below:

1. The unit hydrograph peaks as well as their time characteristics such as their periods of rise and widths at various fractions of the peak discharge can be correlated with watershed areas and population density to provide statistically significant relations which enable hydrologists to estimate the runoff characteristics of ungaged areas. These relationships were derived from the analysis of hundreds of flood hydrographs from 53 drainage basins from five states. The areas of these basins vary from 0.02 to 743 sq mi and the population densities cover a range from less than 100 to more than 14,000 persons/sq mi.

2. The effect of urbanization is primarily in the production of flood hydrographs of much shorter duration and higher peaks. For example as the population density changes from 100 to 13,000 persons/sq mi the peak rate of surface runoff for a given total surface runoff becomes about 10 times greater while the time parameters decrease to about one tenth of the values for rural areas. For the same population increases

the increase in total runoff due to increased impermeable area is only about 10 percent in Southeastern Michigan.

3. When the 16 basins located in Southeastern Michigan* were studied separately the correlations showed lower unit hydrograph peaks for low population densities than the corresponding relation for all 53 basins. It is suspected that the differences are related to the nature of the drainage networks. The use of local results improved the accuracy in Southeastern Michigan for low population basins over the use of the general curves.

4. Eleven basins located in Texas† exhibited a tendency toward higher peaks for given areas and populations then the trends of the other 53 basins which included many Texas basins at other locations. Further research will be required to determine the cause of this anamolous behavior. However, based on the behavior of the other basins it appears likely that the drainage systems in these 11 basins have been developed in advance of the population growth.

5. Based on the analysis of about 200 flood hydrographs produced by rains equal to or greater than 1 in., the average summer and winter infiltration capacities in Southeastern Michigan are 0.40 and 0.10 in./hr, respectively.

6. The effect of the impermeable area was taken care of by developing the concept of hydrologically significant impermeable area which was found to vary linearly with population density from about 1 percent for 1000 persons/sq mi to about 10 percent for 7500 persons/sq mi.

7. The maximum value of retention on the permeable portion of the basins is about 0.2 in. The average in summer is approximately 0.15 in. and in winter 0.10 in. An estimated retention of 0.05 in. on the impermeable areas gave satisfactory results.

8. An analysis of the frequency of one day occurrences of winter rain plus snowmelt gave values about 2 percent higher than the values for the same frequency determined in the conventional manner from precipitation records, where snowfall is included along with rain.

9. Typical large rainstorms in Southeastern Michigan have a nearly symetrical time distribution with the maximum hour near the center of

*These 16 basins were part of the 53 basins which formed the basis for the general relations.
†These 11 basins were not among the 53 used for developing the general relations.

the rain storm. In winter the maximum hour contains about 24 percent of the rain and in summer the maximum hour usually provides about 55 percent of the total storm rainfall. Information was obtained permitting the formation of typical time-intensity precipitation patterns from 24-hr rains of any frequency.

SECTION II

RECOMMENDATIONS

The evidence provided by this research shows that storm runoff from most drainage basins behaves in a consistant manner when basin size and population density are taken into account. However, there were a number of basins which did not follow this pattern. It is believed that an investigation of these anomolies would be very productive in improving our knowledge of the runoff process. The results to this time indicate that most differences could be explained if more were known about the density and efficiency of the drainage systems. It is suspected that some drainage systems may be developed in advance of population increases whereas in other locations the drainage system may lag behind population increases. Related to this same problem would be land use. For example, highly industrialized areas may not show population densities which are consistant with their storm sewer system. Perhaps in the future some measures of drainage efficiency could be used in place of population density as a measure of urbanization.

Although there is no substitute for field investigations and the use of real rainfall and runoff records to find these answers, it is believed that an extension of the mathematical model to more complex drainage networks would be of nearly equal value in establishing a better knowledge of this process.

Research should be continued to determine more accurately the relation between point rainfall and average rainfall on areas of various sizes for the same frequencies. The form of precipitation time-intensity pattern should also be studied at other locations as should the effect of including snowmelt with precipitation in frequency studies.

In general it is strongly recommended that hydrograph analysis be carried on systematically to determine the various parameters such as infiltration capacities, retentions, hydrologically significant impermeable areas, and unit hydrograph characteristics for basins in

various locations. Population densities and drainage patterns should also be determined. These data will be needed to provide accurate design procedures even if in the future other methods are found to be more satisfactory than the one suggested here.

SECTION III

INTRODUCTION

The objective of this project was to gain a better understanding of the factors which control the relationship between rainfall or snowmelt and the resulting storm runoff and to determine the effect of urbanization on this runoff process. The benefits would include the prevention of flood damage by means of improved design of storm sewers and waterways and would provide the data needed for the improved design and operation of facilities for control of pollution due to storm water and/or combined sewage. A basic approach was adopted which would provide a better understanding of the surface runoff process in rural and urban areas while concurrently examining and testing known methods of predicting flood peaks. The development of any practical procedure for predicting peak discharges obviously needed to be based on known surface runoff events. Therefore, the largest portion of the effort was gathering and analyzing storm runoff events from small drainage basins at various stages of urbanization. Data were gathered and analyzed from 69 basins located in five states and varying in size from 0.02 to 473 sq mi. In addition to the testing and development of practical flood prediction procedures a simple mathematical model was developed in which runoff could be computed for various rainfall inputs. The model served to check and extend information derived from the study of actual rainfall and runoff data.

SECTION IV

THE STATE-OF-THE-ART

An intensive study of procedures and literature dealing with runoff processes was carried out at the beginning of the research. In Addition to studying the literature, the Principal Investigator visited centers and researchers working on this phase of hydrology in the U.S. and Europe. The review of the subject included a reevaluation of methods which had been used in the past as well as those in current usage. In a general way, these procedures can be separated into the following categories; statistical methods, procedures utilizing empirical equations or curves, storage routing procedures and unit hydrograph procedures. The later two categories refer to the way in which the surface runoff hydrograph is formed; the total volume of runoff being usually determined by the use of the infiltration capacity concept.

Statistical methods utilize flood records on a particular basin. Sometimes they are applied regionally by assuming similar rainfall, snowmelt and drainage basin characteristics. These methods are usually limited in accuracy because of lack of sufficient records to make a significant statistical analysis as compared with methods using rainfall as input in which frequency can be determined from the much longer precipitation records. They lack the flexibility to determine the effect of urbanization or other watershed changes. The various empirical methods also require a fairly long period of records to determine the necessary constants in particular locations and again they do not lend themselves to modification for changing conditions.

Most of the attention was given to methods which combined the determination of flood volumes by deducting infiltration from precipitation and forming flood hydrographs by storage routing or unit hydrographs. These procedures provide models which attempt to represent the actual runoff process.

Peak flood di charges are controlled by two independent processes.

One process determines the time rate of input to the system and the other establishes the response of the system which is the flood hydrograph. The system input is rainfall plus snowmelt minus infiltration and other minor retentions. This process is dependent on the frequency and nature of the rain and snowmelt as well as the variations of the infiltration capacity of the soil. Since the concept of infiltration capacity was first introduced[1] a number of investigators have studied the variations of infiltration capacity with time during a rain[2-5] as well as its seasonal variation.[6-8] Its variation from place to place has also been noted.[9,10] The factors which control infiltration capacity are quite well understood but quantitative values for any region must be obtained from the analysis of rainfall and surface runoff events on drainage basins within the region. For example, previous work on this project has provided more than 200 values of infiltration capacity for Southeastern Michigan from which average seasonal values have been determined.[8]

The second process which deals with the response of the system and controls the shape of the flood hydrograph is a function of the input and of the physical characteristics of the drainage basin. Knowledge gained from this aspect of the runoff process is not limited to regional conditions but can be expected to be applicable to all locations. The important input parameters are intensity, duration and spacial distribution of rain and snowmelt. The physical characteristics are those of the flow system. The flow system consists of a series of surfaces which receive the input and contribute to the stream system. Throughout the system, flow is spatially variable and unsteady. For simplified basins the flow can first be computed over the land surfaces[11-14] and then through the channels.[15,16] Combining the two phases provides a useful mathematical model.[17,18] For practical flood predictions a simpler approach is essential. Various methods of routing input through storage have been proposed.[19-21] The storage-discharge relation is usually derived from the recession side of a hydrograph. In some cases the input is transferred to the outlet by a convolution process after estimating the time of travel from various segments of the drainage area. All of these procedures have been explored in this research program. The unit hydrograph procedure has shown the best results when considering simplicity as well as sensitivity to urbanization and other physical parameters.

The unit hydrograph idea was first proposed[22,23] for large watersheds, but it is also a useful tool for small watersheds.[24] Many investigators have studied the effect of drainage basin characteristics on unit hydrographs.[25-32] Previous research has shown that drainage basin size is one of the most important factors in influencing the

shape of the unit hydrograph.[9] This project has provided much more evidence that the area is one of the most important factors[8,17,33,34] and has produced quantitative evidence that population density is a very important parameter.[8]

SECTION V

COLLECTING DATA

It was clearly recognized from the beginning of this research that any effort that would provide a better understanding of surface runoff processes and eventually lead to a dependable method of predicting runoff from rainfall would require the analysis of many rainfall and/or snowmelt and runoff events from many different sizes and types of drainage basins.

A great deal of effort was devoted to searching for available runoff and rainfall records. It became obvious early in the work that the effect of urbanization would be one of the most important factors in the relations dealing with hydrograph shape. Many runoff records from urbanized areas are unpublished and must be obtained by copying from the original hydrographs where they are stored. Many were not published in sufficient detail and therefore it was necessary to work from the original gage charts or tapes in the U.S.G.S. offices to obtain the records. In the case of Red Run, a highly urbanized basin in Southeastern Michigan, it was also necessary to combine the runoff from the gaging station with the discharge diverted into the sewer system. Another part of the analysis consisted of the determination of the weighted hourly precipitation for each event and the computation of snowmelt when it occurred. Each event was then plotted as shown in Figure 1. It is estimated that the collection of data along with the hydrograph analysis mentioned above required about 70 percent of the total effort.

In Table 1 is presented a list of the watersheds that were studied. The location, the U.S.G.S. number, area, population density and the number of rain gages are also shown in the table. The number of drainage basins studied was 69, varying in size from 0.02 to 734 sq mi with 54 basins having areas of less than 20 sq mi. Population densities vary from less than 100 to more than 36,000 persons/sq mi. The number of hydrographs analyzed for each basin is also shown. The total number of hydrographs analyzed was 1620.

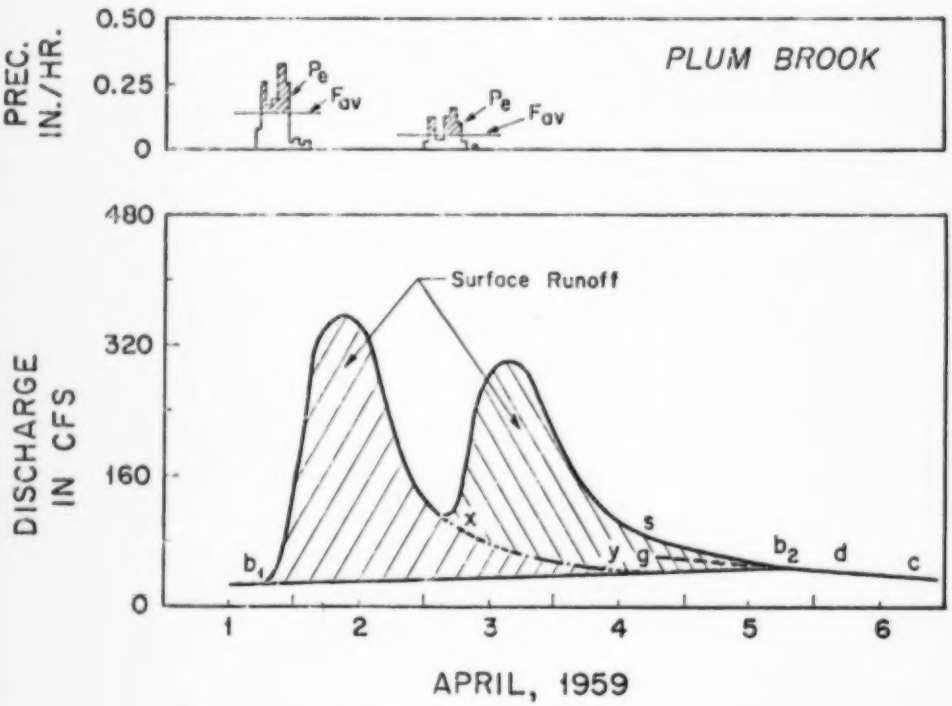

Figure 1. Typical hyetographs and hydrographs.

Table 1. FLOOD RUNOFF DATA

Legend

Column 6:
- T = Total number of gages
- R = Number of recording gages

Column 7:
- VA = Velocity-area station
- VAC = Velocity-area station with concrete control
- VAS = Velocity-area slope station
- VACS = Velocity-area partial hydrograph
- CCC = Concrete culvert control
- SSC = Shopping center, high P_d assumed
- PF = Parshall flume
- PAF = Parabolic flume

(1)	(2)	(3)	(4)	(5)	(6)		(7)	(8)	(9)
No.	Drainage basin (name and location)	U.S.G.S. No.	No. of flood hydrographs analyzed	Years of records	Rain gages T	Rain gages R	Type of gaging station	Area in sq mi	Population in persons per sq mi
1	Big Beaver Crk nr Warren, MI	4-1629.0	9	5	3	3	VA	23.5	774
2	Plum Brook nr Utica, MI	4-1633.0	93	10	2	2	VA	22.9	731
3	Rouge Rr, Birmingham, MI	4-1660.0	72	14	5	5	VAC	36.9	1212
4	Rouge Rr, Southfield, MI	4-.661.0	81	9	8	8	VA	88.0	1390
5	Lower Rouge Rr, Inster, MI	4-1680.0	80	14	4	4	VA	82.9	1100

Table 1 (continued). FLOOD RUNOFF DATA

(1)	(2)	(3)	(4)	(5)	(6)		(7)	(8)	(9)
No.	Drainage basin (name and location)	U.S.G.S. No.	No. of flood hydrographs analyzed	Years of records	Rain gages T	R	Type of gaging station	Area in sq mi	Population in persons per sq mi
6	Rouge Rr, Detroit, MI	4-1665.0	56	14	13	13	VA	185.0	2710
7	Clinton Rr, nr Fraser, MI	4-1640.0	21	21	20	20	VA	445.0	1650
8	Clinton Rr, Mount Clemens, MI	4-1655.0	45	31	22	22	VAS	734.0	1000
9	McBride Drain nr Macomb, MI	4-1644.5	32	5	2	2	VA	5.8	114
10	Tupper Brook, Ray Center, MI	4-1642.5	28	5	4	4	VA	8.6	60
11	Evans Ditch, Southfield, MI	4-1662.0	80	9	6	6	VAC	9.5	2376
12	East Branch Coon Cr, Armada, MI	4-1643.0	47	5	2	2	VAC	13.0	56
13	Gloede Ditch nr Waldenburg, MI	4-1652.0	33	5	3	3	VA	16.0	560
14	Upper Rouge Rr, Farmington, MI	4-1663.0	40	9	5	5	VAC	17.5	1129
15	Red Run nr Royal Oak, MI		91	14	9	9	VA	36.5	7500
16	Galloway Grk nr Auburn Heights, MI	4-1611.0	37	8	3	3	VAC	17.8	1112
17	Northwood Drainage Area Baltimore, MD		14	2	2	2	PF	.0742	9620

Table 1 (continued). FLOOD RUNOFF DATA

(1) No.	(2) Drainage basin (name and location)	(3) U.S.G.S. No.	(4) No. of flood hydrographs analyzed	(5) Years of records	(6) Rain gages T	(6) Rain gages R	(7) Type of gaging station	(8) Area in sq mi	(9) Population in persons per sq mi
18	Gray Haven, Baltimore, MD		29	4	1	1	PF	.364	38460
19	Oakdale, Chicago, ILL		13	5	1	1	PAF	.0201	36600
20	Boneyard Crk, ILL	3-3370.0	29	6	5	5	VAC	3.58	8900
21	Stoney Brook St Ditch, Houston, T	8-0737.5	16	4	4	1	VACS	.50	3306
22	Bintliff Ditch, Bissonet St., Houston, T	8-0748.5	13	2	5	2	VACS	4.29	4346
23	Berry Bayou, Gilpin St., Houston, T.	8-0755.5	15	5	2	2	VACS	3.26	2279
24	Hunting Bayou, U.S. Hwy 90-A, Houston, T	8-0757.7	19	6	6	4	VA	14.4	4614
25	Hunting Bayou, Calvalcade St., Houston, T	8-0757.5	22	6	5	2	VACS	1.03	8189
26	Bering Ditch, Woodway Drive, Houston, T	8-0738.0	21	7	4	2	VACS	2.74	4430
27	Berry Crk, Galveston Rd. Houston, T	8-0757.0	13	6	6	3	VACS	4.86	1546
28	Hunting Bayou, Falls St., Houston, T	8-0757.6	14	6	3	3	VACS	3.42	6726

Table 1 (continued). FLOOD RUNOFF DATA

(1)	(2)	(3)	(4)	(5)	(6)		(7)	(8)	(9)
			No. of		Rain gages				
No.	Drainage basin (name and location)	U.S.G.S. No.	flood hydrographs analyzed	Years of records	T	R	Type of gaging station	Area in sq mi	Population in Persons per sq mi
29	Berry Bayou, Forest Oaks St., Houston, T	8-0756.5	19	6	4	4	VA	11.1	2518
30	Berry Bayou, Globe St., Houston, T	8-0756.0	20	6	6	6	VACS	1.58	1447
31	Willow Waterhole Bayou, Landsdown St., Houston, T	8-0749.0	20	7	4	2	VACS	11.2	1021
32	Brickhouse Gully, Coasta Rica St., Houston, T	8-0742.5	21	6	6	5	VA	10.5	2245
33	Brickhouse Gully, Clarblake St., Houston, T	3-0742.0	11	6	2	2	VACS	2.01	529
34	Clear Crk Trib., Hall Rd, Houston, T	8-0771.0	15	5	2	2	VACS	1.27	664
35	Greens Bayou, U.S. Hwy 75 nr Houston, T	8-0759.0	12	5	4	3	VA	35.5	85
36	Greens Bayou, Cutten Rd. nr Houston, T	8-0757.8	10	6	2	2	VACS	8.73	60
37	Halls Bayou, Deertrail St., nr Houston, T	8-0762.0	12	6	3	3	VACS	5.27	807
38	Cole Crk, Guhn Rd., Houston, T	8-0741.0	15	6	5	3	VACS	7.05	243

Table 1 (continued). FLOOD RUNOFF DATA

(1) No.	(2) Drainage basin (name and location)	(3) U.S.G.S. No.	(4) No. of flood hydrographs analyzed	(5) Years of records	(6) Rain gages T	(6) Rain gages R	(7) Type of gaging station	(8) Area in sq mi	(9) Population in Persons per sq mi
39	Keegans Bayou, Roark Rd., nr Houston, T	8-0748.0	12	6	5	2	VA	9.66	125
40	Sims Bayou, Hiram Clarke St., Houston, T	8-0753.0	17	6	4	3	VA	20.2	939
41	Sims Bayou, Carlsbad St., Houston, T	8-0753.0	14	6	2	2	VACS	4.99	676
42	Cole Crk, Deihl Rd., Houston, T.	8-0741.5	13	6	5	4	VA	8.81	286
43	Keegans Bayou, Keegan Rd., nr Houston, T	8-0747.8	10	6	5	3	VACS	5.77	125
44	Waller Crk, 23rd St., Austin, T	8-1575.0	58	11	3	3	VAC	4.13	5500
45	Waller Crk, 38th St., Austin, T	8-1570.0	52	11	4	2	VAC	2.31	4200
46	Wilbarger Crk nr Pflugerville, T	8-1591.5	10	6	4	3	VAC	4.61	32
47	Bachman Br, Dallas, T	8-0557.0	18	5	6	6	VA	10.0	2950
48	Turtle Crk, Dallas, T	8-0565.0	24	7	5	5	VAC	7.98	5660
49	White Rock Crk, Keller Springs Rd., Dallas, T	8-0571.0	19	8	4	4	VA	29.4	238

Table 1 (continued). FLOOD RUNOFF DATA

(1)	(2)	(3)	(4)	(5)	(6)		(7)	(8)	(9)
No.	Drainage basin (name and location)	U.S.G.S. No.	No. of flood hydrographs analyzed	Years of records	Rain gages T	Rain gages R	Type of gaging station	Area in sq mi	Population in persons per sq mi
50	White Rock Crk, Greenville Ave., Dallas, T	8-0572.0	24	8	12	12	VA	66.4	708
51	White Rock Crk, White Rock Lake, Dallas, T	8-0573.0	8	3	18	18	VAC	100.0	981
52	Sycamore Crk Trib., Interst Hwy 35-W, Fort Worth, T	8-0485.4	7	1	2	2	VA	1.35	5590 +SSC
53	Little Fossil Crk, Interst Hwy 820, Fort Worth, T	8-0488.2	3	1	2	2	VACS	5.64	585
54	Seminary S. Shopping Ctr, Fort Worth, T		5	1	1	1	ROUTING	.38	SSC
55	Dry Br, Blanding St., Fort Worth, T	8-0485.5	9	2	2	2	VACS	1.08	610
56	Little Fossil Crk, Mesquite St., Fort Worth, T	8-0488.5	6	2	3	3	VAC	12.3	494
57	Dry Br, Fain St., Fort Worth, T	8-0486.0	8	2	2	2	CCC	2.15	2310
58	Sycamore Crk Trib. above Seminary S. Shopping Ctr, Fort Worth, T	8-0485.3	6	1	2	2	CCC	.97	7400

Table 1 (concluded). FLOOD RUNOFF DATA

(1)	(2)	(3)	(4)	(5)	(6)		(7)	(8)	(9)
No.	Drainage basin (name and location)	U.S.G.S. No.	No. of flood hydrographs analyzed	Years of records	Rain gages T	Rain gages R	Type of gaging station	Area in sq mi	Population in persons per sq mi
59	Sycamore Crk, at Interst Hwy 35-W, Fort Worth, T	8-0485.2	5	1	2	2	VA	17.7	1300
60	Olmos Crk, Dresden Dr., San Antonio, T	8-1777.0	6	2	4	4	VA	21.2	1120
61	Alazan Crk, St. Cloud St., San Antonio, T	8-1783.0	9	2	2	2	VACS	3.26	3210
62	Salado Crk Trib., Bitters Rd., San Antonio, T	8-1786.9	8	2	1	1	VACS	.26	5630
63	Hudson Crk, nr Bryan, T	8-1110.5	7	2	3	3	VA	1.94	10
64	Burton Crk, Villa Maria Rd., Bryan, T	8-1110.25	9	3	2	2	VAC	1.33	3150
65	17th St., Sewer, Louisville, KY		7	5	1	1	VAS	.22	13600
66	N.W. Trunk Sewer, Louisville, KY		7	5	2	2	VAS	1.90	13150
67	W. Outfall Sewer, Louisville, KY		6	5	5	5	VAS	2.77	14450
68	S. Outfall Sewer, Louisville, KY		9	5	9	9	VAS	6.43	9350
69	S.W. Outfall Sewer, Louisville, KY		6	5	6	6	VAS	7.52	6400

SECTION VI

HYDROGRAPH ANALYSIS

Hydrograph analysis on perennial streams for the purpose of determining the surface runoff, infiltration capacity, the duration of precipitation excess, and the form of the surface runoff hydrograph requires the separation of surface runoff from ground water discharge or base flow. The method conventionally used was based to some extent on judgment. Furthermore, it has been common practice to neglect initial retention (the portion of the rain which is intercepted by vegetation or the ground surface and never becomes infiltration or surface runoff) and the effect of runoff from impervious areas on the computations of infiltration capacity. Therefore, one of the initial goals of this project was to develop objective methods of carrying out this operation including the effect of retention and impermeable area.

SEPARATION OF GROUND WATER DISCHARGE FROM SURFACE RUNOFF

The first step in hydrograph analysis is to select lines such as b_1b_2 in Figures 1 and 2, to separate ground water discharge from surface runoff. Various logical subjective selections of this line could be made. Usually the range of reasonable locations where this line could be established is not great enough to create substantial differences in the computed values of either the infiltration capacity or the unit hydrograph ordinates. However, in the interest of better uniformity the following method was derived. There is little difficulty in selecting the point b_1 where surface runoff begins, but locating the point b_2 where surface runoff ends is more difficult. Consequently, it was decided to make use of the ground water depletion curve to determine the location of such points. The ground water depletion curve is the hydrograph of river discharge during a time of no precipitation and it depicts a rate of decrease in discharge that is much smaller than that of the recession side of a flood hydrograph such as sb_2 in Figures 1 and 2. If point b_2 correctly locates the end of surface runoff, then a ground water depletion curve for the basin should closely fit the hydrograph to the right of b_2 but should depart from the hydrograph to the left of b_2. This is illustrated by the ground water

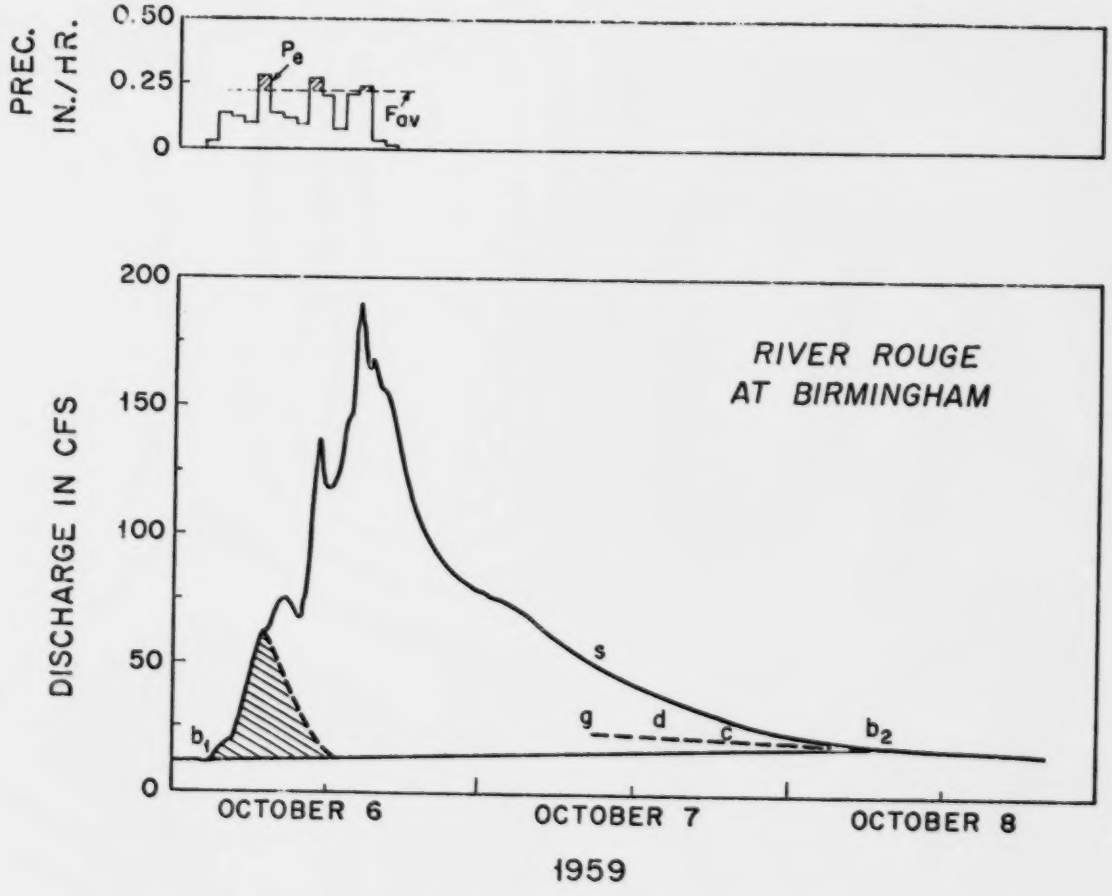

Figure 2. Complex hyetograph and hydrograph.

depletion curves gdc in Figures 1 and 2.

The practice of deriving ground water depletion curves by graphically fitting together portions of the curve permits the exercise of considerable judgment. Consequently, a more objective procedure was sought. The method selected is based on the idea that insofar as there exists a consistent relationship between ground water discharge and storage on the drainage basin, there must also exist a consistent relationship between discharge (Q), which is the ordinate of a point on the depletion curve, and its slope ($\Delta Q/\Delta T$), and that the equation for this relationship can be solved to obtain the equation for the ground water depletion curve. Values of Q and $\Delta Q/\Delta T$ were read from only those portions of the hydrographs preceded by a period of at least 3 days during which there was neither rain nor snowmelt. Examples of plotted values of $\Delta Q/\Delta T$ versus Q are shown in Figures 3 and 4. In all river basins for which this derivation has been made, the relationship between $\Delta Q/\Delta T$ and Q appeared to be linear. For example, the numerical value of the linear correlation coefficient (r) for the group of points in Figure 4 is 0.93, which is much greater than the value of 0.7 required to indicate that there is only one chance in 1000 that linearity is a fortuitous occurrence. The equations relating $\Delta Q/\Delta T$ to Q were derived by the method of least squares. The equation for Plum Brook (Figure 4) is

$$dQ/dT = 0.102 + 0.124Q \qquad (1)$$

Solution of this differential equation yields

$$Q = (Q_o + 0.82)e^{-.124T} - 0.82 \qquad (2)$$

in which Q_o is the value of Q selected for T = 0. This is the equation of the ground water depletion curve. A segment of this curve is plotted as line gdc in Figure 1.

A point of interest regarding the relation between $\Delta Q/\Delta T$ and Q is that none of the straight lines such as those in Figures 3 and 4 pass through the 0,0 coordinate. There seems to be no physical reason why they should. On the other hand, the data are probably not sufficiently accurate to give any significance to the location of the lower end points of these lines.

Having eliminated most of the subjectivity from selecting point b_2, it remains to decide on the form of the line connecting b_1 and b_2. Logical deduction would suggest that the ground water discharge would continue to recede for a time beyond b_1 and then rise in an s curve to point b_2. However, until this process is better defined quantitatively, it was decided to use a straight line connecting points b_1 and b_2. The straight line has

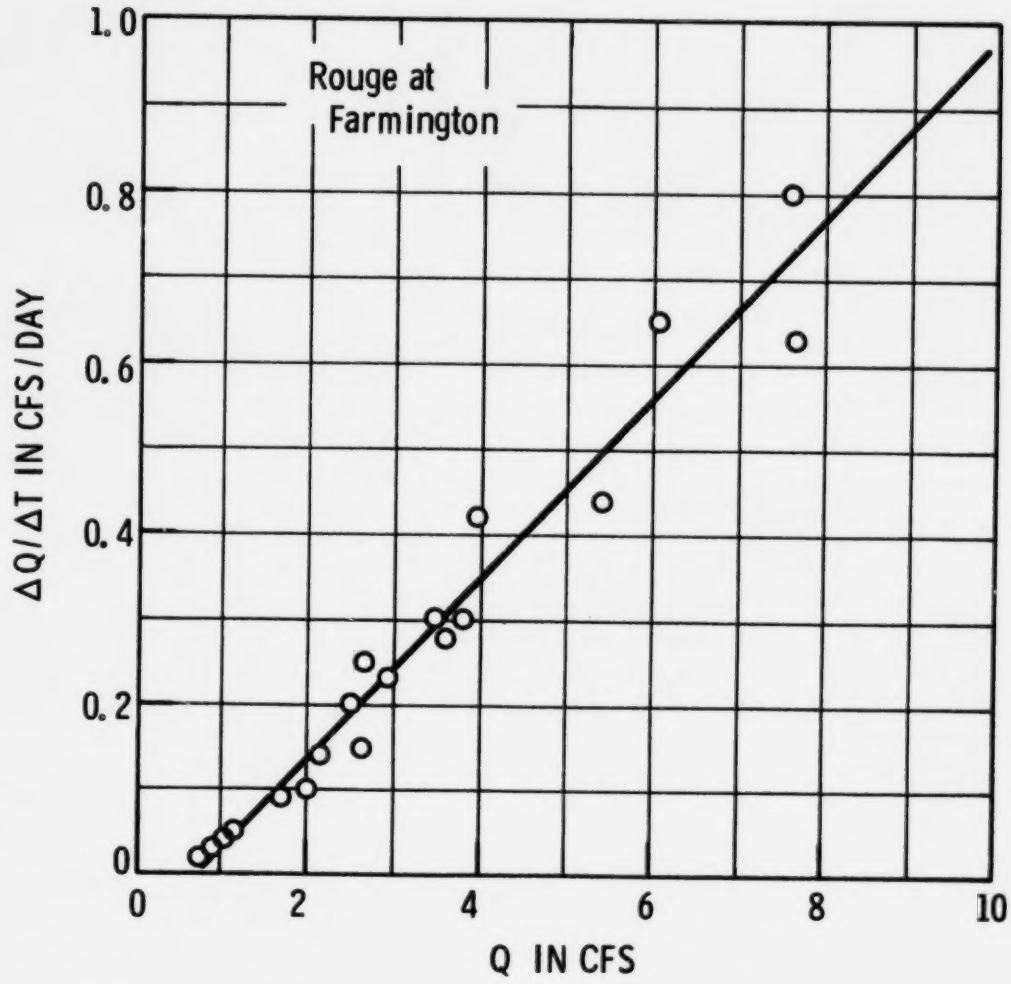

Figure 3. Relation between slope and discharge on ground water depletion curve.

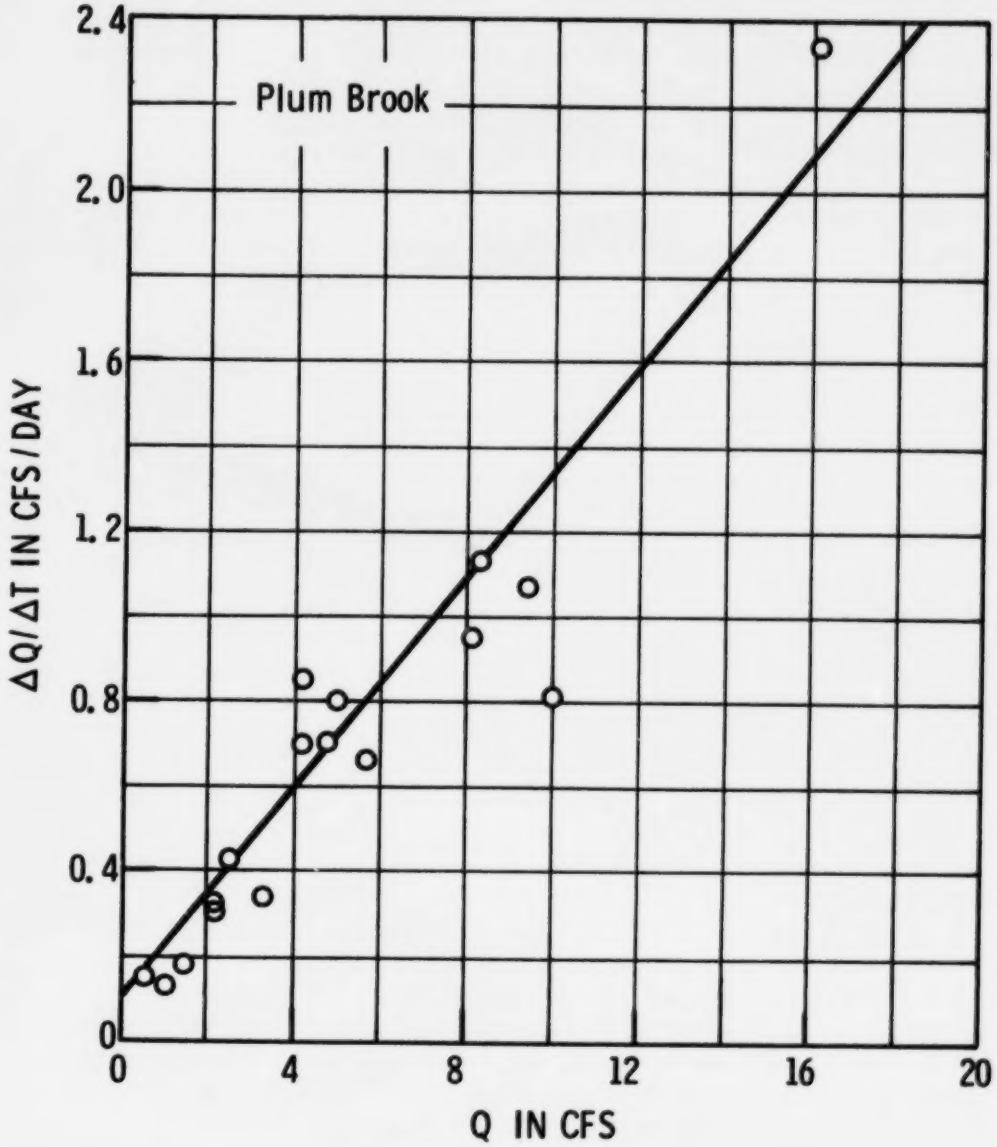

Figure 4. Relation between slope and discharge on ground water depletion curve.

the advantage of providing a consistent method of making this separation and eliminating any imaginative approach, even though it is based on logic.

Once the line b_1b_2 is established, the surface runoff may be computed by finding the area between this line and the hydrographs. The example shown in Figure 1 is complicated by the occurrence of a second rain before the surface runoff from the preceding one has ended. In such cases, a recession line such as xy is drawn having the same form as the recession sb_2. After the initial retention and the runoff from the impermeable area are taken into consideration, the average value of infiltration capacity (f_{av}) is obtained by trial, assuming that the precipitation excess (Pe) is equal to the surface runoff.

RETENTION

Before overland flow begins, or during its early stages, a small portion of the initial rainfall is stored and permanently abstracted from surface runoff by interception and surface or depression storage. The interception evaporates, and the depression storage either evaporates or infiltrates after the end of rainfall. The interception is abstracted from the beginning of rainfall, whereas depression storage accumulates only after the rain intensity exceeds the infiltration capacity. However, for the purpose of flood prediction it is convenient to combine the two abstractions. In this discussion, the total of these two abstractions will be referred to as retention (R). There is evidence[4] that interception continues to accumulate until the rainfall has reached 2 or more inches, and it seems logical to assume that depression storage may also increase toward some top limit as the rain continues at high intensities. Therefore, small rains are not likely to fulfill the maximum possible abstractions. The values of retention that have been estimated in the past presumably refer to the upper limit. Tholin and Keifer[18] have suggested values of retention of 1/16 in. for pavements and 1/4 in. for grass land. For small paved areas, values reported by Viessman[35] range from 0.04 to 0.10 in. Values of this order of magnitude could be considered as inconsequential when dealing with large floods. However, for smaller stream rises, variations in the selected magnitudes of this factor produce significant differences in the computed values of infiltration capacity. For example, for the hydrographs shown in Figure 1, values of f_{av} computed first by neglecting this abstraction and then by assuming a value of 0.2 in. have the ratio of about 3 to 2, respectively, for the first stream rise and 4 to 1 for the second stream rise.

Although quantitative values of depression storage cannot be determined directly from the analysis of individual hydrographs, it is possible to

gain a reasonably good idea of the maximum values of retention by arranging the data for total precipitation and surface runoff in the manner shown in Figures 5, 6, and 7. In these figures Line A is drawn near the left side to represent the condition of 100 percent surface runoff which could only occur if there were no infiltration ($f = 0$) and no retention ($R = 0$). If the vertical and horizontal coordinates were drawn to the same scale this would be a 45-degree line. Any points falling near Line A represent stream rises which must have occurred when the infiltration capacity on the permeable portion of the basin was very low.*

Another line, Line B, is then drawn through the points nearest to Line A and above and to the left of the main body of points. The magnitude of the retention can be estimated by assuming that points falling on Line B have zero infiltration and that all of the precipitation becomes either surface runoff or retention. Therefore the retention is the vertical distance between Lines A and B. It will be seen that for Plum Brook and Big Beaver Creek (Figures 5 and 6) nearly all of the points fall below and to the right of the lines representing an R of 0.2 in., thus indicating that the probable maximum value of R is slightly more than 0.2 in. For Red Run (Figure 7) more points fall above the 0.2-in. line than in the cases of Plum Brook or Big Beaver Creek. However, it may be noted that most of these points are designated in Figure 7 by black circles which represent winter rains which occurred within 15 hr after antecedent precipitation. Therefore, the portion of the retention caused by interception on vegetation was very low and there is also a good possibility that there was residual retention from the previous rain. The four summer storms falling between Line A and B in Figure 7, designated by triangles, were very small rainstorms ($P < 0.2$ in.) for which the retention capacity may not have been filled. It may be inferred, therefore, that the value of R on Red Run for summer rains greater than 0.2 in. and not preceded by a rain within 15 hr is approximately 0.2 in., but that it may be smaller for winter rains.

Although the maximum value of R appears to be about 0.2 in., it is clear that the average value during large rains is less. The determination of typical average values to be used in flood prediction was carried out in the analysis of the runoff hydrographs by assuming several values of R and computing the time of beginning of precipitation excess, recognizing

*The significance of the points on these graphs which lie toward the lower right, near the line labelled "SRO from A_i only," is discussed in a later section of this report. The points in the central portion of the graph represent stream rises during which there occurred both surface runoff from and infiltration into the permeable portion of the basin.

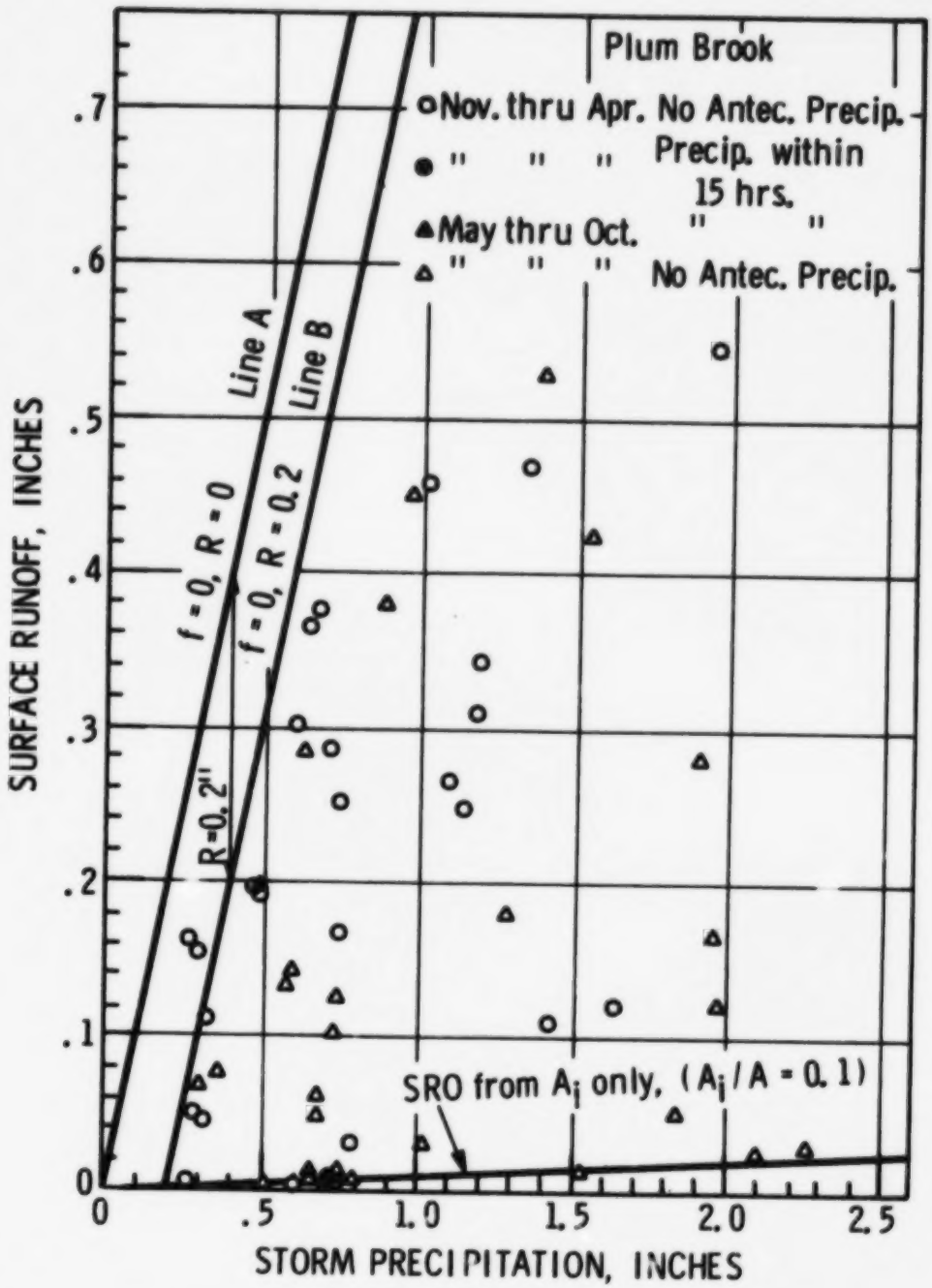

Figure 5. Surface runoff vs. precipitation.

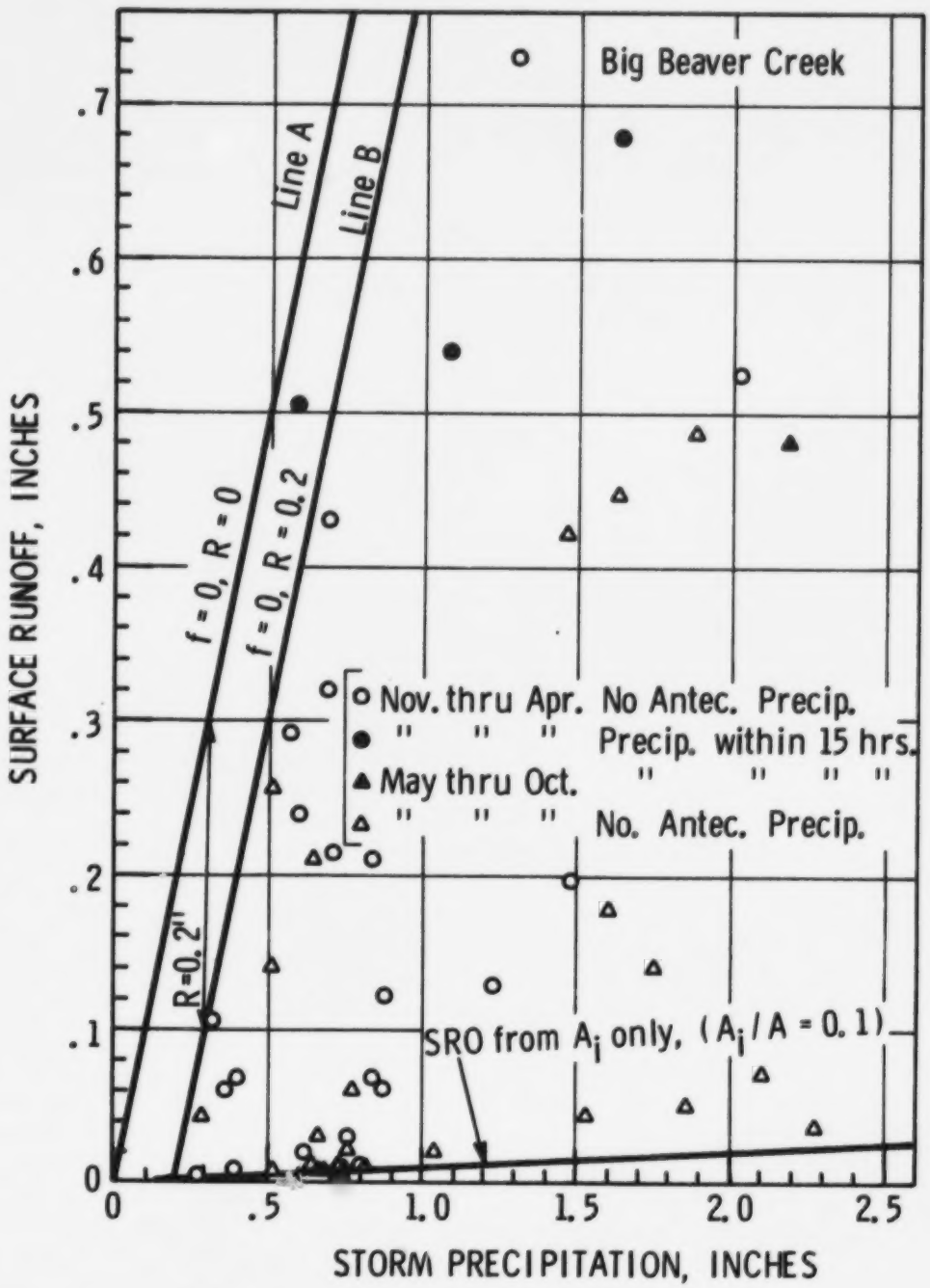

Figure 6. Surface runoff vs. precipitation.

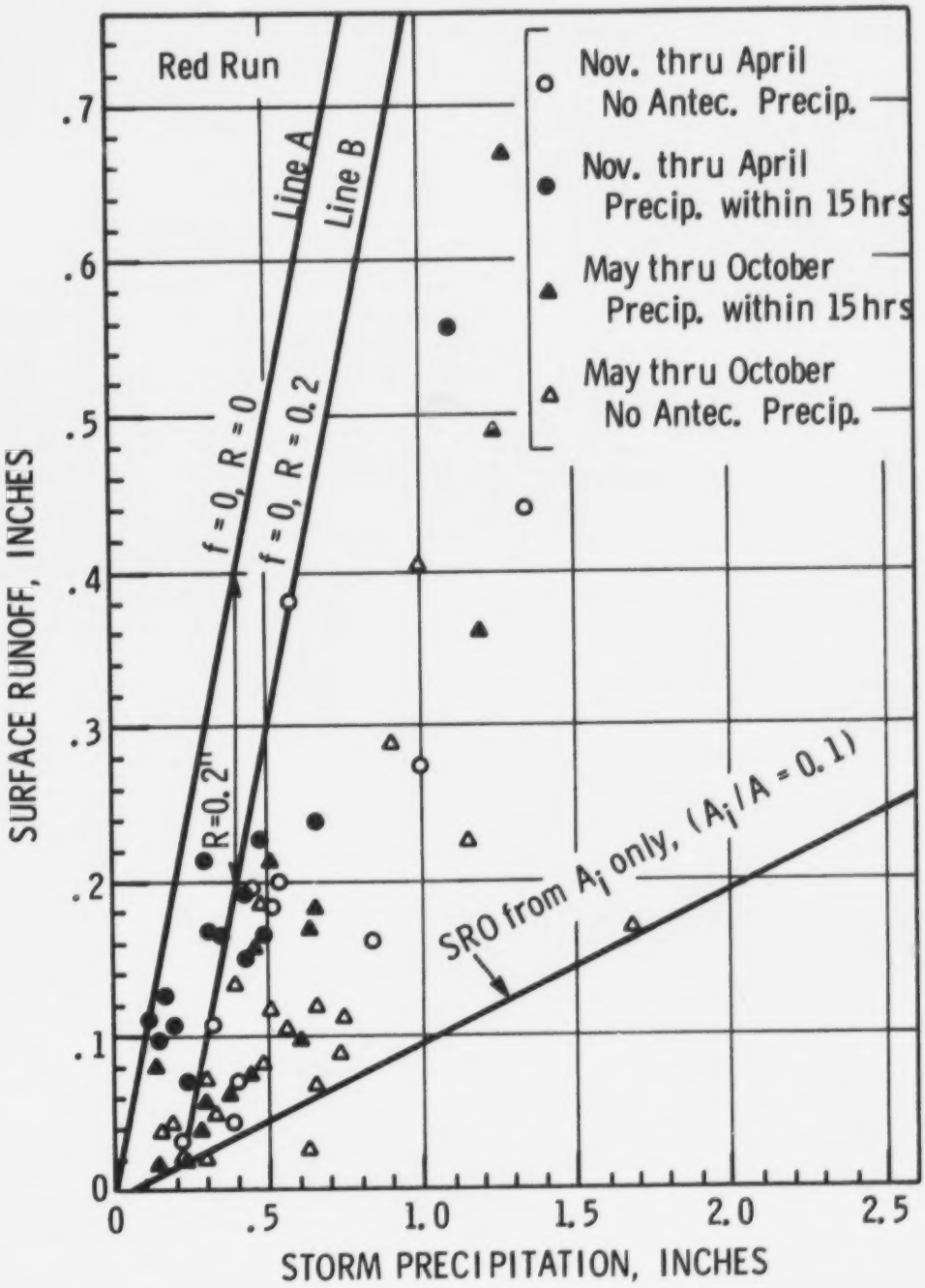

Figure 7. Surface runoff vs. precipitation.

that the initial precipitation excess would become retention. For each storm the value was selected which produced the best time relation between the beginning of precipitation excess and the beginning of surface runoff. For all rain storms over 1 in. in magnitude the values of R for the permeable portion of the basins varied from zero to 0.2 in. and the average value for summer was 0.15 in. and for winter 0.09 in. The latter value was rounded to 0.10 in. for practical application to flood prediction. For the impermeable portion of the basins a value of 0.05 in. gave satisfactory results.

A value of retention of 0.15 in. determined as described above represents the weighted average of the retention on the impermeable portion of the basin (R_i) and the retention on the permeable portion of the basin (R_p). If a value is assumed for R_i, then the value of R_p can be computed from the following equation:

$$RA = R_i A_i + R_p A_p \qquad (3)$$

in which A is the total area of the basin, and A_i and A_p are the areas of the impermeable and permeable portions, respectively. The solution will be illustrated for Red Run by assuming R_i = 0.05 in. and making use of the fact (demonstrated later) that A_i is 10 percent of the total area. Then

$$0.15A = 0.05A_i + R_p A_p$$

and

$$0.15 = 0.05A_i/A + R_p A_p/A$$

Since A_i/A = 0.1 and A_p/A = 0.9, R_p is found to be 0.16 in. This example is presented to illustrate that even for a basin in which 10 percent of the area is impermeable, there is only a small difference between R and R_p, probably less than the uncertainty in the estimated value of R. For less urbanized areas such as Plum Brook and Big Beaver Creek, this difference would, of course, be even smaller.

IMPERMEABLE AREAS

Shortly after the time when Horton[36] recognized the now obvious fact that surface runoff is produced when precipitation intensity exceeds the infiltration capacity of the soil, studies made by the senior author on storm runoff from small watersheds seemed to indicate a flaw in this concept.[24] Typical flood hydrographs were being observed on watersheds having such permeable soils that surface runoff was assumed to be impossible. It was

only after surveys of the stream channel area were made that it became clear that the precipitation falling on the streams themselves and the immediately adjacent banks produced unit hydrographs exactly similar to those from adjacent, less permeable areas. This discovery indicated that a thorough study of the characteristics of infiltration capacity must take into consideration the nearly 100 percent runoff from water surfaces and other impervious areas. Similar findings have since been reported for other drainage basins.[37]

The extent of the effectively impervious area is of particular interest in this research, because it appears obvious that this is one of the important factors whereby urbanization influences storm runoff. It is recognized that the effectively impervious portion of the basin may be larger during wet seasons than during dry periods. This might be caused by increased area of water surfaces on the basin but also by portions of the permeable portions of the basin that might become nearly impervious after prolonged rainfall or snowmelt. It was decided to approach the problem by attempting to determine what portion of the drainage basin acted as an impermeable area under all conditions. This area, expressed as the percentage of the total area, has been called the 'hydrologically significant impermeable area,' (HSIA). (HSIA = 100 (A_i/A), where A_i is the impermeable area and A is the total area of the drainage basin). It was reasoned that this area could be computed from hydrographs produced during periods of very high infiltration capacity when the entire hydrograph of surface runoff can be attributed to the rainfall minus retention (P - R_i) on the HSIA.

Although such hydrographs can be found from a search of the records, they can also be isolated readily by plotting the surface runoff against precipitation for all stream rises of record, as shown in Figures 5, 6, and 7. The hydrographs, which are of the type mentioned above, provide the points on the lower right side of Figures 5, 6, and 7, near the line labeled 'SRO from A_i only.' The slope of this line (A_i/A) multiplied by 100 gives the value of the HSIA. The two drainage basins for which such data are plotted in Figures 5 and 6 are relatively unurbanized when compared with highly populated areas. They contain farm land, some scattered housing along main roads, and several industrial parks. The population density of Plum Brook is about 700/sq mi and that of Big Beaver Creek approximately 800/sq mi. (Population density data were compiled by the Detroit Metropolitan Area Regional Planning Commission.) It may be seen that the lines drawn for an HSIA of 1.0 percent of the basin area and for an assumed value of retention on the impermeable area (R_i) of 0.05 in. form envelopes that include nearly all of the lowest points. (If R_i were assumed to be zero, the line for the same hydrologically significant area would have the same slope but would pass through the

origin.) A similar plotting for Red Run, shown in Figure 7, reveals an HSIA area of about 10 percent of the drainage basin. The population density of the Red Run basin is approximately 7500. Thus, it is indicated that, for these particular basins, the HSIA increases in about the same way as the population density. As additional rainfall and runoff data are analyzed for other drainage basins, the relation of the HSIA to other measures of the degree of urbanization, as well as to natural physical characteristics of the drainage basin, will be examined.

The small amount of HSIA in the Plum Brook and Big Beaver watersheds makes little difference in the computed values of f_{av} when there is a substantial contribution of surface runoff from the pervious portions of a drainage basin. However, even such small amounts of HSIA as 1.0 percent can, if ignored, lead to the computation of meaningless values of f_{av} for those summer or autumn floods produced entirely by runoff from impervious areas. The importance of taking into consideration the runoff from even a small percentage of impervious areas is illustrated by the stream rise for the River Rouge at Birmingham shown in Figure 2. It may be seen that the surface runoff started on October 6 at 0300, whereas the rainfall excess did not begin until 0600. This is illogical, unless the runoff from the HSIA is included as a separate item. If the HSIA were 1.8 percent, which is typical for that population density, then the rainfall occurring before 0600 would have produced a runoff from the impermeable area of the amount shown by the hatched area in Figure 2. The beginning of surface runoff from precipitation excess on the permeable area would then be at 0700, or an hour later than the beginning of rainfall excess, and the entire hydrograph becomes a reasonable output from the precipitation pattern.

Values of HSIA were determined for 12 basins in Southeastern Michigan. When plotted against population density the trend of the points was closely represented by the following equation

$$HSIA = 1.38P_d \qquad (4)$$

where P_d is the population density in thousands of persons per square mile and HSIA is in percent of total area.

SECTION VII

INFILTRATION CAPACITY

The prediction of the peak flow resulting from a specific input from rainfall and/or snowmelt requires knowledge of the portion of the total input which will be abstracted as infiltration and surface retention. Of these abstractions, infiltration is by far the most important. Unlike the shapes of the unit hydrographs which depend primarily on the areas of the drainage basins and on other physical characteristics of the basins which are not related to a particular geographical region, the infiltration capacity (f) depends to a large extent on the soil in the particular location where flood predictions are to be made. Therefore one of the principle parameters sought from hydrograph analysis is the infiltration capacity and its seasonal variation.

The determination of infiltration capacity for a runoff event may be described with reference to Figure 1. The amount of surface runoff which is the hatched area for each stream rise is computed first, then the average infiltration capacity during a storm is computed by trial by finding the value which makes the precipitation excess, P_e on the rain intensity diagram, equal to the surface runoff, after taking into consideration retention and runoff from impermeable portions of the basin. Sketching this value of infiltration capacity on the hyetograph as shown in Figure 1, then establishes the duration of precipitation excess which becomes an important parameter in the formation of the surface runoff hydrograph. Infiltration capacity decreases during rain storms as illustrated by the two rains in Figure 1 and it also varies seasonally as shown in Figure 8.

Because of the variation of f with time during a rain the actual value during a particular rain depends on whether there has been recent antecedent precipitation. The scatter of points in Figure 8 is largely due to this factor. The only method of determining the average infiltration capacity of a particular drainage basin is by means of hydrograph analysis. This type of analysis yields the average value of infiltration capacity (f_{av}) for each stream rise. The variation of f with

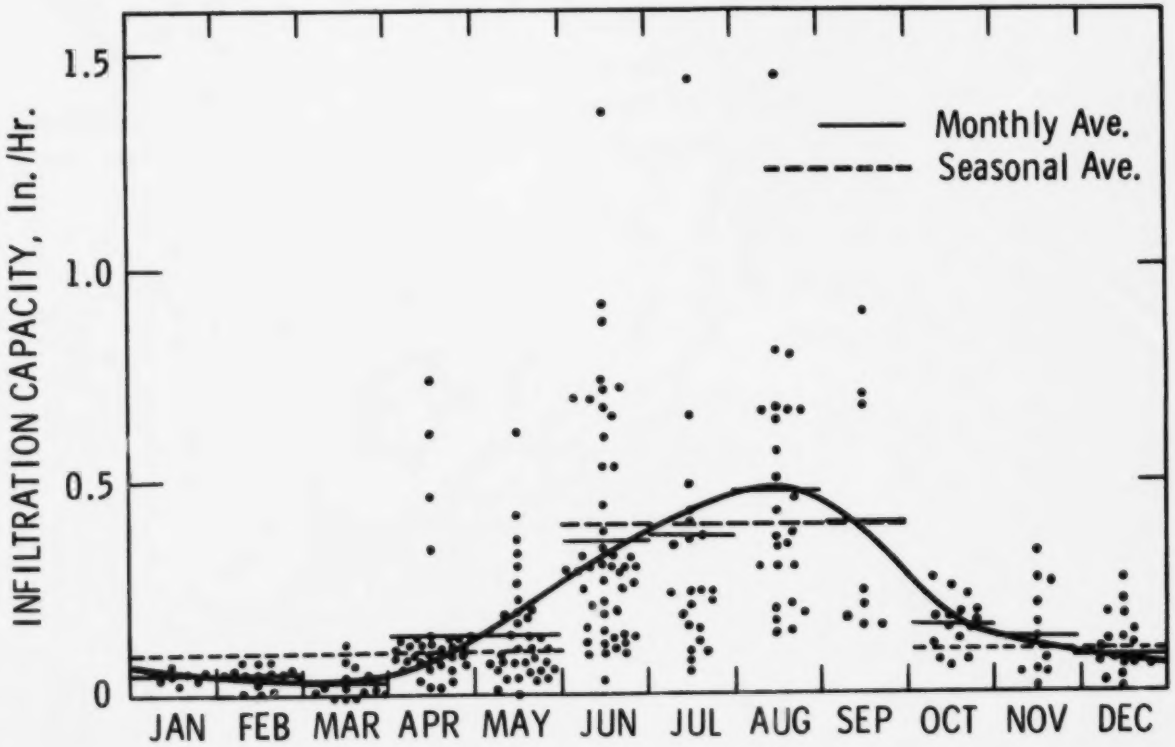

Figure 8. Seasonal variation of infiltration capacity.

time can be obtained from a closely spaced series of stream rises as shown by an example in the next section on "Unit Hydrographs."

Each of the more than 200 points in Figure 8 was determined by hydrograph analysis on the 16 basins in Southeastern Michigan. These basins have quite similar soils and therefore the infiltration capacity did not vary greatly from one basin to another. The average value for summer which included June, July, August, and September was 0.4 in./hr and the average for winter, which included the other eight months, was 0.10 in./hr. The values should not be used in other regions. Enough hydrographs must be analyzed in any region to establish the order of magnitude of infiltration capacity. The computed value of infiltration capacity depends to some extent on whether retention and runoff from impermeable areas are included in the computations. The latter factor becomes particularly important for highly urbanized areas where the impermeable area becomes large. In the analysis, the total surface runoff (SRO) is taken to be equal to the surface runoff from impermeable portion of a basin (SRO_i) plus that from the permeable portion (SRO_p). These values are defined by the following equations

$$SRO_i = P - R_i \tag{5}$$

$$SRO_p = P - F - R_p \tag{6}$$

where P is the average precipitation, R_i is the retention on the impermeable area, F is the total infiltration and R_p is the retention on the permeable area. A detailed description of the determination of the impermeable area and the retention has been presented in the section on Hydrograph Analysis.

The computations for determining the infiltration capacity for the first stream rise in Figure 1 are presented here to illustrate the procedure.

Area of Drainage Basin, A = 22.9 sq mi
Impermeable area, A_i = .02A
Retention on impermeable area, R_i = 0.05 in.
Retention on permeable area, R_p = 0.15 in.
Weighted average precipitation, P = 1.35 in.

The first step is the computation of the surface runoff. This requires that a line separating surface runoff from groundwater discharge be drawn

such as b_1b_2 in Figure 1. The procedure used to do this was explained earlier in this report in the section on hydrograph analysis. In the example shown in Figure 1, it was also necessary to draw the line xy to separate the hydrograph produced by the first rain from one resulting from the second rain. This is done by sketching a line having the same form as sb_2 which represents the same release of storage as would have occurred at the end of the first hydrograph. Ordinates from the first hydrograph were tabulated for 2-hr intervals as shown in columns 1 and 2, Table 2. The surface runoff in inches on the basin is then computed from the summation of column 2 by multiplying by the number of second in 2 hr dividing by the area of the basin and multiplying by 12 as shown as follows.

$$SRO = \frac{3456 \times 2 \times 3600}{22.9 \times 5280 \times 5280} \times 12 = .468 \text{ in.}$$

The surface runoff from the impermeable area (SRO_i) is computed using Eq. (5) and then converting to inches on the entire basin by multiplying by the ratio of the impermeable area to the total area as follows

$$SRO_i = \frac{A_i}{A} (P - R_i) \qquad (7)$$

$$= .02 (1.35 - .05) = .026 \text{ in. on A}$$

The surface runoff from the permeable area (SRO_p) is then the difference between the total surface runoff and SRO_i and is (.468 - .026) = .442 expressed in inches on the total basin. This value is converted to inches on the permeable portion of the basin as follows:

$$SRO_p = \frac{A}{A_p} \times (.442) = \frac{100}{98} \times .442 = .451 \text{ in. on } A_p$$

The total precipitation excess on the permeable area (P_{ep}) is then obtained by adding the retention (R_p) as follows:

$$P_{ep} = SRO_p + R_p \qquad (8)$$

$$= .451 + .15 = .601 \text{ in. on } A_p$$

Table 2. COMPUTATIONS OF SURFACE RUNOFF AND UNIT HYDROGRAPH ORDINATES FOR RAIN OF APRIL 1, 1959, ON PLUM BROOK
(Drainage Area = 22.9 sq mi)

Number of 2-hour Intervals	Average rate of surface runoff, cfs	Unit hydrograph, cfs/sq. mi./in.
1	28	2.6
2	116	10.8
3	230	21.5
4	294	27.4
5	308	28.8
6	320	29.9
	(324)	(30.3) (peak)
7	320	29.9
8	308	28.8
9	280	26.1
10	240	22.4
11	190	17.7
12	148	13.8
13	120	13.8
14	96	9.0
15	80	7.5
16	66	6.2
17	56	5.2
18	48	4.5
19	40	3.7
20	36	3.4
21	32	3.0
22	26	2.4
23	22	2.1
24	18	1.7
25	14	1.3
26	10	0.9
27	7	0.7
28	3	0.3
	3456	

[a]Typical computation of unit hydrograph ordinate:

$$\frac{28 \text{ cfs}}{22.9 \text{ sq mi} \times 0.468 \text{ in.}} \equiv 2.6 \text{ cfs/sq mi/in.}$$

The infiltration capacity of the permeable area is now computed by trial. The final trial computations are shown in Table 3 in which hourly precipitation is given in column 2, the assumed infiltration capacity in column 3 and the precipitation excess in column 4. The total of column 4 multiplied by 60/60 to convert from inches per hour to inches is 0.600 which agrees with the value of P_{ep} computed above. Therefore the infiltration capacity of the permeable portion of the basin is 0.114 in./hr. This procedure applies to simple hydrographs which can readily be assigned to a particular rain. For more complex storms the method involves an application of the unit hydrograph and will be described later.

Table 3. COMPUTATION OF INFILTRATION CAPACITY

Hours	Precipitation intensity, in./hr.	Infiltration capacity, in./hr.	Precipitation excess, in./hr.
17	.00	.114	-
18	.07	.114	-
19	.26	.114	0.146
20	.16	.114	0.046
21	.18	.114	0.066
22	.32	.114	0.206
23	.25	.114	0.136
24	.03	.114	-
25	.04	.114	-
26	.01	.114	-
27	.03	.114	-
28	.00	.114	-
			0.600

SECTION VIII

UNIT HYDROGRAPHS

By far the major portion of the research effort was devoted to studying unit hydrograph characteristics. This procedure in its simplest form is based on the assumption that the important characteristics of a surface runoff hydrograph for any basin are essentially constant if the duration of precipitation excess is less than some critical value, that the ordinates of this hydrograph vary linearly with the magnitude of rainfall excess and that various complex rainfall or snowmelt inputs can be transformed into a complete hydrograph by a linear additive convolution process.

The unit hydrograph is obtained from a surface runoff hydrograph produced by a precipitation excess having a duration less than some critical duration to be defined later by taking the surface runoff ordinates for successive arbitrarily selected uniform time intervals and converting them to cfs per square mile per inch of rainfall excess. This is done by dividing the ordinates in cfs by the area of the drainage basin in square miles and by the rainfall excess in inches as illustrated in Table 2. The ordinates of a unit hydrograph could also be expressed in percentage of total surface runoff. In this form the graph is often referred to as a distribution graph. This latter form is not used in this report. The example shown in Table 2 is for the first of the two hydrographs of Figure 1. In Figure 9 are shown five unit hydrographs from this same basin. These five show typical variations for a basin. It should be noted that they are relatively consistent even though the total surface runoff for the largest of the five was about four times the smallest as shown by the values of surface runoff tabulated in Figure 9. The average unit hydrograph is also shown in Figure 9.

The most important characteristic of a unit hydrograph is its peak because this is the value used to predict peak flood flows. However, in order to construct a complete flood hydrograph the entire set of unit hydrograph ordinates and abscissas must be known as shown in tabular form in columns 1 and 3 in Table 2 or graphically in Figure 9. A very useful

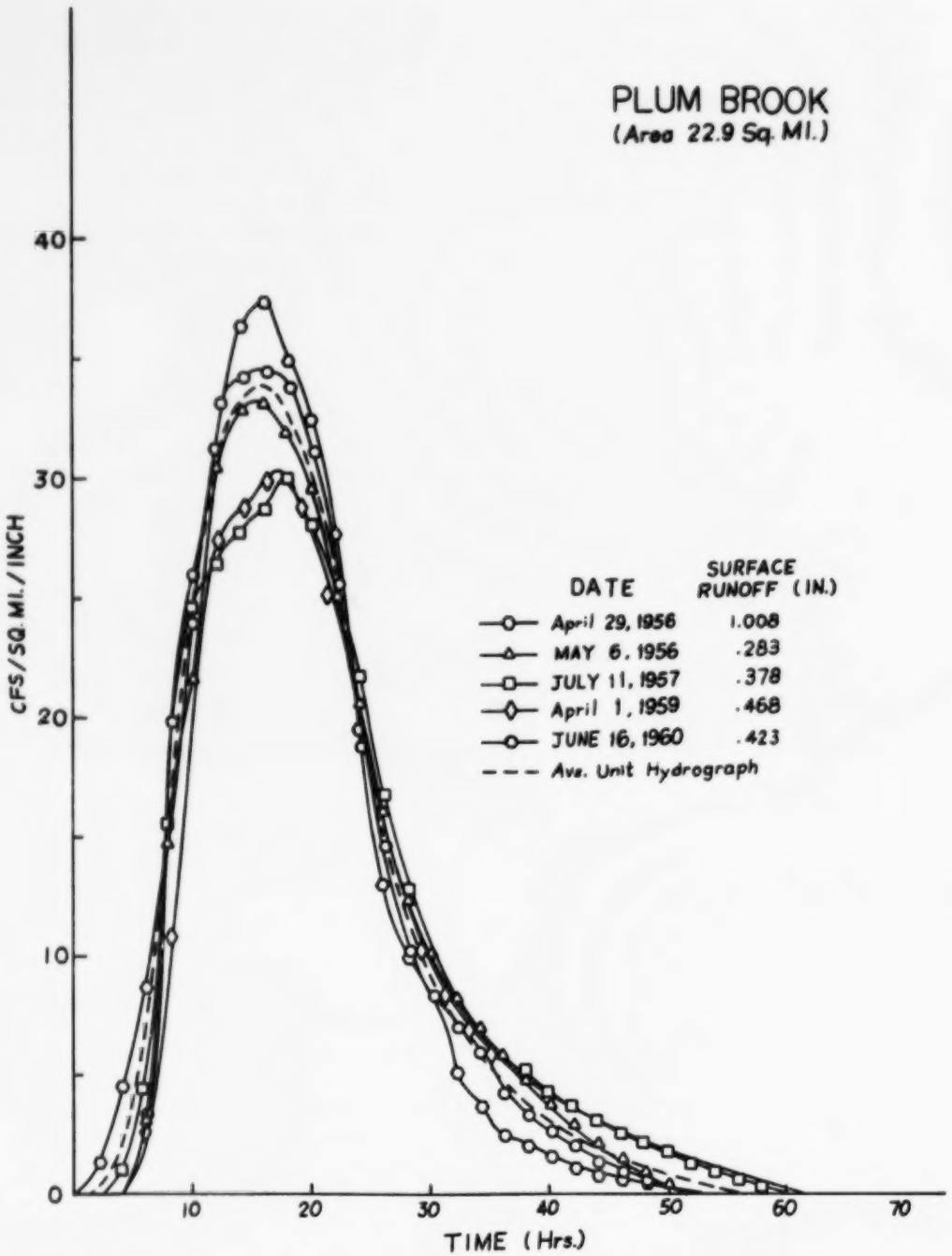

Figure 9. Five unit hydrographs from the same basin.

application of the unit hydrograph is in determining the progressive variation of infiltration capacity during a closely spaced series of storms. This process also provides a test of the accuracy of the unit hydrograph procedure by applying the unit hydrograph for a drainage basin to a complex rain storm in which the contributions from various portions of the rainfall excess must be added taking into account the sequential time of occurrence of the periods of rainfall excess and comparing the computed hydrograph with the actual hydrograph. A typical example is shown in Figure 10. When a unit hydrograph is applied to successive portions of a long complex series of rains such as those in Figure 10, the infiltration capacity is computed for each separate stream rise and adjusted by trial until the summation of the overlapping hydrographs fits the actual hydrograph. The curve of infiltration capacity (f_{av}) shown in Figure 10 is based on five values of f_{av} determined for the five bursts of rainfall. The volumes of precipitation excess (P_e) are shown by the hatched areas of the hyetograph above the infiltration capacity curve. The derived hydrograph shown by the dashed line was computed by applying the average unit hydrograph for that basin five times to the five values of precipitation excess (P_e) and adding overlapping ordinates. This latter process is sometimes called convolution.

For the purpose of relating unit hydrograph shape to basin characteristics the average unit hydrographs for each basin was defined in terms of the peak (q_{pA}), the period of rise (T_r), the significant period of rise (t_r), the width of the graph at the base (W_0) and at 25, 50, and 75 percent of the peak discharge (W_{25}, W_{50}, and W_{75}). These parameters are defined graphically in Figure 11. The average values of these parameters for 53 of the basins* are presented in Table 4. The numbers in column 1 of Table 4 provide a convenient method of identifying each watershed by reference

*Sixteen of the 69 basins listed in Table 1 are not included in Table 4. Basins 43 and 59 had not experienced enough large rains to define the unit hydrograph. Basins 5, 16, and 42 were omitted because the flood hydrographs were double peaked thus making it difficult to define their shape. The double peaks appear to be caused by highly urbanized areas in the lower reaches of an otherwise less urbanized basin. Eleven basins in the Austin (44-46), Dallas (47-51), and San Antonio (60-62) regions were omitted because they displayed runoff characteristics which indicated high urbanization even though their values of P_d are very low. It is suspected that the storm drainage systems of these eleven basins may have been developed in advance of anticipated urban growth. As with the double peaked basins, a detailed study of the drainage system is expected to reveal the causes of the anomolous behavior. This additional research was beyond the scope of this project.

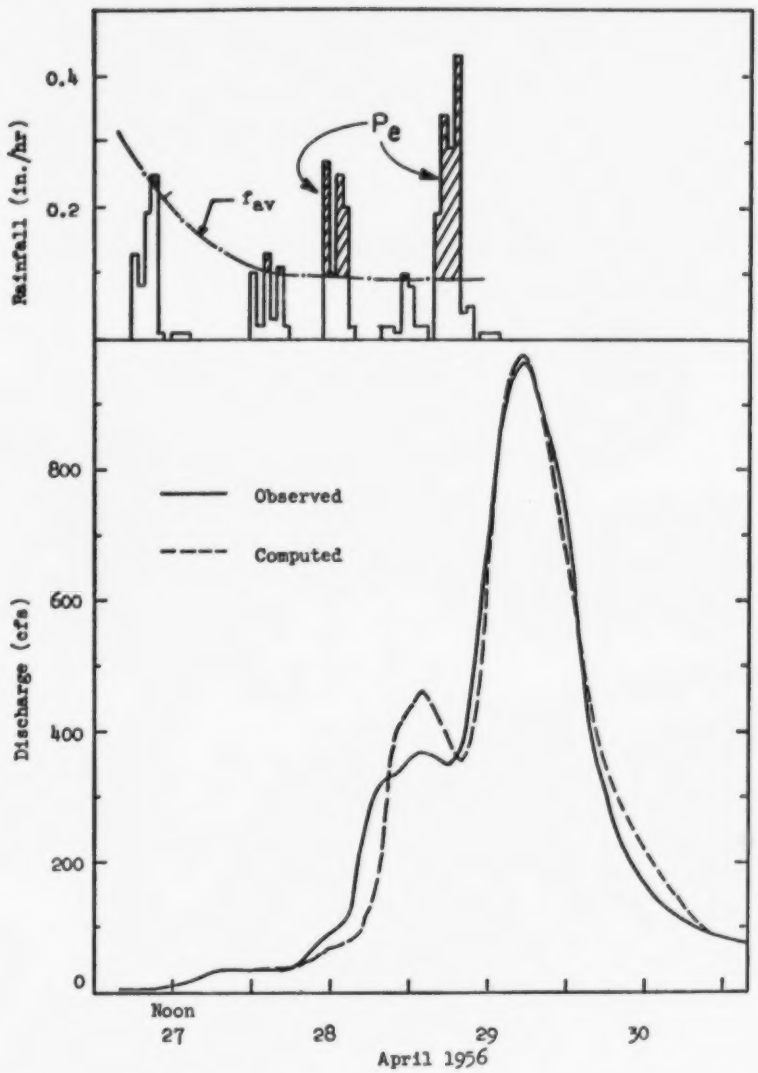

Figure 10. Reproduction of a complex hydrograph for the flood of April 27-30, 1956 on Plum Brook (area = 22.9 sq mi).

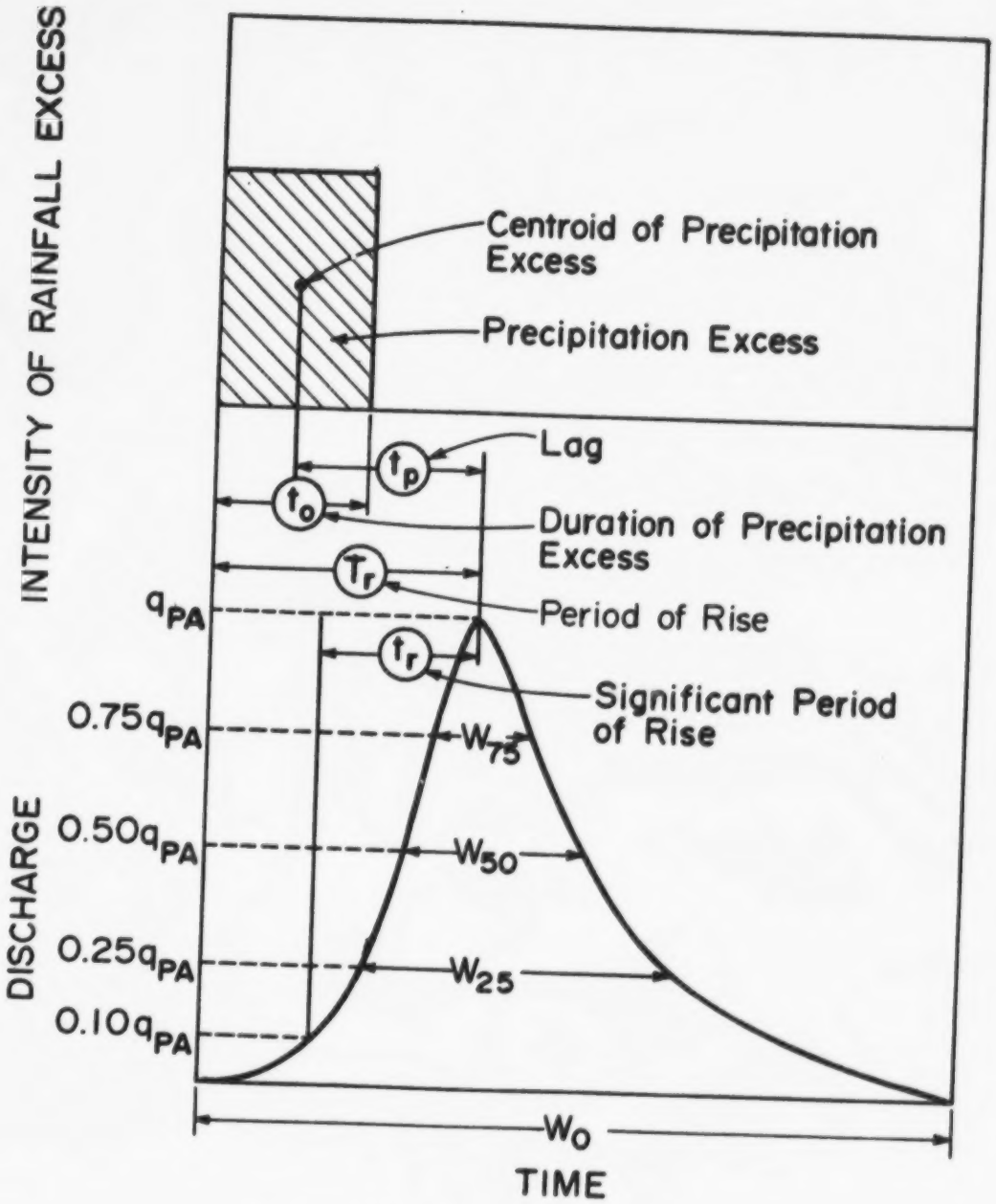

Figure 11. Definition sketch.

Table 4. UNIT HYDROGRAPH PARAMETERS

Legend

No. = Number assigned to basin in Table 1
A = Area in sq mi
P_d = Population density in persons/sq mi
q_{pA} = Pk. in cfs/sq mi/in.
t^r = Significant period of rise in hours
T^r = Period of rise in hours
W^r_0 = Width of base in hours
W_{xx} = Width at xx percent of peak in hours
SC = Shopping center, high P_d. assumed

No.	A	P_d	q_{pA}	t_r	T_r	W_0	W_{25}	W_{50}	W_{75}
				High population density					
15	36.5	7500	140	2.40	4.00	23.0	6.10	4.10	2.40
17	0.074	9620	7370	0.025	0.063	0.300	0.124	0.076	0.038
18	0.036	38460	3010	0.103	0.133	0.616	0.283	0.192	0.117
19	0.02	36600	2850	0.117	0.150	0.800	0.307	0.185	0.103
20	3.58	8900	496	0.516	0.660	4.40	1.72	1.04	0.62
25	1.03	8189	188	1.25	1.50	13.0	4.95	2.95	1.55
28	3.42	6726	140	1.35	1.75	16.0	6.20	3.55	1.85
52	1.35	5590 +SC	1000	0.333	0.450	3.00	0.833	0.525	0.317
54	0.38	SC	2020	0.167	0.167	1.50	0.375	0.226	0.117

Table 4 (continued). UNIT HYDROGRAPH PARAMETERS

No.	A	P_d	q_{pA}	t_r	T_r	W_0	W_{25}	W_{50}	W_{75}
58	0.97	7400	1165	0.250	0.333	2.67	0.633	0.417	0.266
65	0.22	13600	1612	0.167	0.217	0.875	0.536	0.374	0.220
66	1.90	13150	934	0.342	0.484	1.83	0.900	0.642	0.400
67	2.77	14450	513	0.342	0.416	3.17	1.73	1.17	0.716
68	6.43	9350	513	0.683	0.917	3.34	1.60	1.13	0.717
69	7.52	6400	694	0.350	0.584	3.33	1.17	0.750	0.483
				Low population density					
1	23.5	774	34	9.5	13.0	53.0	27.2	16.3	9.5
2	22.9	731	34	10.6	15.9	51.2	24.8	17.6	12.4
3	36.9	1212	30	10.0	12.5	67.0	29.1	17.2	10.2
8	734.	1000	13.4	32.0	38.0	120.	64.0	43.0	27.0
9	5.8	114	38.5	6.8	9.3	47.5	22.9	14.8	8.60
10	8.6	60	37.	3.1	5.	80.	22.8	13.6	7.30
12	13.0	56	40.	7.3	10.	58.	23.	11.9	5.70
13	16.0	560	27.	8.6	14.1	94.	30.5	18.1	12.0
14	17.5	1129	40.	7.2	10.	78.	20.8	12.0	6.1
31	11.2	1021	140.	0.75	1.4	19.	4.83	2.62	1.38
33	2.01	529	74.2	2.8	3.3	24.	11.1	7.	4.20
34	1.27	664	175.	1.4	1.8	14.	5.	3.05	1.83
35	35.5	85	47.7	3.9	4.8	38.	19.4	11.4	6.50
36	8.73	60	40.8	5.60	7.20	40.0	18.9	14.8	9.20
37	5.27	807	102.	2.08	2.08	19.0	9.0	5.7	3.30
38	7.05	243	91.5	2.65	3.70	20.0	9.55	5.95	3.75
39	9.66	125	54.0	3.00	5.50	40.0	16.7	10.0	5.00

Table 4 (concluded). UNIT HYDROGRAPH PARAMETERS

No.	A	P_d	q_{pA}	t_r	T_r	W_0	W_{25}	W_{50}	W_{75}
40	20.2	939	58.7	4.00	5.20	33.0	16.8	9.3	5.00
41	4.99	676	56.6	4.50	6.05	34.0	15.8	9.1	5.75
53	5.64	585	167.	3.00	3.25	10.8	5.25	3.0	1.75
55	1.08	610	426.	0.833	0.833	4.16	1.97	1.33	0.833
56	12.3	494	137.	1.83	2.90	18.0	5.95	3.60	2.30
63	1.94	10	194.	2.25	2.75	11.0	4.25	2.60	1.75
				Intermediate Population Density					
4	88.0	1390	26.0	11.5	15.0	79.0	35.0	22.0	12.1
6	185.	2710	20.0	21.0	27.0	100.	41.0	28.3	17.0
7	445.	1650	15.0	Time Parameters Not Determined					
11	9.5	2376	63.5	6.8	12.0	41.0	12.6	8.8	5.6
21	0.50	3306	580.	0.300	0.500	5.75	1.25	0.75	0.50
22	4.29	4346	201.	1.10	1.42	9.00	4.29	2.78	1.85
23	3.26	2279	164.	1.50	1.67	16.0	5.00	3.15	1.70
24	14.4	4614	62.7	4.50	6.00	34.0	14.9	8.45	4.65
26	2.74	4430	211.	1.05	1.40	11.5	4.10	2.35	1.30
27	4.86	1546	114.	1.45	2.20	22.0	9.90	2.80	1.60
29	11.1	2518	168.	1.50	2.16	16.5	5.50	3.40	2.05
30	1.58	1447	172.	1.05	1.70	15.0	5.40	2.75	1.40
32	10.5	2245	140.	0.75	1.17	16.5	5.75	3.75	2.00
57	2.15	2310	300.	1.17	1.42	5.25	2.75	2.04	1.55
64	1.33	3150	540.	0.881	1.25	4.25	1.48	1.05	0.667

to Table 1. All of the parameters are used to define the shape of a unit hydrograph. However, t_r is also the critical time characteristic which is related to the maximum duration of rainfall excess which will produce a single unit hydrograph.

It was previously discovered that for a group of watersheds from within the same large watershed system there was a relatively consistant relationship between the two most important unit hydrograph characteristics, their peaks and periods of rise, and the areas of the drainage basins.[9] The research reported here provided an opportunity to determine if such relationships exist for a wide variety of watersheds from different regions. The relations between unit hydrograph peak and area and between the various time parameters and area were found to be quite consistant for all watersheds if the degree of urbanization was accounted for. At this stage in the research the population density (P_d) seems to be a very significant factor in expressing the degree of urbanization. Satisfactory practical relationships were developed for varying population densities. This factor appears to be much more important than such factors as watershed shape, channel slope, or roughness.

The investigation of the effect of population density was carried out by arranging the basins in the three groups shown in Table 4. The first group "High Population Density" consists of 15 basins having population densities greater than 5,590 persons/sq mi. The average value of P_d for this group of 13,300 persons/sq mi. The second group in Table 4 "Low Population Density" consists of 23 basins having population densities less than 1,200 persons/sq mi, the average for this group being 539 persons/sq mi. Finally Table 4 shows 15 watersheds under the heading "Intermediate Population Density" for which values of P_d were in the range 1,400-4,700 and the average P_d was 2,689 persons/sq mi.

The unit hydrograph peaks are shown plotted against P_d in Figure 12. The symbols used in Figures 12-20 are explained in Table 5. Best fit equations based on the use of a least squares analysis were derived for the three groups of points representing three degrees of urbanization in Figure 12. These are Eqs. (9), (15), and (13) in Table 6 and the straight lines represented by these equations are shown in Figure 12. Table 6 also shows the number of points used to derive each equation, the average P_d for each graph and the linear correlation coefficient (r). All values of r are well above the value needed to indicate a one percent chance that the linear relationship is accidental. Also shown in Figure 12 is a dashed line which represents Eq. (11). In the derivation of Eq. (11) two points representing basins 25 and 28, both from the Huntington Bayou area of Houston, were omitted. These points fell well below the other high P_d points as can be seen in Figure 12. It might therefore be inferred that

Table 5. LEGEND FOR FIGURES 12-20

Symbol		Figures
△	P_d* ≤ 5590, P_d Av. = 13300 All basins	12, 13, 15, 16, 18, 19
□	$P_d \leq 1200$, P_d Av. = 539 All basins	12, 15, 18
×	$1400 \geq P_d \leq 4700$, P_d Av. = 2763 or 2689 All basins	12, 15, 16, 18, 19
○	$P_d \leq 1200$, P_d Av. = 610 Michigan basins	13, 16, 19
◨	$P_d \leq 1200$, P_d Av. = 488 All basins except Michigan	13, 16, 19
○	$1400 \leq P_d \leq 2700$, P_d Av. = 2038 Michigan basins	13
⧗	$1400 \geq P_d \leq 4700$, P_d Av. = 2926 All basins except Michigan	13
◇	Michigan basins	14, 17, 20
▲	All basins except Michigan	14, 17, 20
0	Values obtained from Figures 13, 16 and 19 at A = 10 sq mi for all drainage basins.	14, 17, 20
θ	Values obtained from Figures 13, 16 and 19 at A = 10 sq mi for Michigan basins only.	14, 17, 20

*P_d = Population density in persons/sq. mi.

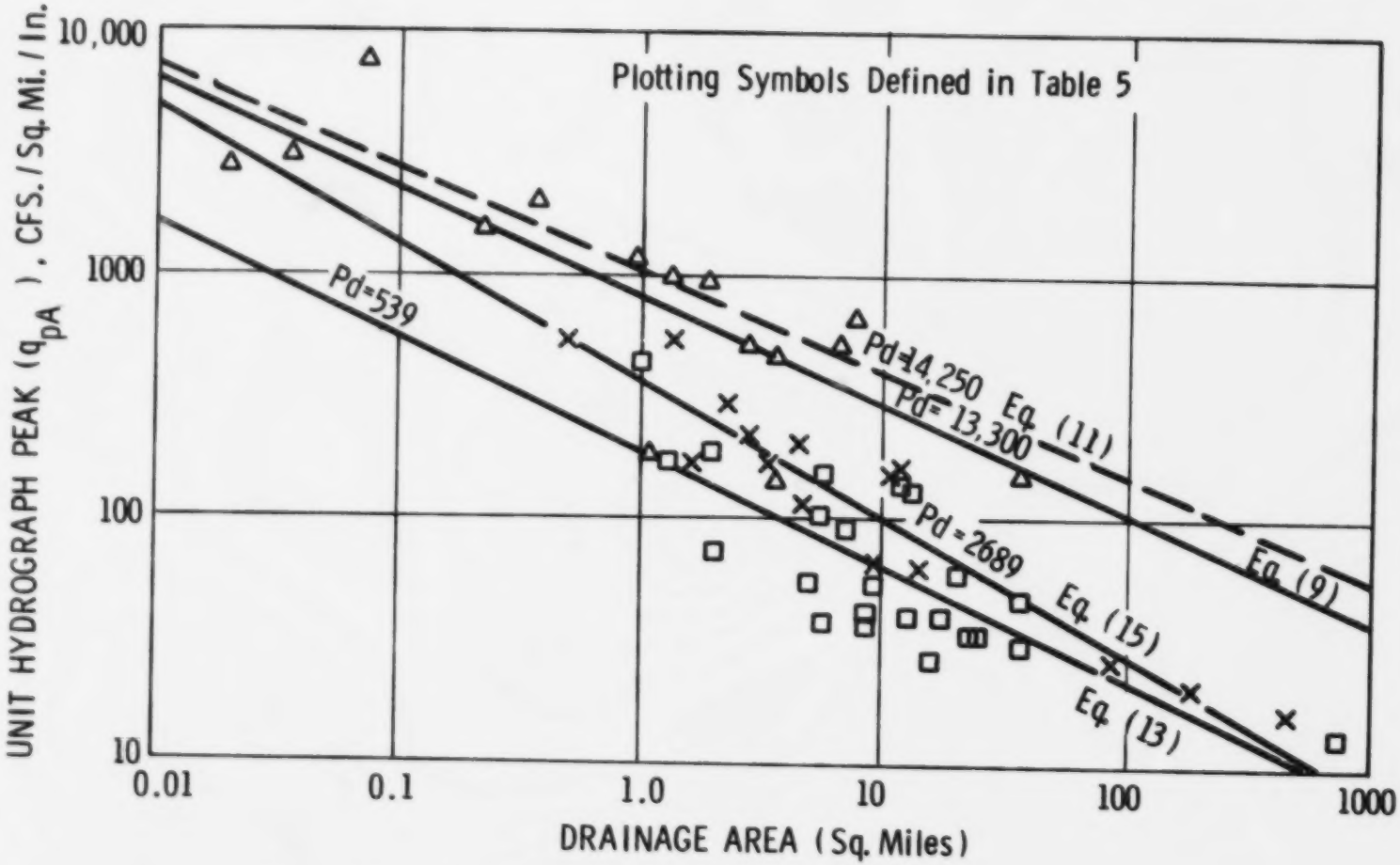

Figure 12. Unit hydrograph peaks vs. area (original data).

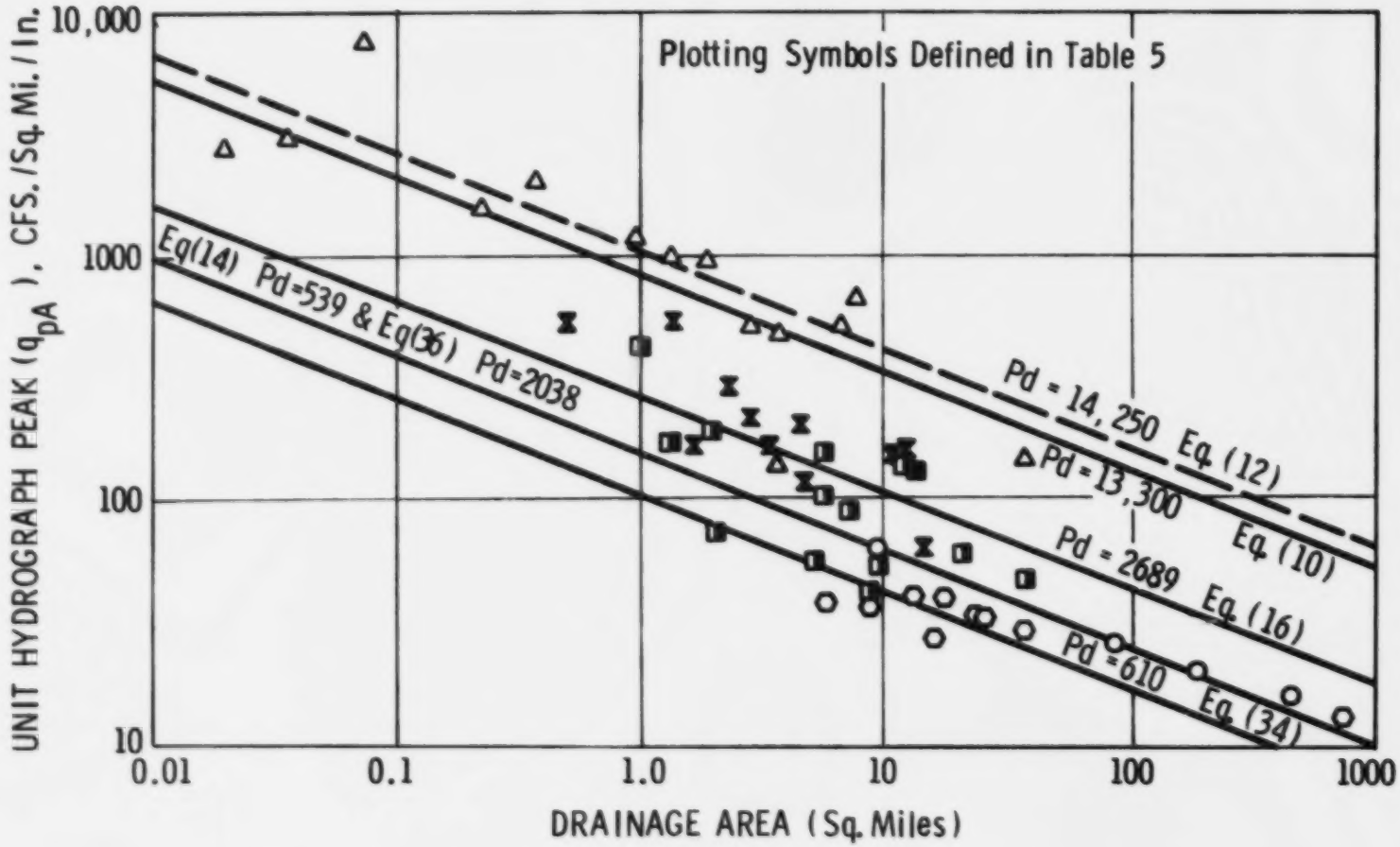

Figure 13. Unit hydrograph peaks vs. area with uniform slopes.

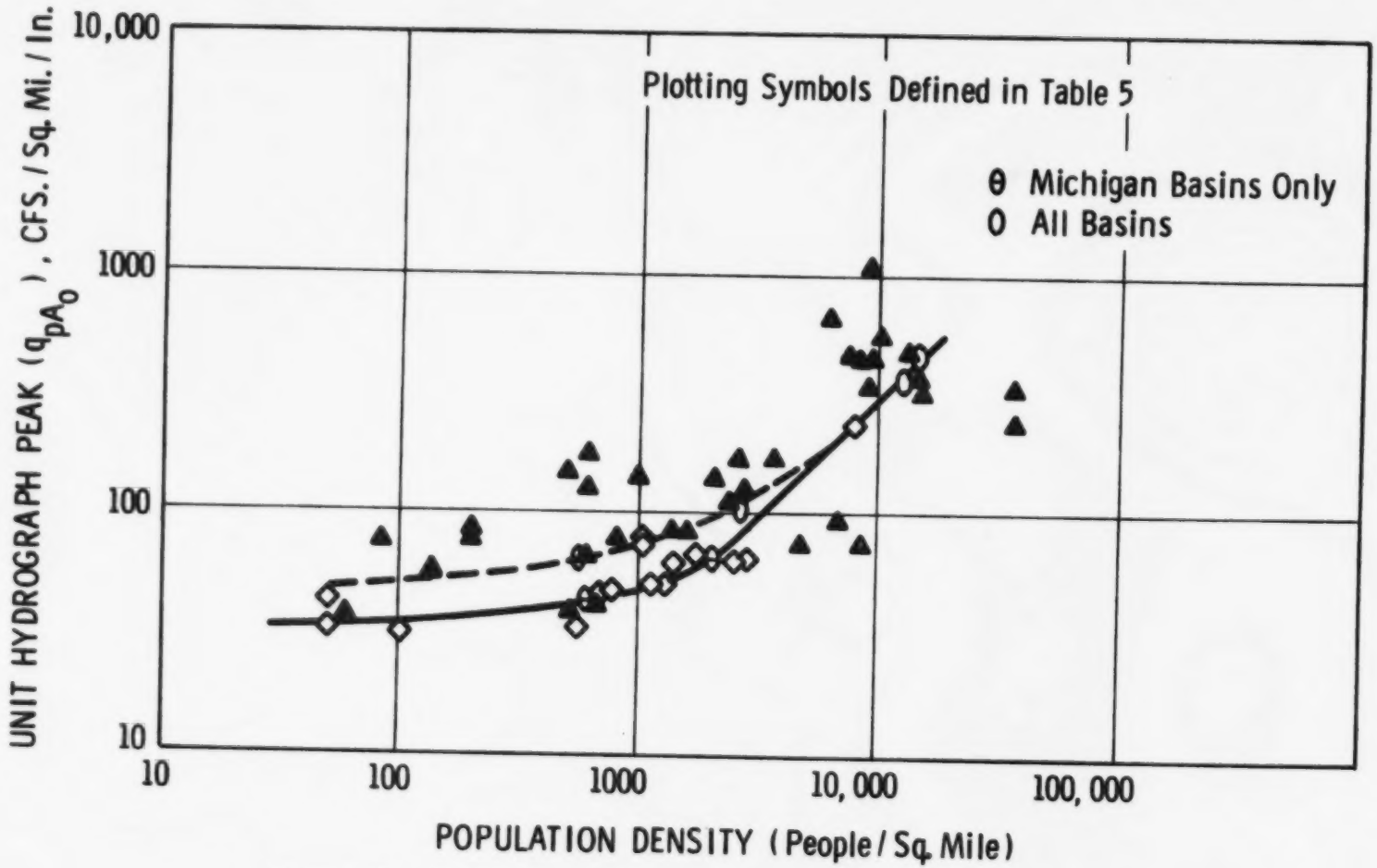

Figure 14. Unit hydrograph peaks vs. population density.

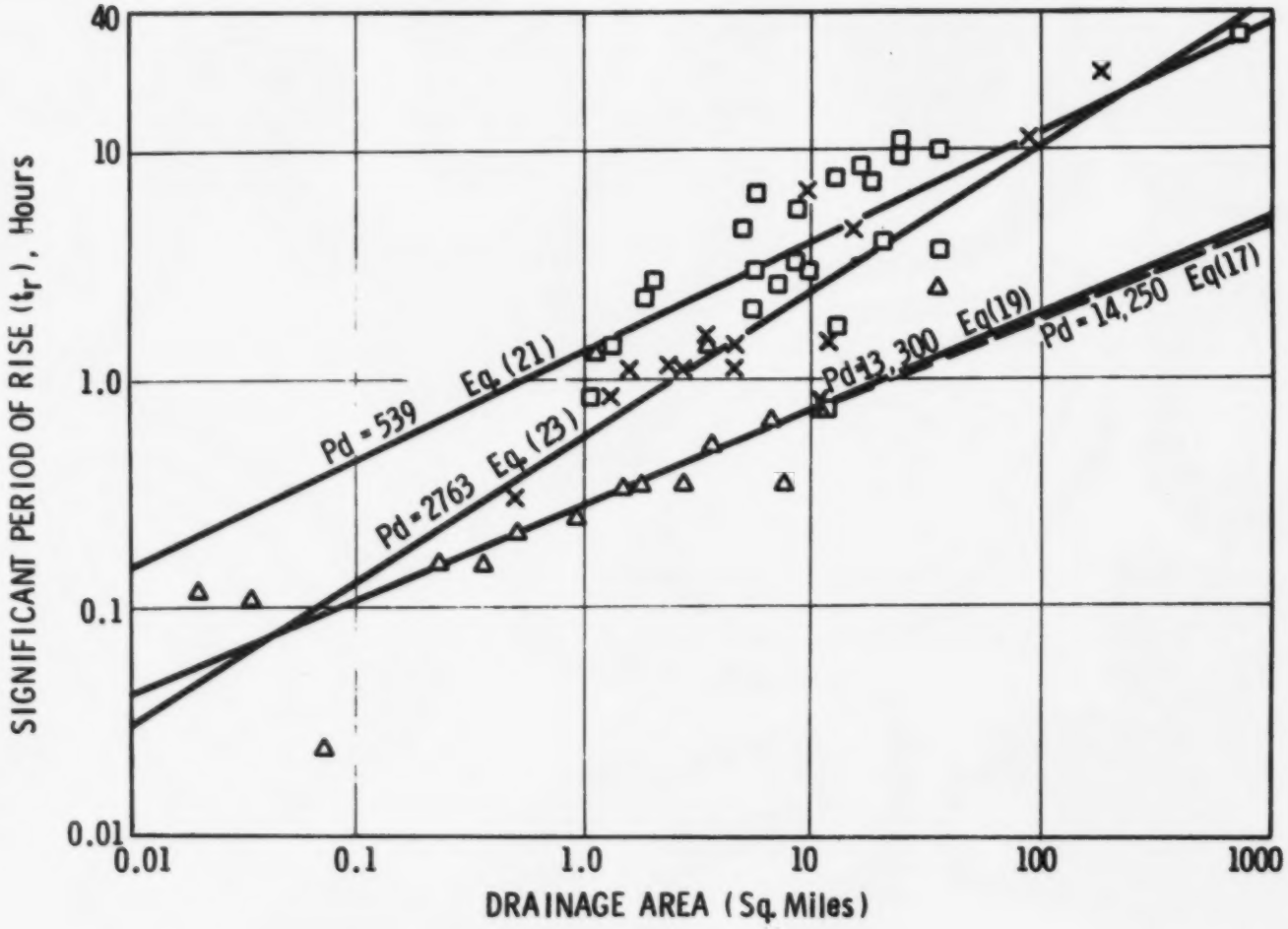

Figure 15. Significant period of rise vs. area.

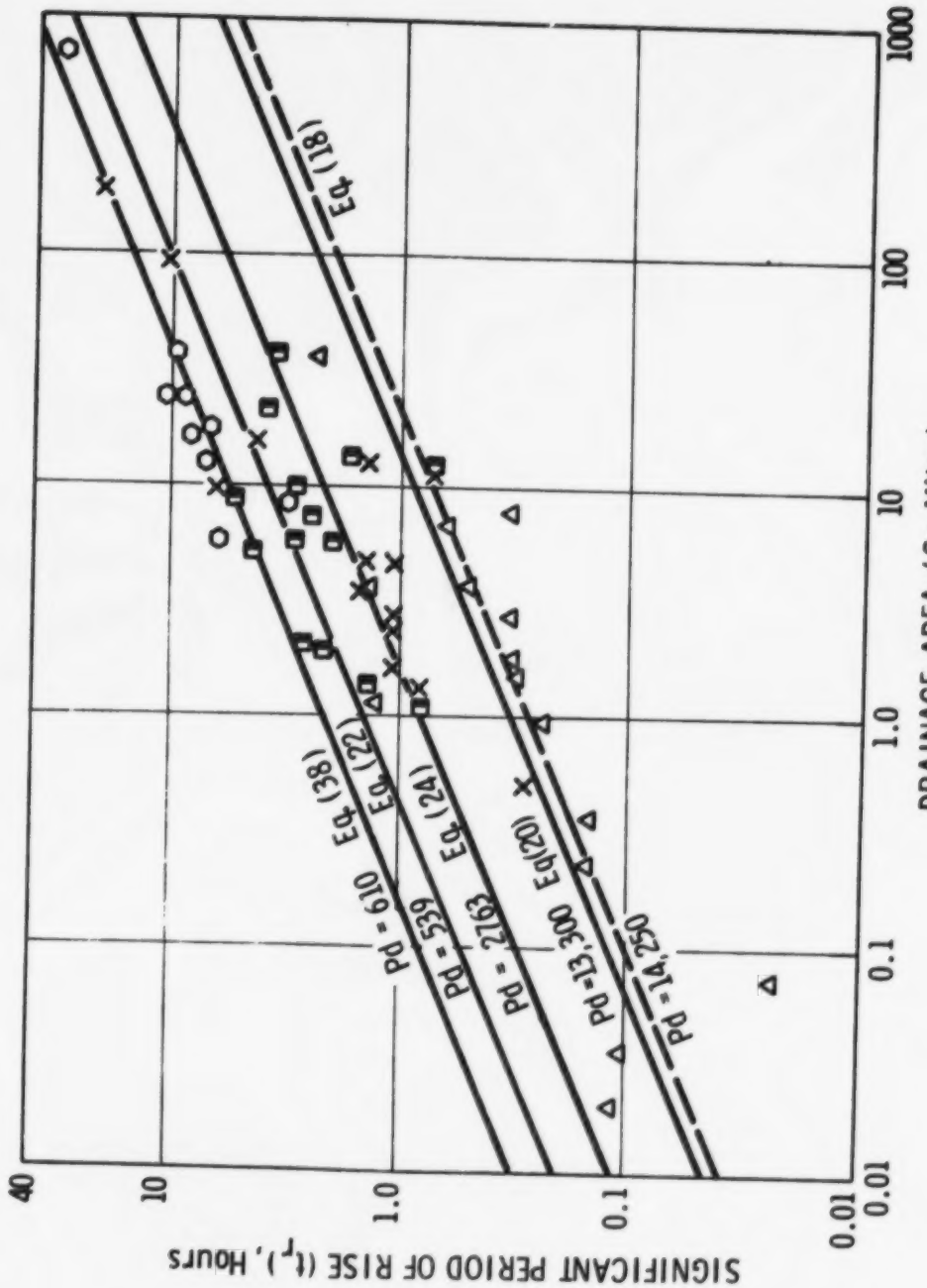

Figure 16. Significant period of rise vs. area with uniform density.

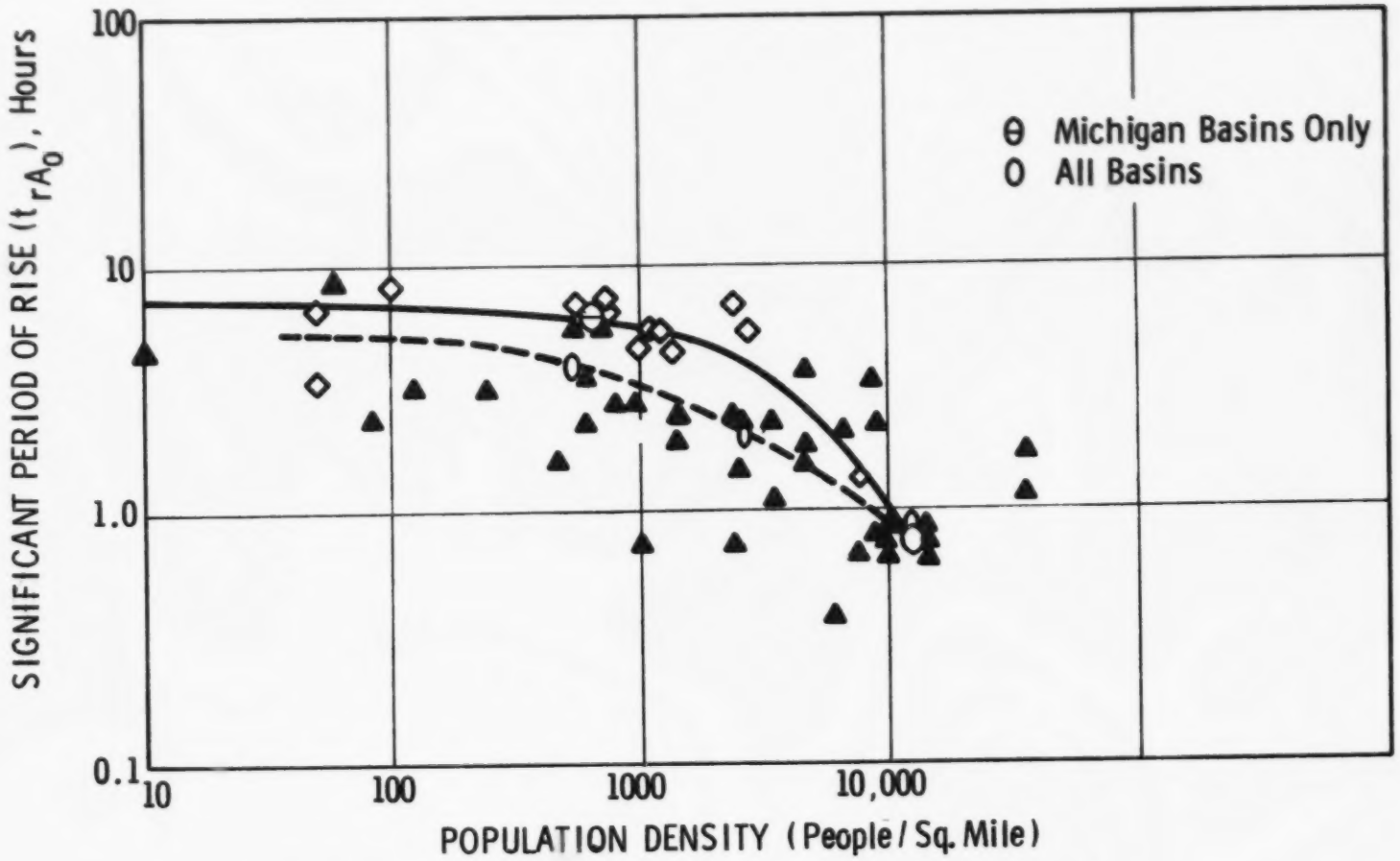

Figure 17. Significant period of rise vs. population density.

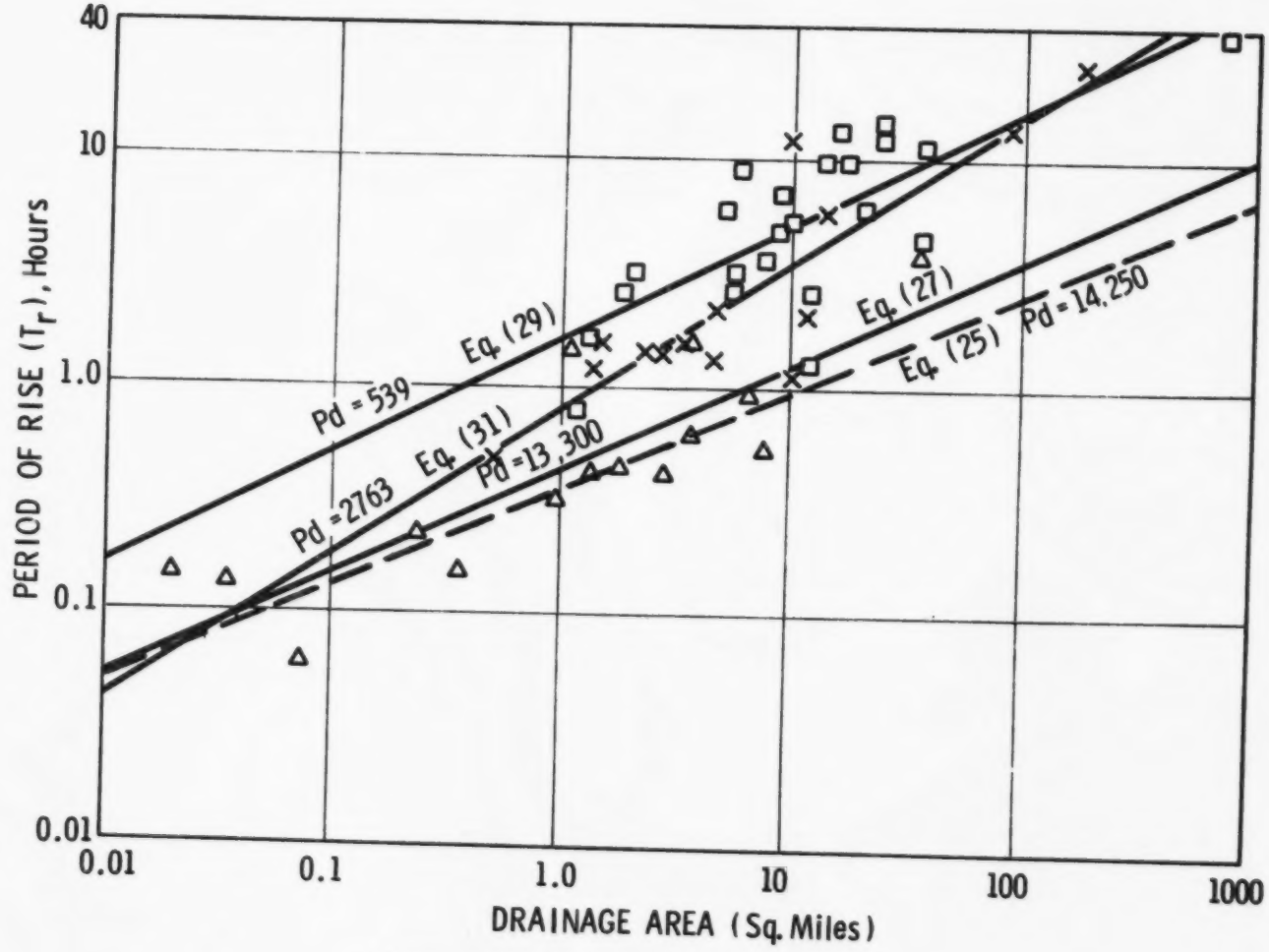

Figure 18. Period of rise vs. area.

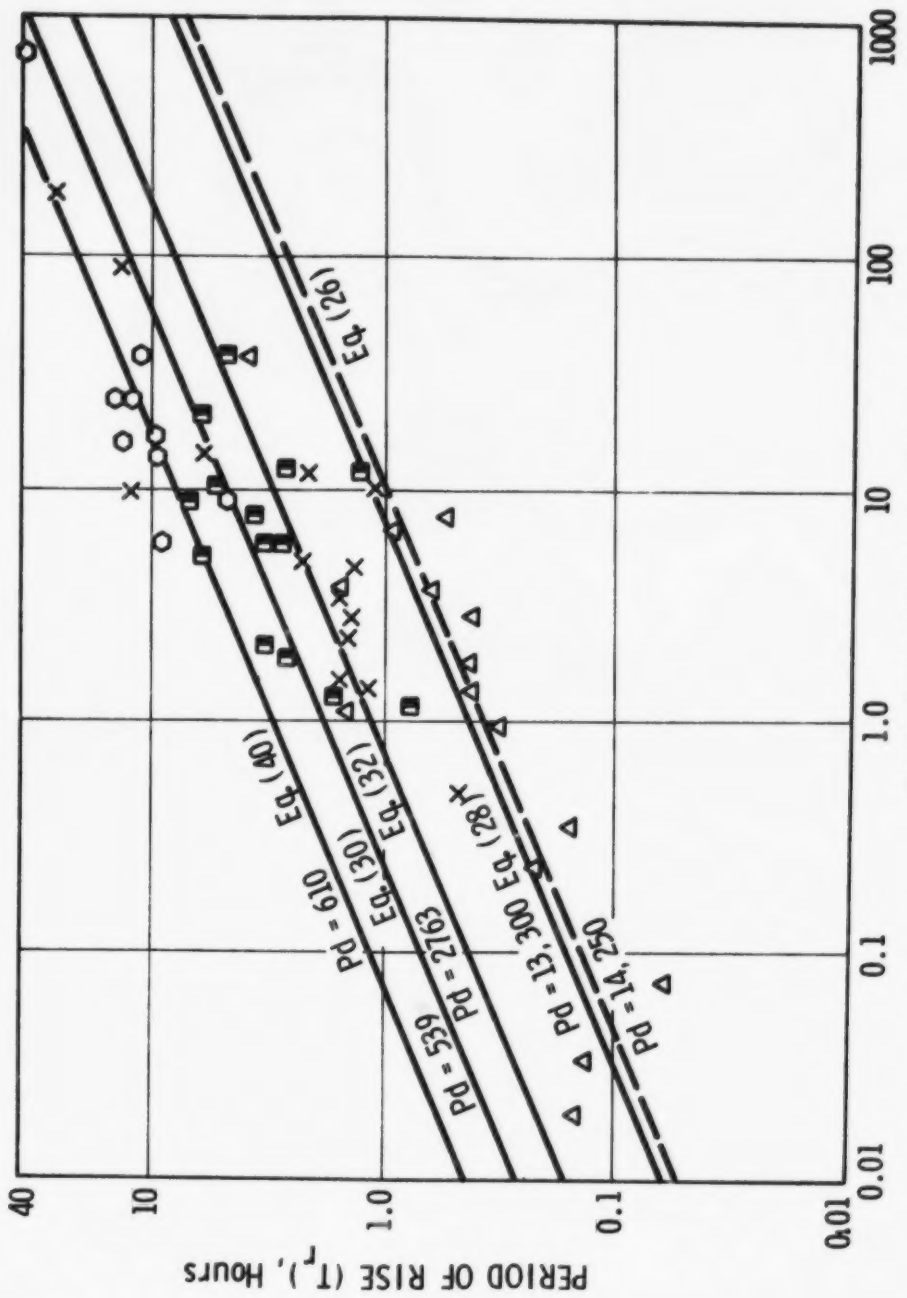

Figure 19. Period of rise vs. area with uniform slope.

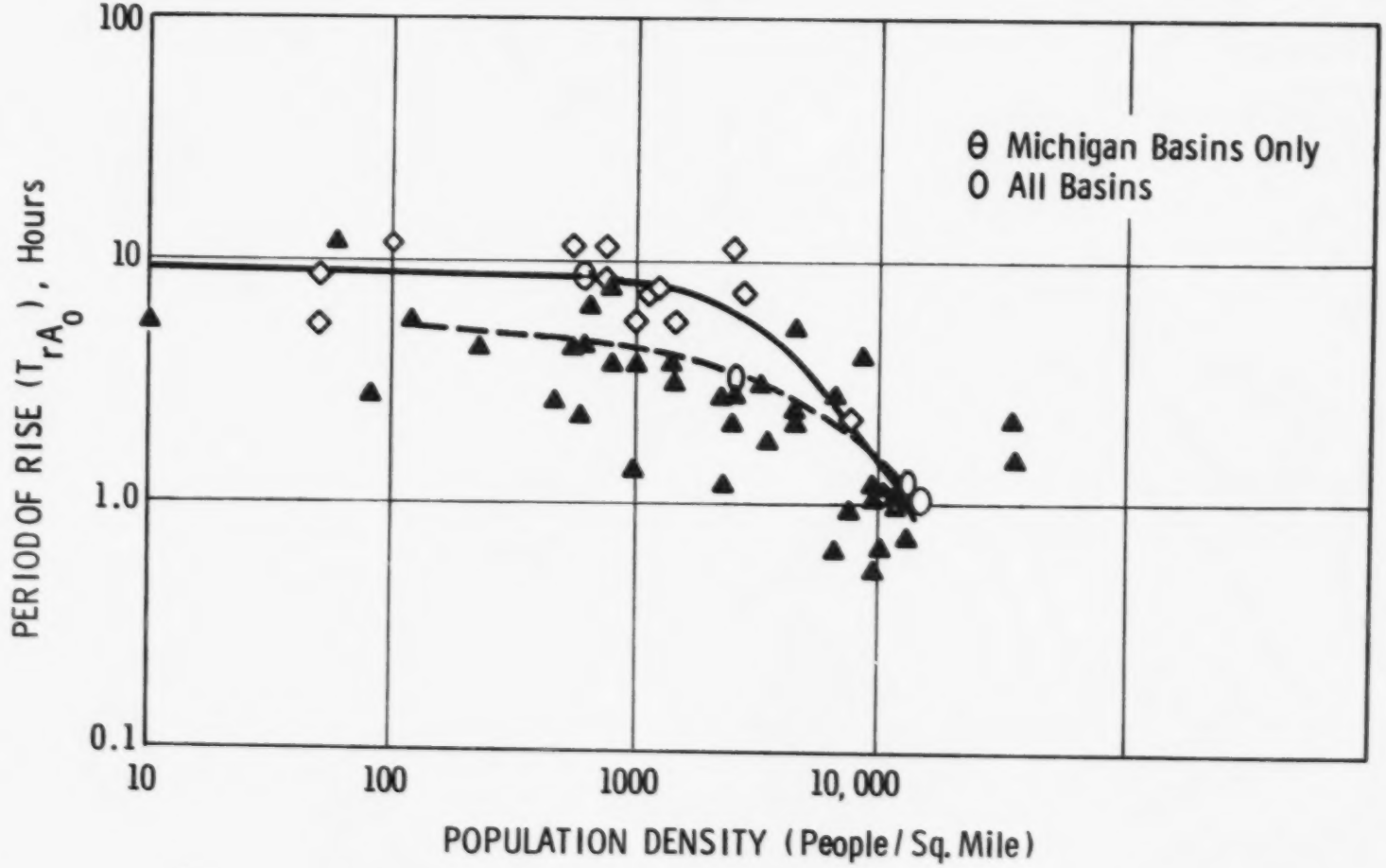

Figure 20. Period of rise vs. population density.

Table 6. EQUATIONS AND STATISTICAL PARAMETERS FOR LINES ON FIGURES 12, 13, 15, 16, 18, AND 19

N = Number of drainage basins
P_d = Population density in persons per square mile
r = Linear correlation coefficient

(1)	(2)	(3)	(4)	(5)
Eq. No.	Equation	N	Av. P_d	r
9	$q_{pA} = 834A^{-.448}$	15	13,300	-0.81
10	$q_{pA} = 835A^{-.400}$	15	13,300	
11	$q_{pA} = 1032A^{-.416}$	13	14,250	-0.92
12	$q_{pA} = 1034A^{-.400}$	13	14,250	
13	$q_{pA} = 184A^{-.458}$	23	539	-0.77
14	$q_{pA} = 161A^{-.400}$	23	539	
15	$q_{pA} = 375A^{-.558}$	15	2,689	-0.95
16	$q_{pA} = 269A^{-.400}$	15	2,689	
17	$t_r = .274A^{.422}$	13	14,250	0.87
18	$t_r = .274A^{.437}$	13	14,250	
19	$t_r = .325A^{.445}$	15	13,300	0.81
20	$t_r = .325A^{.437}$	15	13,300	
21	$t_r = 1.292A^{.486}$	23	539	0.75
22	$t_r = 1.447A^{.437}$	23	539	
23	$t_r = .572A^{.655}$	14	2,763	0.90
24	$t_r = .849A^{.437}$	14	2,763	
25	$T_r = .383A^{.425}$	13	14,250	0.91
26	$T_r = .384A^{.437}$	13	14,250	
27	$T_r = .449A^{.446}$	15	13,300	0.85
28	$T_r = .448A^{.437}$	15	13,300	
29	$T_r = 1.688A^{.504}$	23	539	0.78
30	$T_r = 1.968A^{.437}$	23	539	

Table 6 (concluded). EQUATIONS AND STATISTICAL PARAMETERS FOR LINES ON FIGURES, 12, 13, 15, 16, 18, AND 19

(1)	(2)	(3)	(4)	(5)
31	$T_r = .835A^{.635}$	14	2,763	0.88
32	$T_r = 1.196A^{.437}$	14	2,763	
	Michigan Basins Only			
33	$q_{pA} = 65.0A^{-.23}$	9	610	0.95
34	$q_{pA} = 112A^{-.400}$	9	610	
35	$q_{pA} = 159A^{-.395}$	4	2,038	0.99
36	$q_{pA} = 162A^{-.400}$	4	2,038	
37	$t_r = 3.78A^{.26}$	9	610	0.90
38	$t_r = 2.18A^{.437}$	9	610	
39	$T_r = 4.18A^{.34}$	9	610	0.88
40	$T_r = 3.06A^{.437}$	9	610	

some unusual conditions exist on these two basins which can only be determined from more detailed investigation. If these two points are omitted the average population density of this group of points becomes 14,250 persons/sq mi.

The lowest group of points in Figure 12 is for drainage basins having population densities less than 1,200 persons/sq mi and with an average density of 539 persons/sq mi. These points are plotted with a distinguishing symbol which may be identified in Table 5.

It is significant to note that the slopes of these lines as determined by a least squares analysis, are -0.448 and -.416 for the upper two lines which represent highly populated basins and -0.458 for the lowest line which was derived for low values of P_d. A similar set of unit hydrographs peaks derived from the mathematical model (discussed in the next section) produced a slope of -0.4 when plotted in the same fashion.

The center group of points representing an average population density of 2,689 when fitted by least squares (Eq. (15)) produced a somewhat steeper line having a slope of -0.558. One explanation for this difference in slope is that the development of a drainage system is probably not always a gradual process related directly to gradual changes in population density but it may lag behind or jump ahead of population increases thus creating anomolous situations. Because of the fact that there is so much evidence that the slopes of these lines should be about -0.4, the least squares method was applied again to find the best fit with a slope of -0.4. Five curves for which this was done, are shown in Figure 13. Three of these represent the upper three groups of points from Figure 12, the fourth and fifth lines represent the low population basins (average population density is 610) and intermediate population basins (average population density is 2,038) in Southeastern Michigan. The line representing Eq. (14) for all of the low population basins coincides with the line representing Eq. (36) for the intermediate population basins in Southeastern Michigan. The equation numbers are shown in Figure 13 to enable the reader to locate the corresponding equations in Table 6. The average population densities are also shown on the graphs. The lines for Southeastern Michigan were included in order to provide for the most accurate application to that region. These lines fell somewhat below lines representing all of the low population basins. The difference between the more general lines and the one for Southeastern Michigan will be discussed in the next portion of the report.

Although interpolation between the lines showing unit hydrograph peaks for various population densities might be carried out on Figure 13, a new parameter q_{pA_o} which eliminates area as a variable was found more useful

for this purpose. This factor is defined by the following equation

$$q_{pA_o} = \left(\frac{A}{A_o}\right)^{.40} q_{pA} \qquad (41)$$

in which q_{pA} is the unit hydrograph peak for any area A in cfs/sq mi/in. and q_{pA_o} is the corresponding unit hydrograph peak for a selected base area A_o. The value q_{pA_o} is obtained for any basin from its value of q_{pA} by means of Eq. (41) or by following along a line such as those in Figure 13 to the base area A_o. In this case A_o was chosen as 10 sq mi but any other size of basin could be selected for this purpose. The resulting points may then be plotted against population density as shown in Figure 14. It will be seen that the trend is quite clear and that the basins from Southeastern Michigan (white diamonds) follow a slightly different trend than those from other areas (black triangles). Also shown in Figure 14 are values of P_d vs. q_{pA_o} read from the six straight lines in Figure 13, two of which are coincident. The symbol ⊖ is used for the four points derived from all 53 basins and the symbol ⊖ for the points from the two lines representing the 16 Southeastern Michigan basins.

The solid curve shown in Figure 14 is drawn to best represent Southeastern Michigan. A more general curve such as the dashed line represents all basins. The curve in Figure 14 was used to derive design curves for Southeastern Michigan.

The relation of the unit hydrograph time parameters to area and population density were analyzed and correlated in the same manner as the peak discharges. The values of t_r, the significant period of rise (see Figure 11), are plotted against area in Figure 15. The top line represents the "Low Population Density" basins and the lower two lines represent "High Population Density" basins. These lower two lines differ only in the omission of two data points from the dashed line as previously described. Equation numbers are shown to aid in identifying the corresponding equations and statistical parameters in Table 6.

The slopes of these lines are 0.422, 0.445, and 0.486, respectively, which are again similar to the slope derived from unit hydrographs developed by the model which was 0.437. Also, as in Figure 15 the intermediate population basins showed a different trend. Figure 16 shows the best fit lines converted to a common slope of 0.437 and Figure 17 gives the relation of t_{rA_o} with population density. The correlation coefficients and equations for the regressions are shown in Table 6. Similar correlations for T_r are presented in Figures 18, 19, and 20. The equations and statistical parameters are shown in Table 6. The

corresponding derivations for W_0, W_{25}, W_{50}, and W_{75} are not presented in this report but the final results are given as described in the following paragraph.

In order to provide a more convenient way of deriving the form of the unit hydrograph for any area and population density curves such as those shown in Figures 14, 17, and 20 were used to provide values of q_{pA}, t_r, T_r, W_{75}, W_{50}, W_{25}, and W_0 for an area of 10 sq mi for various population densities. Lines with the proper slope were then constructed as shown in Figures 21-27 for round numbered values of population density. These curves make interpolation much easier than in the original graphs. Results from streams in Southeastern Michigan were given the most weight in deriving these curves. Therefore the curves apply more accurately there than elsewhere. The use of these curves will be demonstrated in the section titled Predicting Flood Magnitudes and Frequencies.

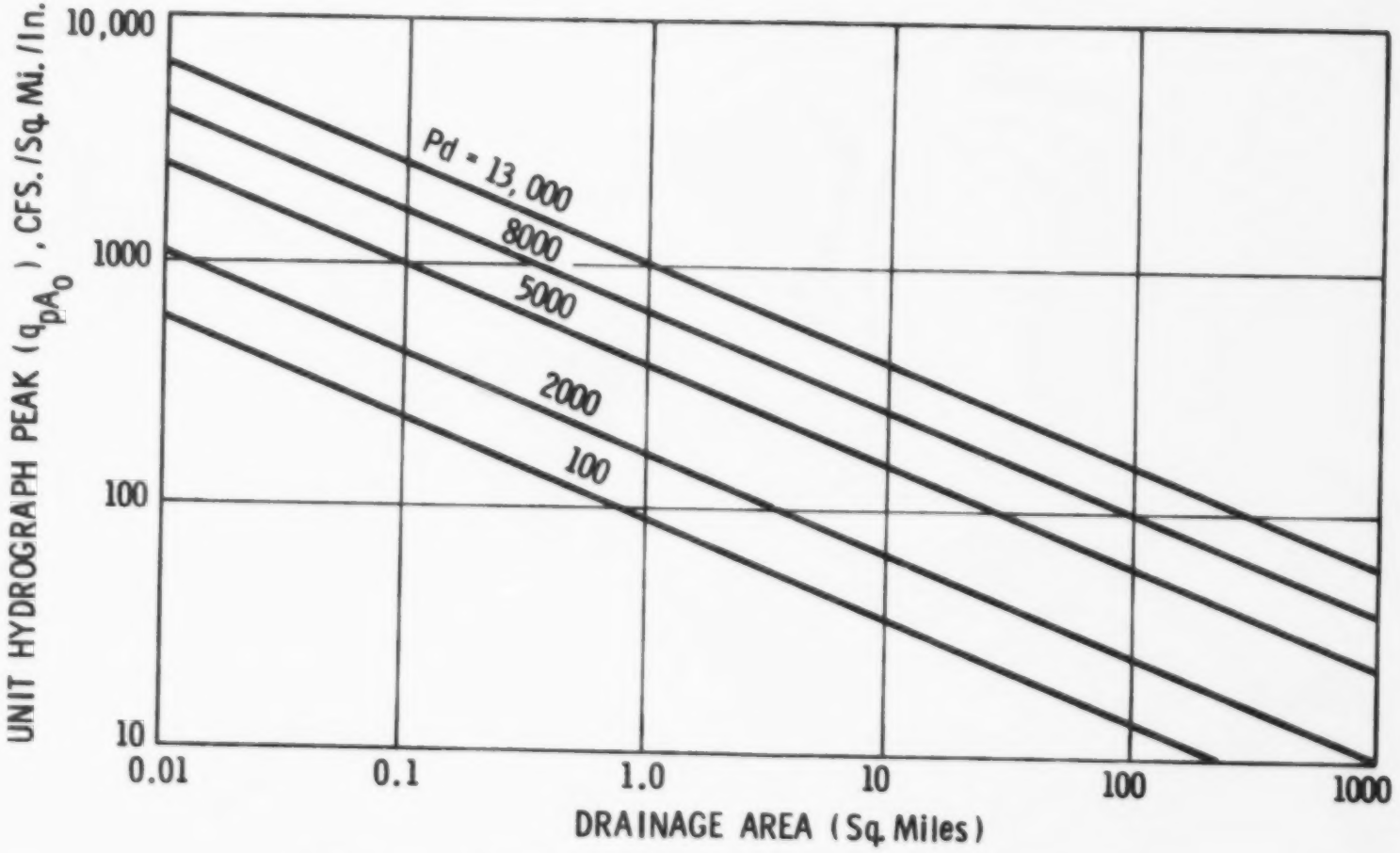

Figure 21. Unit hydrograph peak vs. area-design curves.

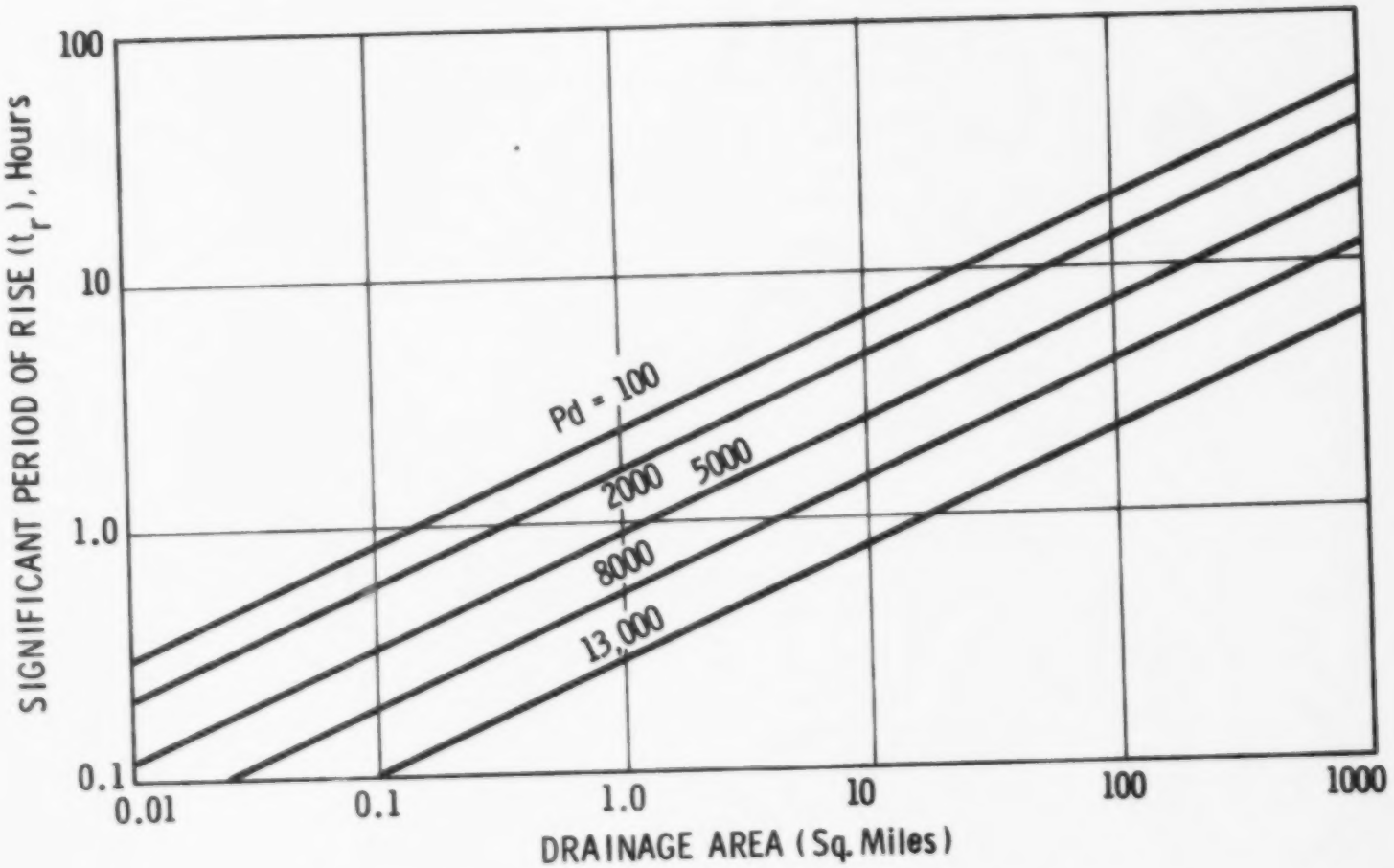

Figure 22. Significant period of rise vs. area-design curves.

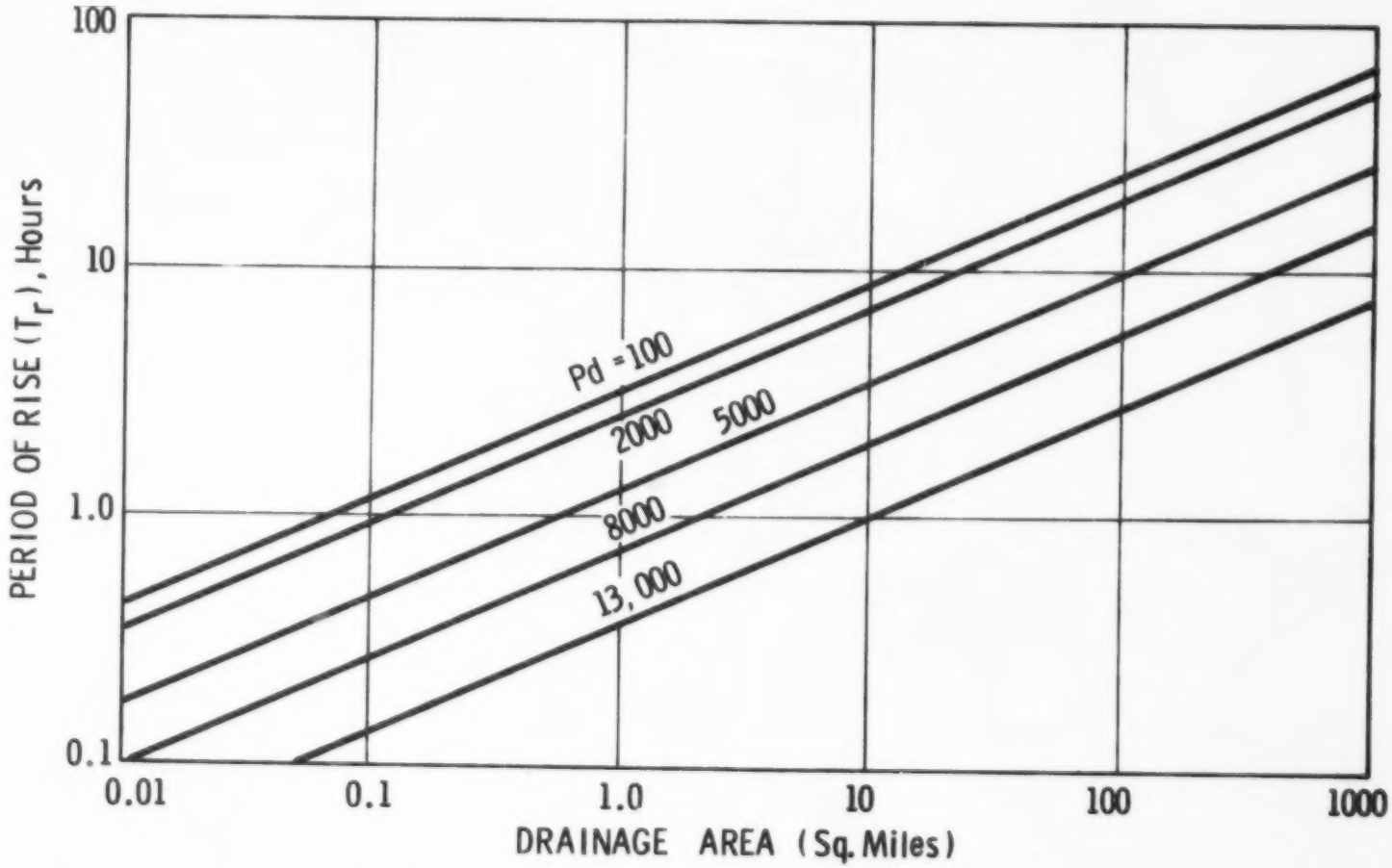

Figure 23. Period of rise vs. area-design curves.

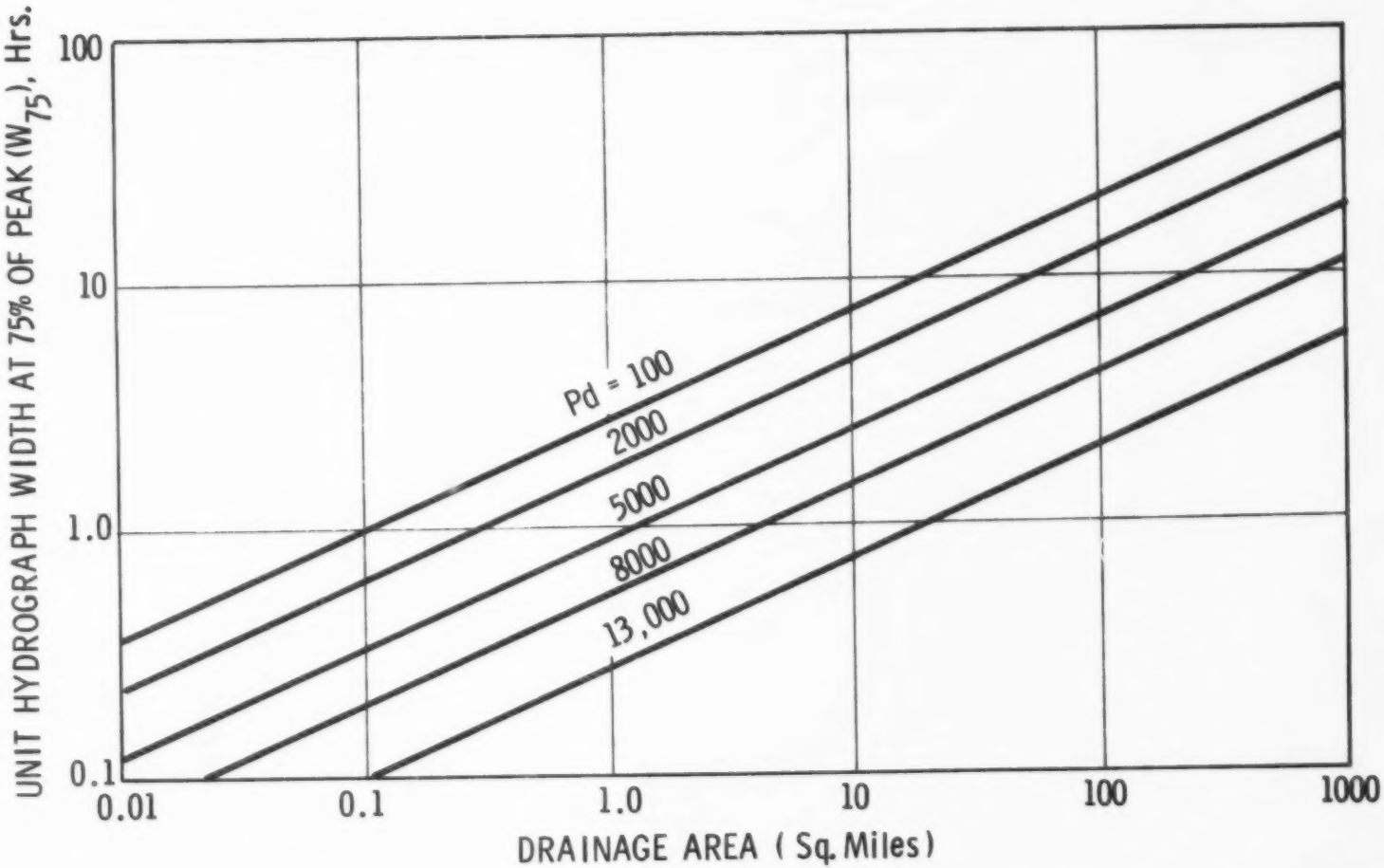

Figure 24. Width at 75 percent of peak vs. area-design curves.

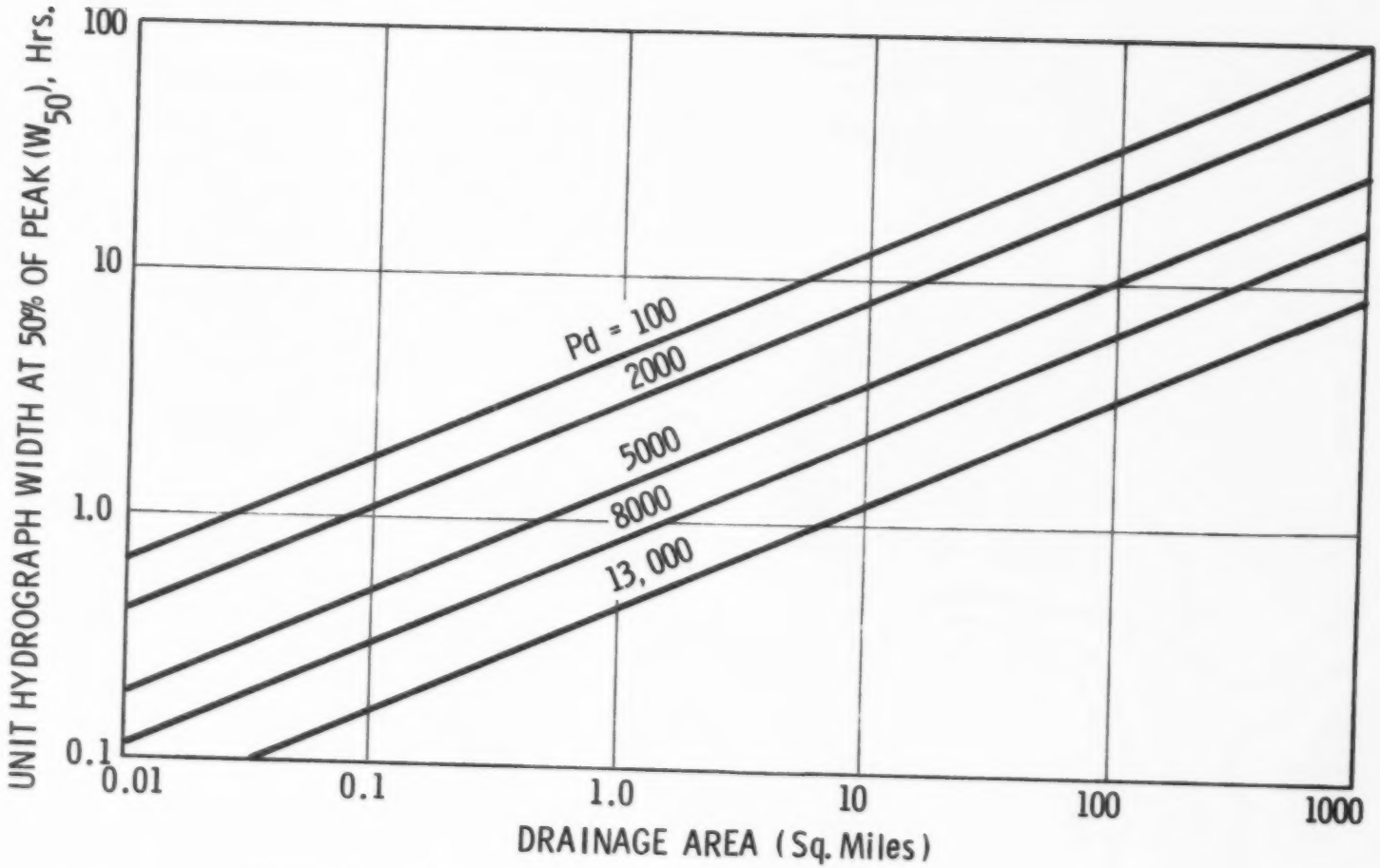

Figure 25. Width at 50 percent of peak vs. area-design curves.

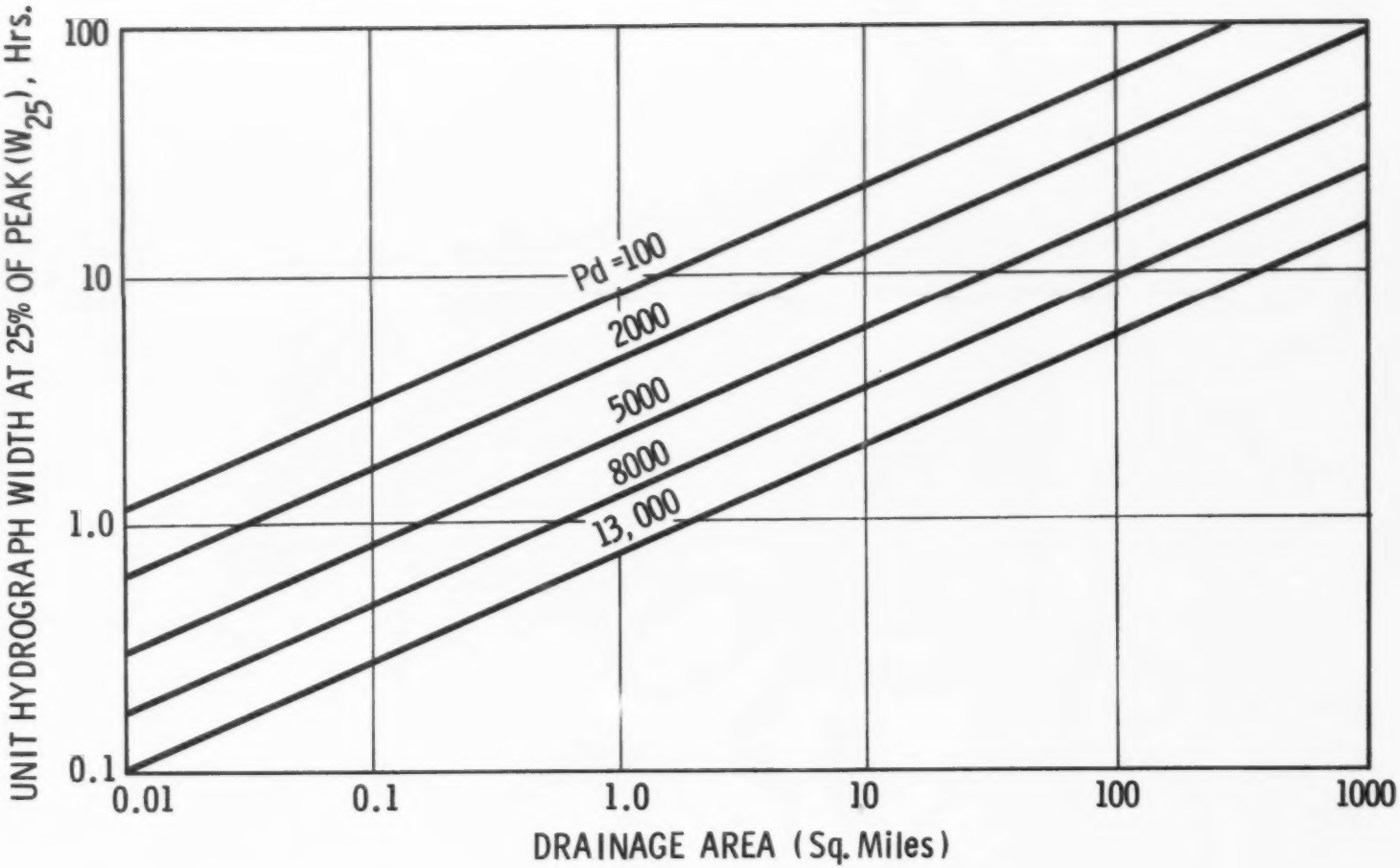

Figure 26. Width at 25 percent of peak vs. area-design curves.

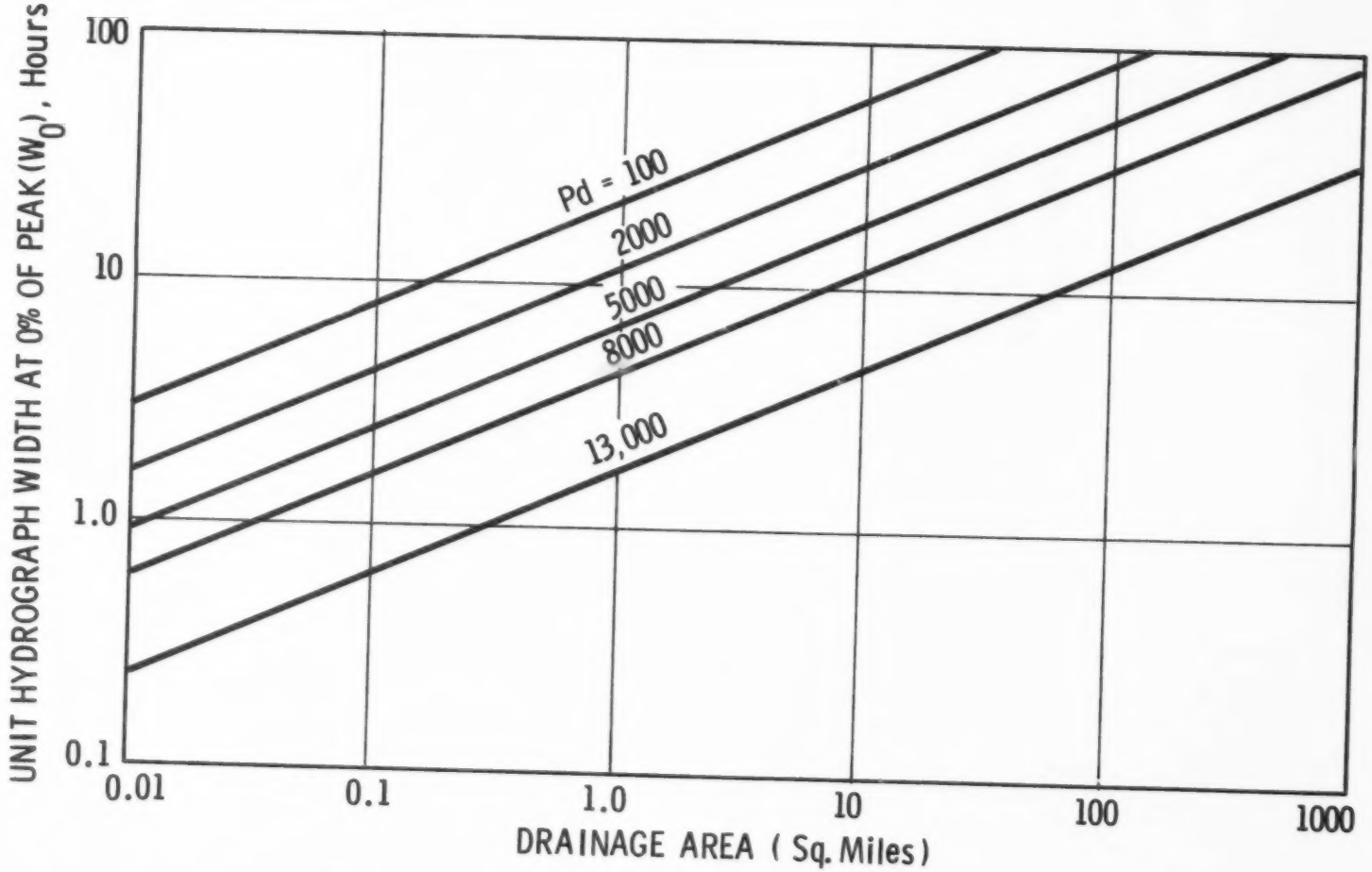

Figure 27. Width of base vs. area-design curves.

SECTION IX

MATHEMATICAL MODEL

It became apparent early in the work that an analytical approach to the surface runoff problem would be an exceedingly valuable goal if it could be developed well enough to simulate natural watershed responses from precipitation inputs. Consequently, a mathematical model was constructed which fulfills these requirements to a certain point (the next step is to incorporate more complex drainage networks into the model). The model simulates the runoff process in a conceptual watershed consisting of a plane rectangular basin with a stream flowing in the middle. The model performs a two phase transformation on the rainfall excess input. For the first or land phase, the kinematic wave theory is used to transform the precipitation excess into an overland flow hydrograph. For the second or channel phase, the complete equations of motion are used to transform the overland flow hydrograph, which is now taken as the lateral inflow to the main channel, into the output from the watershed. These equations are formulated in a direct implicit method using a fixed rectangular grid, and the resulting system of simultaneous nonlinear finite difference equations is solved using the generalized Newton-Raphson procedure on an IBM 360-67 digital computer.[17] The model functions well even in the difficult conditions of very low initial flows (less than 1 percent of peak flow). The results are independent of any reasonable downstream boundary conditions imposed.

The model was investigated first to determine the effect of the duration of rainfall excess (t_o) on the peak discharge (Q_p) and on such time parameters as T_r, t_p, W_{50}, W_{75} (Figure 11) which define the form of the unit hydrograph. This was done by running the model for various values of t_o with the total input (D) held constant. These runs indicated that the form of the unit hydrograph varies little when $t_o < t_p/2$ and for $t_o < t_p$ the variation is small for practical purposes. The meaning of t_p is shown in Figure 11. These results agree with those obtained from natural watersheds where t_r was used instead of t_p. The values of t_r and t_p were found to be nearly the same in natural watersheds and t_r is more useful and easier to obtain.

The second set of runs was made holding to t_o constant at a value less than t_p and varying the input D. It was found that the relation between peak discharge and input was expressed by the following equation

$$Q_p = CD^G \qquad (42)$$

If G is unity the relation between peak and volume is linear. For trapezoidal channels the value of G was found to be about 1.4 whereas for parabolic channels with the sides concave downward G was about 1.2. It is believed that this latter shape tends to simulate natural rivers and flood plains much more clearly than does a trapezoidal channel. If the roughness is allowed to increase with increasing depth natural conditions are simulated even more closely and the value of G in the model was reduced to 1.05. These findings helped explain why many natural basins have a linear relation between peak and total input. The effects of roughness, slope, and channel length on the value of G were found to be much less important than changing the shape of the channel.

In addition to providing a better understanding of the storm runoff process as described above, the model provides qualitative information on the effect of certain parameters which are likely to have only a limited range in gaged natural watersheds. For example, under urban conditions some watersheds are changed artificially so that they are much more slender than typical natural basins. The model enables one to determine how such parameters as unit hydrograph peak vary as the shape of the model watershed is changed from nearly square to very slender. Such results can be used to indicate what trends can be expected for the same parameters in real watersheds. Specific references to comparisons of specific phases of the runoff process in the model and in natural watersheds are given at appropriate places in this report.

SECTION X

FREQUENCY STUDIES

The determination of the winter rainfall frequency is complicated in Michigan by the fact that recorded precipitation may be snowfall rather than rainfall and should therefore be excluded. Furthermore, rapidly melting snow whether or not accompanied by rainfall produces precipitation excess and such events should be included in the frequency analysis. Fortunately, including snowfall tends to compensate for leaving out snowmelt in the frequency analysis of precipitation, however, the extent to which they do so needed to be determined. The frequency investigation was made by analyzing 535 station-years of records from 16 stations in Southeastern Michigan. The recorded daily precipitation and average temperature were determined from records of the U.S. Environmental Data Service. For each winter season at each weather station a continuous record was developed of the water equivalent of snow on the ground by adding snowfalls and deducting daily snowmelt. The recorded precipitation was considered to be snowfall when the average of the daily maximum and minimum temperature was 32° or lower. Snowmelt from rain was computed by means of Eq. (43)

$$M = \frac{P\,(T_a - 32)}{144} \qquad (43)$$

and snowmelt resulting from atmospheric heat was computed by the degree-day method using the following equation

$$M = 0.05\,(T_a - 34) \qquad (44)$$

In these equations M is the water derived from melt in inches per day, T_a is the average of the daily maximum and minimum temperature and P is the 24-hr rainfall. Examination of these two equations will show that melt due to rainfall tends to be very small compared with that

caused by atmospheric heat. Although Eq. (44) only indirectly includes the significant amount of heat transferred to the snow by condensation it has given satisfactory results in accounting for snowmelt in Michigan based on the analysis of several hundred hydrographs from many drainage basins.

The recorded daily rainfalls used in this analysis have been corrected to a 24-hr basis by adding half of the largest rain which occurred on an adjacent day. This procedure is based on the fact that the maximum 24 hr of rain could have included an amount recorded for an adjacent day varying from zero to the full recorded value. Shown in Figure 28 are winter frequencies for rainfall plus snowmelt, for rainfall plus snowfall (conventional recorded precipitation) and, for comparitive purposes, the values for rainfall alone are also shown. In the lower frequencies, up to about 30 years, the curve of rainfall plus snowmelt is about 2 percent above the curve for rainfall only. The fact that the correct curve (rainfall plus snowmelt) falls only 2 percent above the conventional precipitation curve is accounted for by the fact that including snowfall while excluding snowmelt nearly equals the effect of including snowmelt while excluding snowfall. This is fortunate because a great deal of time and expense is involved in computing snowmelt for a large number of years. It is, of course, not known, whether the error would be this small in other latitudes or at other geographical locations at the same latitude. A frequency study was also made for 1950 station-years of conventional rainfall to determine if 535 station-years was long enough to provide a good estimate of frequency. The 535 station-years used in the snowmelt studies are included in the longer period of records and all stations are in a meteorologically homogeneous area in Southeastern Michigan and Northwestern Ohio. The longer period of record included enough larger rains to raise the curve an average of 2 percent for recurrence intervals up to 30 years. The two curves are shown in Figure 29.

It can then be assumed that the best estimate of the frequency of winter rain plus snowmelt can be obtained by drawing a curve about 2 percent higher than the conventional curve for the 1950 station-years of record. This corrected curve is shown in Figure 30 along with the curve giving frequencies of summer rains as determined from the 1950 station-years of record. The winter curve of Figure 30 differs from the winter curve in Figure 29 in that after adding 2 percent for snowmelt the month of October has been included with the winter months and eliminated from the summer months. This was done because infiltration capacities (discussed previously) and time-intensity rainfall patterns (discussed in next section) in October were found to be more like the winter months than the summer months.

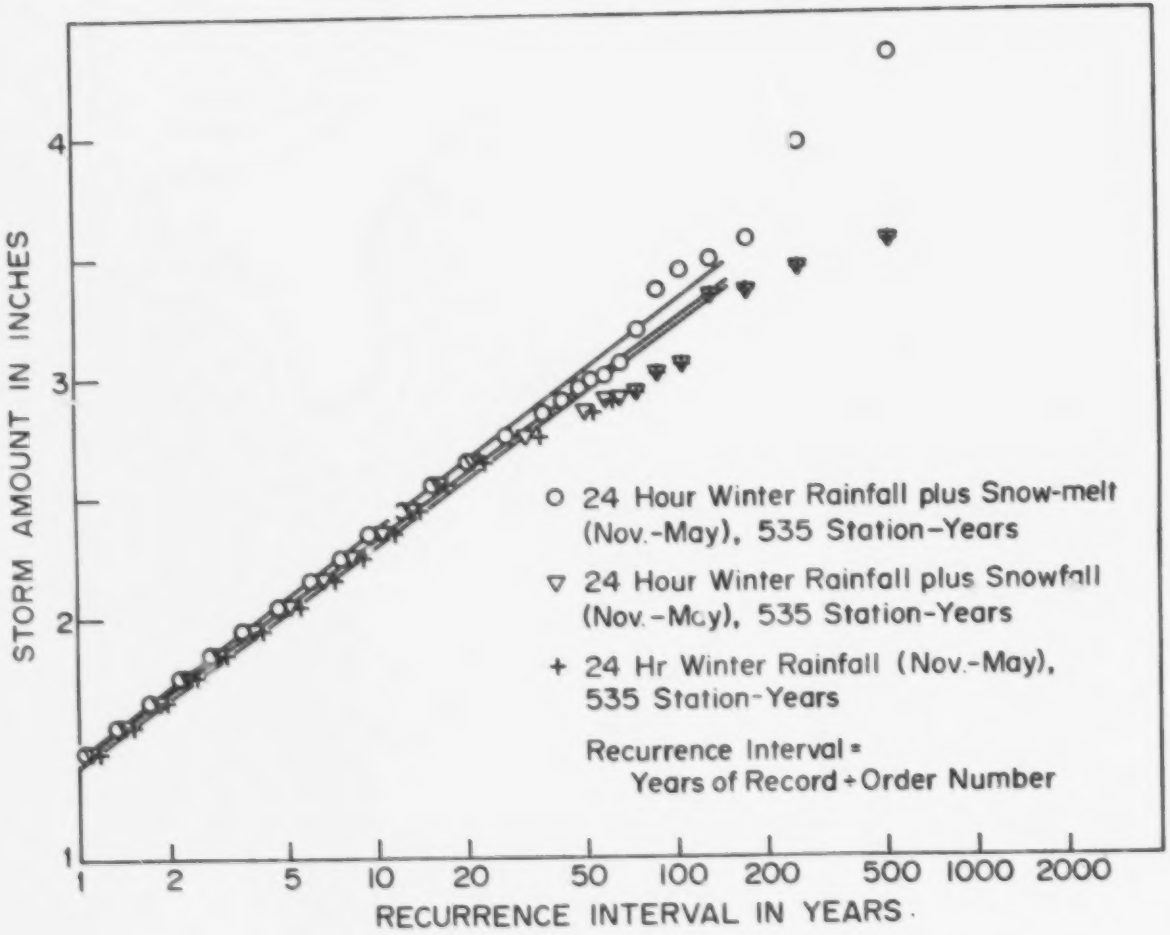

Figure 28. The effect of snowmelt on frequency.

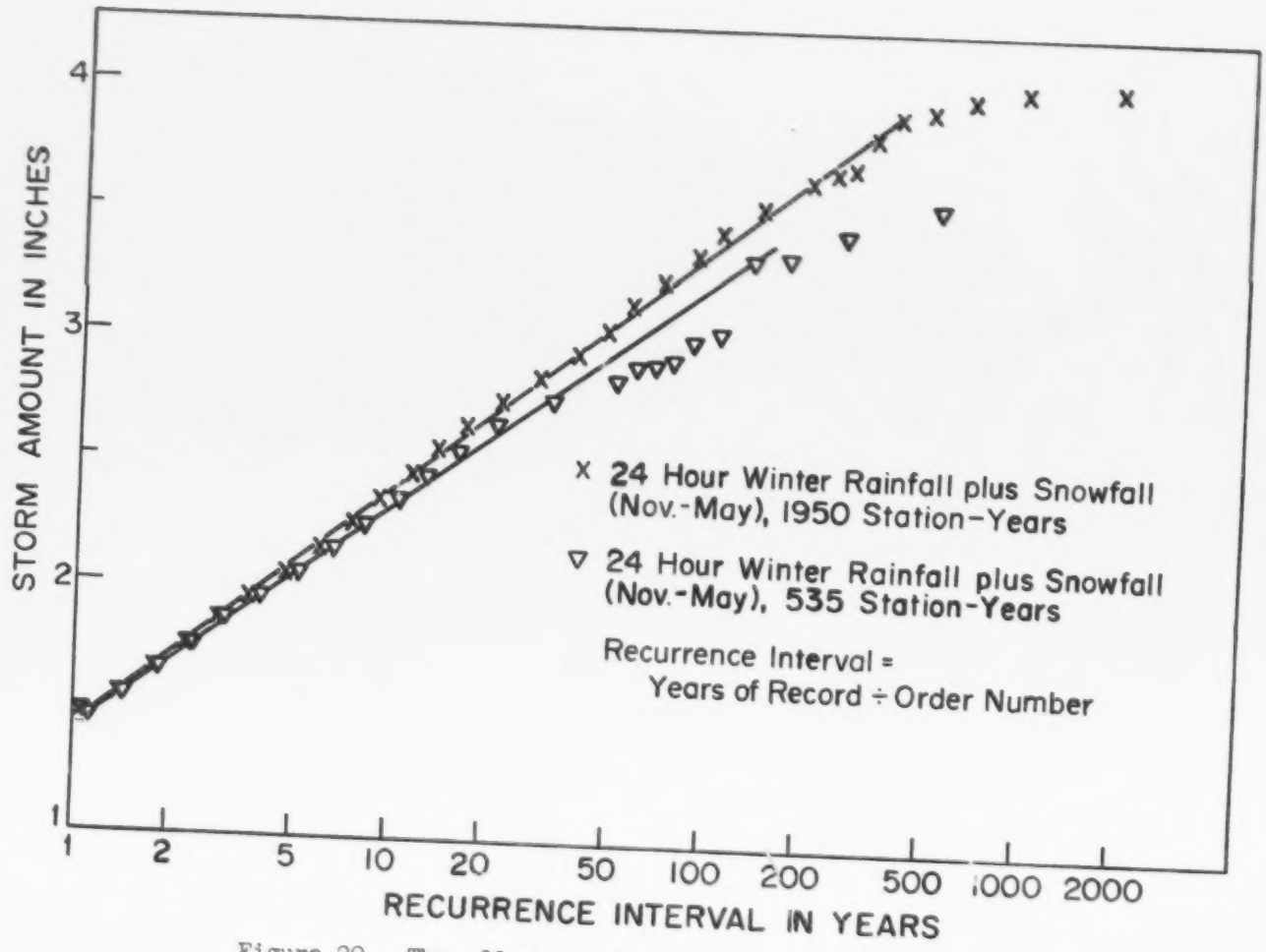

Figure 29. The effect of length of record on frequency.

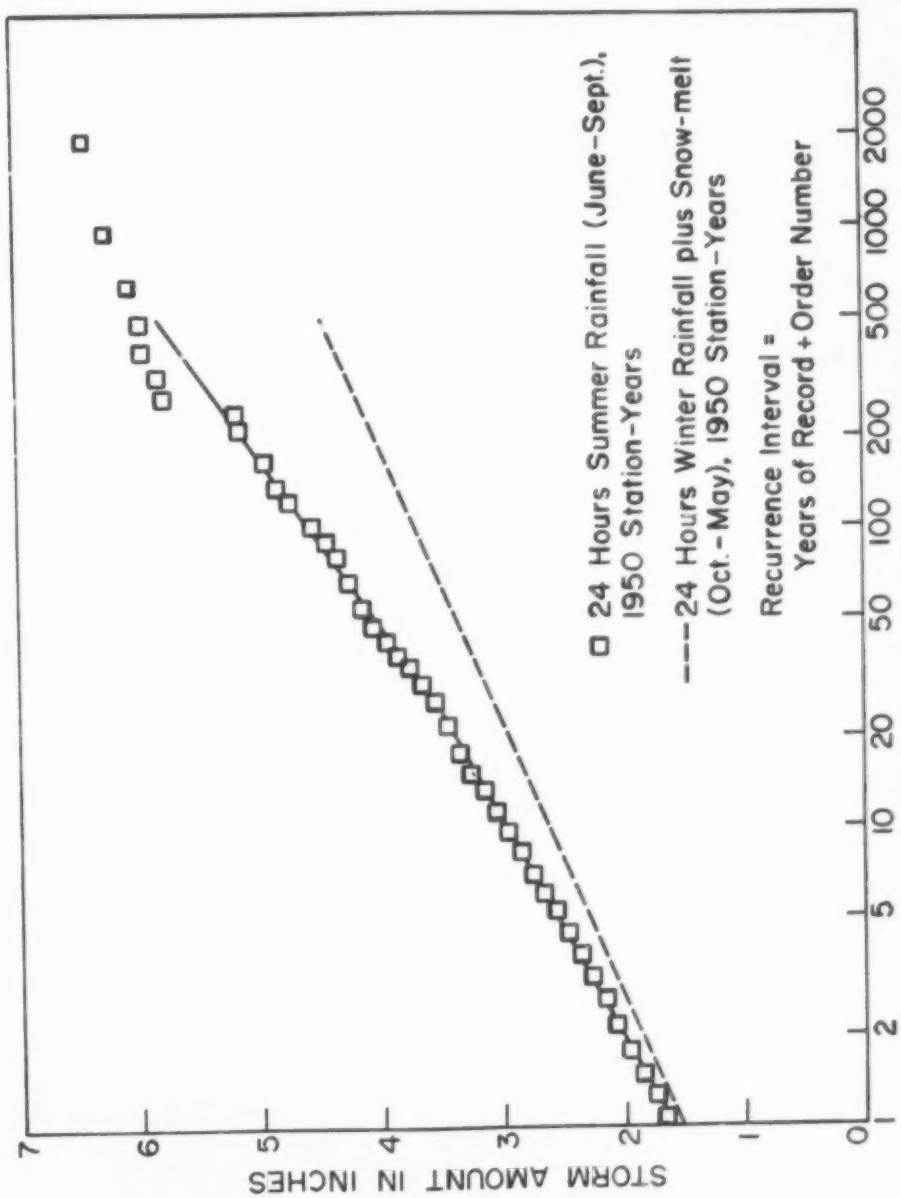

Figure 30. Final seasonal frequency curves.

SECTION XI

TIME-INTENSITY RAINFALL PATTERNS

The analysis of rainfall and runoff for natural drainage basins smaller then about 100 sq mi as well as for all sizes of urbanized basins requires the use of rain intensities for time intervals smaller than 24 hr. The unit hydrograph-infiltration capacity method of flood frequency prediction requires the use of time intervals as small as one hour on natural basins of about 0.2 sq mi, and for urbanized drainage basins of about 10 sq mi. When drainage basins are smaller than about 0.2 sq mi for rural areas or about 10 sq mi for densely populated areas the rainfall intensities must be broken down to smaller than hourly time intervals. Although frequency studies can be made for durations less than 24 hr there is much less information available for these shorter durations. Therefore, greater accuracy can usually be achieved by determining frequencies for 24-hr rains and then finding relationships between shorter duration rains and 24-hr rains. This was done in two ways.[38] One method was to find the values of maximum continuous precipitation of various durations. The other method was to determine the chronological time distributions of rain storms about the maximum hour of rain.

The maximum continuous accumulated rainfall was determined for durations from 1 to 24 hr for 80 summer rains and for 44 winter rains. The rains were selected from a rain gage network located in Southeastern Michigan maintained by the Detroit Metropolitan Area Planning Commission and the U.S. Environmental Data Service. Only rains having a 24-hr rainfall equal to or greater than 1.5 in. were used, and the same rain storm was not used twice even though it may have covered more than one of the rain gages. The period covered was the thirteen years from 1960 through 1972. The results expressed in percent of 24 hr rains along with the standard deviations for each duration are shown in Table 7. The rather large standard deviations indicate the considerable variations among individual values for each duration. The values of P versus t are plotted in Figure 31. Also shown in Figure 31 are values of P derived from U.S. Weather Bureau[39] frequency studies. In Figure 32 the same data are shown as P/t versus t. In this form the ordinates are percentage of 24-rain divided by the

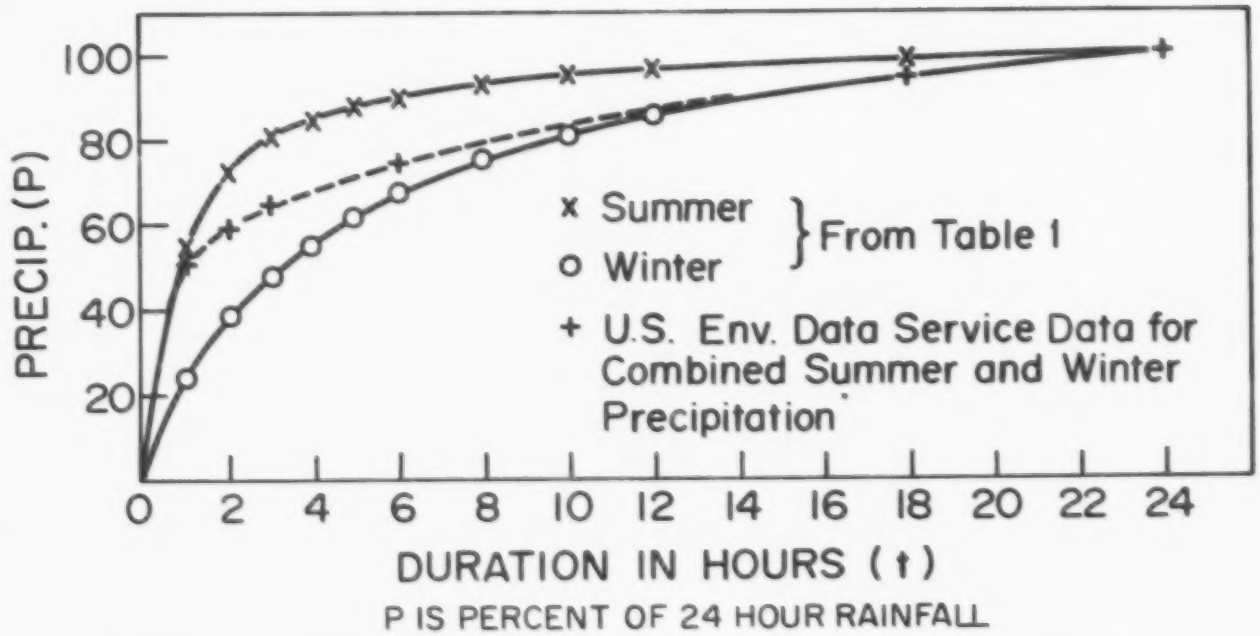

Figure 31. Precipitation-duration expressed as percent of 24-hr rainfall.

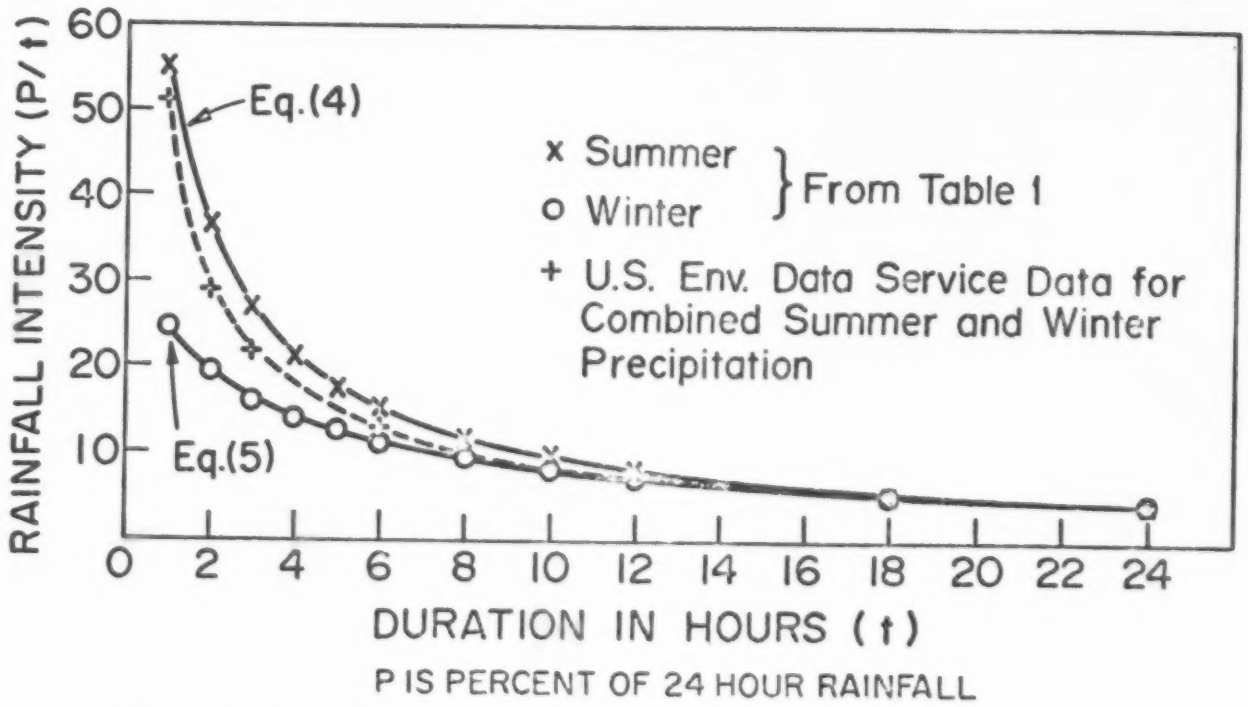

Figure 32. Intensity-duration expressed as percent of 24-hr rainfall.

Table 7. MAXIMUM RAINFALL FOR VARIOUS DURATIONS

t Duration hr	Summer P percent of 24-hr rainfall	Summer Standard deviation of P	Summer P/t percent of 24 hr rainfall/hr	Winter P percent of 24-hr rainfall	Winter Standard deviation of P	Winter P/t percent of 24 hr rainfall/hr
1	55.05	21.24	55.05	24.45	13.56	24.45
2	73.41	20.55	36.71	38.68	19.30	19.34
3	80.34	18.18	26.78	47.87	18.98	15.96
4	84.10	15.70	21.03	55.76	19.38	13.94
5	88.28	13.48	17.66	62.11	19.94	12.42
6	90.20	12.02	15.03	67.67	19.18	11.28
8	93.38	10.29	11.67	75.76	17.32	9.47
10	95.18	8.80	9.52	81.25	14.78	8.13
12	96.89	6.94	8.07	86.03	12.74	7.17
18	99.05	3.31	5.50	95.10	7.35	5.28
24	100.00	0.00	4.17	100.00	0.00	4.17

duration in hours and the curves have the form of the commonly used intensity-duration curves. The equations for these curves have the following form

$$P/t = \frac{A}{(t + B)^n} \tag{44}$$

in which A, B and n are constants. If this equation is expressed in logarithmic form (Eq. 45) it can be reduced to a straight

$$\log P/t = \log A - n \log (t + B) \tag{45}$$

line by the proper selection of B. The optimum value of B was determined by applying the method of least squares to derive linear equations for a series of values of B and selecting the equation for which the linear correlation coefficient was a maximum and the standard deviation from the regression was a minimum.

The resulting equations are, for summer,

$$P/t = \frac{112.0}{(t + 1.0)^{1.026}} \tag{46}$$

and for winter

$$P/t = \frac{68.0}{(t + 2.4)^{.849}} \tag{47}$$

For each of these equations the linear correlation coefficient was very near unity thus indicating a highly linear relationship. The corresponding standard deviation from the regression indicated deviations from the derived equations of less than 2 percent. Among the individual values the most interesting item of information determined from this analysis is that for summer rains the maximum hour of rain included on the average 55 percent of the 24-hr total while for winter the rainfall during the maximum hour was about 24 percent of the 24-hr rainfall. Separate analyses by months indicated that this change takes place quite abruptly at the ends of the two seasons. Additional analyses made by dividing the rains into two groups according to size indicated that the intensity patterns were independent of magnitude of rainfall.

Typical hyetograph ordinates (P_h/t) can be derived from these curves or from Equations (46) and (47) by assuming that the rain for any duration is the maximum for that duration and also contains all of the maximum shorter durations. A convenient way to do this is to express time (t) in terms of uniform time intervals (Δt). Then the rain expressed as percent of 24-hr rain for a duration $N\Delta t$ is $N\Delta t\ (P/t)_N$. If one subtracts the rain for a duration which is smaller by the amount Δt ($(N-t)\Delta t\ (P/t)_{N-1}$), the difference is the rain during the Nth time intervals, ($(P_h/\Delta t)_N \Delta t$). In equation form this relationship becomes

$$(P_h/\Delta t)_N \Delta t = N\Delta t\ (P/t)_N - (N - 1)\Delta t\ (P/t)_{N-1} \qquad (48)$$

Values of (P/t) are computed from Equations (46) and (47), $(P/t)_N$ being the value of (P/t) at time $t = N\Delta t$ and $(P/t)_{N-1}$ being the value at time $t = (N-1)\Delta t$. Then, dividing by Δt the following simple relationship is obtained

$$(P_h/\Delta t)_N = N(P/t)_N - (N - 1)\ (P/t)_{N-1} \qquad (49)$$

Computed values of P/t and $P_h/\Delta t$ are shown in Table 8. These values are plotted as typical hyetographs in Figure 33. In order to change the ordinates to rain-intensity in in./hr it is only necessary to multiply each one by the 24/hr rainfall of the desired frequency.

The order in which the various intensities are arranged in Figure 33 is important if the period of rainfall excess is longer than can be converted to runoff with a single application of the unit hydrograph. Therefore the nature of typical time-intensity patterns was studied. This was done by arranging the 80 summer rains and 44 winter rains previously described in tabular form so that the maximum hours coincided. It was found that on the average the rainfall patterns tended to be symmetrical. The actual volumes of precipitation were about equal before and after the maximum hour when averaged for all the rains. The second largest hour occurred somewhat more often after the peak hour than before for the summer rains and an equal number of times before and after the maximum hour for the winter rains. Based on this study, the hyetographs shown in Figure 33 may be considered as typical for Southeastern Michigan. The use of these curves will be demonstrated in the section on Predicting Flood Magnitudes and Frequencies.

All rainfall frequency data discussed so far in this section are from individual rain gages and are usually referred to as point rainfall. Before

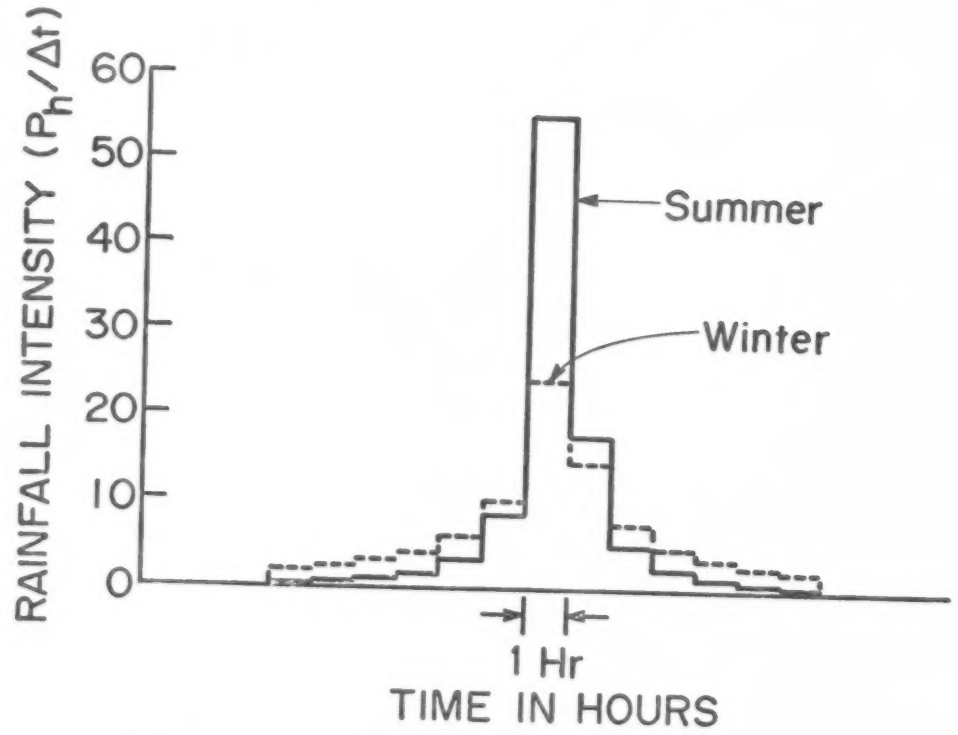

Average Hourly Values Derived by Applying Eq. 7 to Values of P/t Determined from Eq.'s 4 and 5. P_h is Percent of 24 Hour Rainfall.

Figure 33. Typical seasonal hyetographs expressed as percent of 24-hr rainfall.

Table 8. HYETOGRAPH ORDINATES IN PERCENT OF 24-HOUR RAINFALL PER HOUR

Duration in hours (t)	Summer		Winter	
	P/t^a, % of 24-hr rainfall/hr	$P_h/\Delta t^c$, % of 24-hr rainfall/hr	P/t^b, % of 24-hr rainfall/hr	$P_h/\Delta t^c$, % of 24-hr rainfall/hr
1	55.000	55.000	24.059	24.059
2	36.282	17.564	19.329	14.599
3	27.009	8.462	16.245	10.075
4	21.482	4.902	14.062	7.516
5	17.817	3.157	12.432	5.909
6	15.211	2.179	11.163	4.822
7	13.263	1.578	10.147	4.046
8	11.753	1.185	9.312	3.470
9	10.549	0.915	8.614	3.028
10	9.566	0.722	8.020	2.679
11	8.749	0.579	7.509	2.398
12	8.060	0.472	7.064	2.168
13	7.469	0.388	6.673	1.976
14	6.959	0.323	6.326	1.814
15	6.513	0.271	6.016	1.675

[a]From Eq. (46).
[b]From Eq. (47).
[c]From Eq. (49).

these values can be used to predict flood peaks they must be converted to average precipitation of the same frequency for areas of various sizes. The U.S. Weather Bureau[10] has derived ratios between point rainfall and average rainfall of the same frequency for basins up to 400 sq mi. These have been used to derive the curves shown in Figure 34. The curves were extended to larger areas using area-depth curves as a guide.[4]

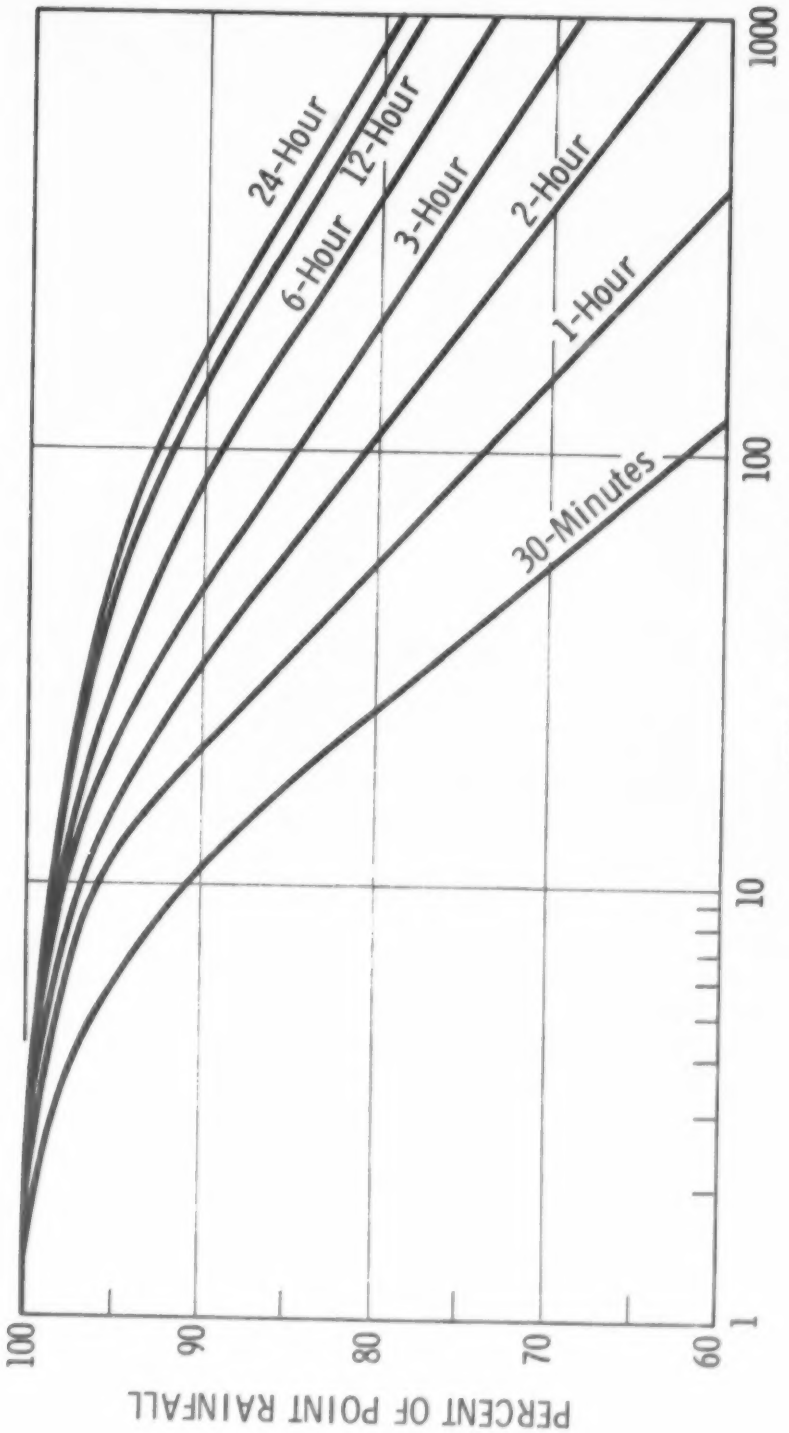

Figure 34. Area-depth curves.

SECTION XII

PREDICTING FLOOD MAGNITUDES AND FREQUENCIES

The procedure presented in this report is based on the idea that rainfall and/or snowmelt can be determined for any desired duration and frequency and that peak surface runoff rate or, if needed, the entire surface runoff hydrograph can be constructed by use of the unit hydrograph taking into account infiltration, the contribution from impermeable areas and retention. For perennial streams this predicted hydrograph must be superimposed on a typical base flow. This procedure has been worked out and is presented here for Southeastern Michigan. The information dealing with precipitation frequency, infiltration capacities, base flows and HSIA are derived from the large group of basirs for which hydrographs were analyzed in Southeastern Michigan. The design curves for estimating unit hydrograph form were derived from basins located in many locations including Southeastern Michigan. However, as discussed in Section VIII more weight was given to results from Southeastern Michigan for low values of population density. The curves based on the average data for all basins would therefore give slightly different results for rural areas. In presenting the steps used in predicting flood peaks for a given watershed a numerical example will be presented. The example selected is Red Run, a 36.5 sq mi basin located in Southeastern Michigan on which the population density is 7500 people/sq mi. It is assumed that a knowledge of a range of flood magnitudes is desired. Therefore a number of solutions are made in order to provide a set of points through which a curve relating flood magnitude to frequency may be plotted.

1. A number of values of 24-hr summer point rainfall and winter point rainfall plus snowmelt of various frequencies are determined from Figure 30 and tabulated in Table 9.

2. Also shown in Table 9 are the corresponding values of average precipitation on 36.5 sq mi. The conversion factors for changing point rainfall to average values were determined from Figure 34 for an area of 36.5 sq mi and for durations which were arbitrarily selected to cover the time required for 95 percent of the rain to fall. Reference to Table 8

Table 9. TWENTY-HOUR HOUR RAINS OF VARIOUS FREQUENCIES

Frequency in yr	WINTER		SUMMER	
	At a point	On 36.5 sq mi	At a point	On 36.5 sq mi
1	1.52	1.45	1.60	1.54
2	1.86	1.77	2.01	1.93
5	2.29	2.18	2.55	2.45
10	2.62	2.50	2.97	2.85
25	3.13	2.98	3.62	3.48
50	3.39	3.23	4.02	3.86
100	3.71	3.53	4.57	4.38

and Eqs. (5) and (7) shows that the duration would be 10 hr for summer rains and 18 hr for winter rains. Then the conversion factors from Figure 34 are .960 for summer and .953 for winter.

3. A typical unit hydrograph is derived for the basin. The unit hydrograph characteristics determined from Figures 21-27 for an area of 36.5 sq mi and a population density of 7500 people/sq mi are as follows:

q_{pA} = 138 cfs/mi^2/in.
t_r = 2.6 hr
T_r = 3.7 hr
W_{75} = 2.8 hr
W_{50} = 4.1 hr
W_{25} = 6.9 hr
W_0 = 22.0 hr

The unit hydrograph shown in Figure 35 is constructed by first placing the peak at the time of rise (T_r). Then the significant period of rise (t_r) is used to sketch in the rising side of the hydrograph. Next, the hydrograph widths at 75 percent, 50 percent, 25 percent of peak plus the base width are used to complete the recession side of the hydrograph. Minor modifications may be necessary to form a unit hydrograph having an area of 1 in.

Also shown in Figure 35 is the average unit hydrograph derived from runoff records on Red Run. The close approximation of the actual unit hydrograph by the one synthesized from generalized curves should not always be expected. It happens that the Red Run unit hydrograph characteristics

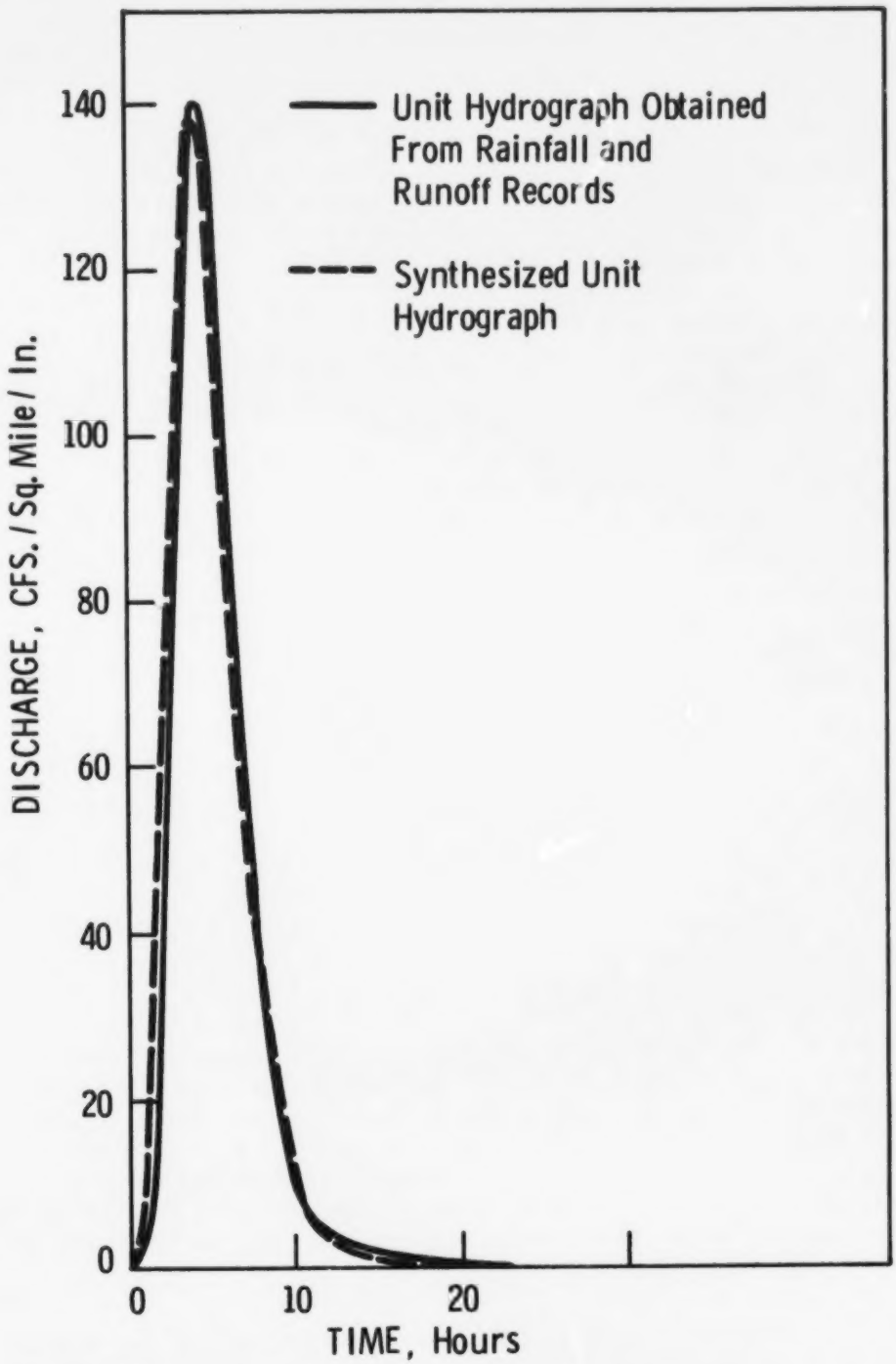

Figure 35. Synthesized and observed unit hydrographs for Red Run.

fall near the best fit lines for the highly urbanized basins.

4. A typical hyetograph of hourly precipitation is derived for summer and winter rain using the arrangement shown in Figure 33 and numerical values from Table 8. An example computation is shown in Table 10 for a 50-yr winter rain. The numerical values of the ratio of 1-hr rain to 24-hr rain are arranged in a typical time sequence in the top line of Table 10. Line 2 shows the corresponding values of hourly precipitation obtained by applying the ratios in row 1 to the 50-yr 24-hr winter rain. The magnitude of the rain was given as 3.23 in. in Table 9.

5. The precipitation excess (P_e) is then computed for each hour by deducting the average hourly winter infiltration which was found to be 0.10 in. for Southeastern Michigan. (See Figure 8.) These values are given in line 3 of Table 10.

6. In line 4, the winter retention (0.10 in.) is deducted from the first 2 hr of P_e. The values in line 4 are in inches on the permeable area. In line 5 these are converted to inches on the entire basin by multiplying by (1 - HSIA/100). The value of HSIA is obtained from Eq. (50). This

$$HSIA = 1.38\ P_d \qquad (50)$$

equation was derived for basins in Southeastern Michigan. HSIA is expressed in percent of total area and P_d in thousands of persons/sq mi.

7. The surface runoff from impermeable area is the total precipitation given in line 2 converted to inches on the total area by multiplying by HSIA/100. These values are shown in line 6 of Table 10. The retention on the impermeable area, 0.05 in., was accounted for by the first several hours of precipitation which are not included in Table 10.

8. Line 7 is the sum of the hourly contributions to surface runoff from the permeable area (line 5) and from the impermeable area (line 6). These are combined into success 2-hr inputs to the drainage system in line 8. This was done because it was shown earlier that the effective period of rise (t_r) is 2.6 hr and therefore the unit hydrograph can be applied to inputs having durations as long as 2.6 hr. The use of 2-hr increments is therefore convenient and reduces the computation time over that required if 1-hr intervals were used.

9. The next step is to convert the 2-hr increments of surface runoff

Table 10. COMPUTATION OF VOLUME OF SURFACE RUNOFF FOR A 50-YEAR WINTER RAIN

1	Ratio of hourly precip. to 24-hr precip.	0.0303	0.0405	0.0591	0.101	0.241	0.146	0.075	0.048	0.035
2	Hourly precip. (P)	0.098	0.127	0.185	0.326	0.778	0.471	0.235	0.151	0.109
3	Precip. excess $P_e = P - F$	0	0.027	0.085	0.226	0.678	0.371	0.135	0.051	0.009
4	$P_e - R_p$ = SRO in in. on permeable area	0	0	0.012	0.226	0.678	0.371	0.135	0.051	0.009
5	SRO_p in in. on total area	0	0	0.011	0.202	0.607	0.332	0.121	0.046	0.008
6	SRO_i in in. on total area	0.010	0.013	0.019	0.034	0.081	0.049	0.024	0.016	0.011
7	$SRO = SRO_p + SRO_i$	0.010	0.013	0.030	0.236	0.688	0.381	0.145	0.062	0.019
8	SRO in 2-hr increments	0.023		0.266		1.069		0.207		

input to hydrographs by means of the unit hydrograph. This is illustrated in Table 11 for the 50-yr winter rain. The first two columns in Table 11 show the coordinates of the unit hydrographs as read from Figure 35. At the top of columns 3, 4, 5, and 6 are shown the successive 2-hr increments to surface runoff derived in Table 10. The values of surface runoff rates shown in these four columns are obtained by multiplying by corresponding unit hydrographs ordinates and by the area, 36.5 sq mi. Column 7 is the summation of Column 3, 4, 5, and 6 and represents the predicted surface runoff hydrograph with a peak of 6631 cu ft/sec.

10. The actual peak discharge is obtained by adding a typical ground water discharge. This value is obtained from Eq. (51) in which Q_{GW} is ground water discharge in cfs and A is the area of the drainage basin in

$$Q_{GW} = .6A \tag{51}$$

square miles. This equation was derived from a study of typical ground water discharge in Southeastern Michigan. The value for Red Run which has an area of 36.5 sq mi is 22 cfs thus making the estimated total peak discharge 6653 cfs.

11. The operations described in steps (11) and (12) are then repeated for all of the rains shown in Table 9. The results are plotted in Figure 36.

12. A curve for total frequency is then obtained by combining the summer and winter curves and is shown in Figure 36. This is done by adding the probabilities which are the reciprocals of the frequencies for floods of selected magnitudes as shown by the following equation in which T_W, T_S and

$$\frac{1}{T_T} = \frac{1}{T_W} + \frac{1}{T_S} \tag{52}$$

T_T are the winter, summer, and total frequencies, respectively. The total frequency is then computed by rearranging Eq. (52) to obtain Eq. (53). Such values of T_T then form the final frequency curve.

$$T_T = \frac{1}{\frac{1}{T_W} + \frac{1}{T_S}} \tag{53}$$

Table 11. COMPUTATION OF COMPOSITE HYDROGRAPH FOR 50-YEAR WINTER RAIN

1	2	3	4	5	6	7
Time from beginning of surface runoff in hr	Unit hydrograph cfs/sq mi/in. (from Figure 35)	Surface runoff input in in. for successive 2-hr time increments				Total SRO cu ft/sec
		.023	.266	1.069	.207	
		Surface runoff in Cu ft/sec				
1	13	11				11
2	55					
3	108	91	127[a]			218
4	138 (pk)					
5	115	97	1047	507		1651
6	83					
7	54	45	1115	4220	98	5878
8	37	31	(805)	(5380)	(415)	(6631)
9	24	20	523	4480	780	6803
10	11					
11	5	4	233	2105	870	3212
12	3.5					
13	2	2	48	937	405	1392
14	1.5					
15	1	1	19	195	184	399
			10	78	38	126
				39	15	54
					7	7

[a] 127 = 13 x 0.266 x 36.5

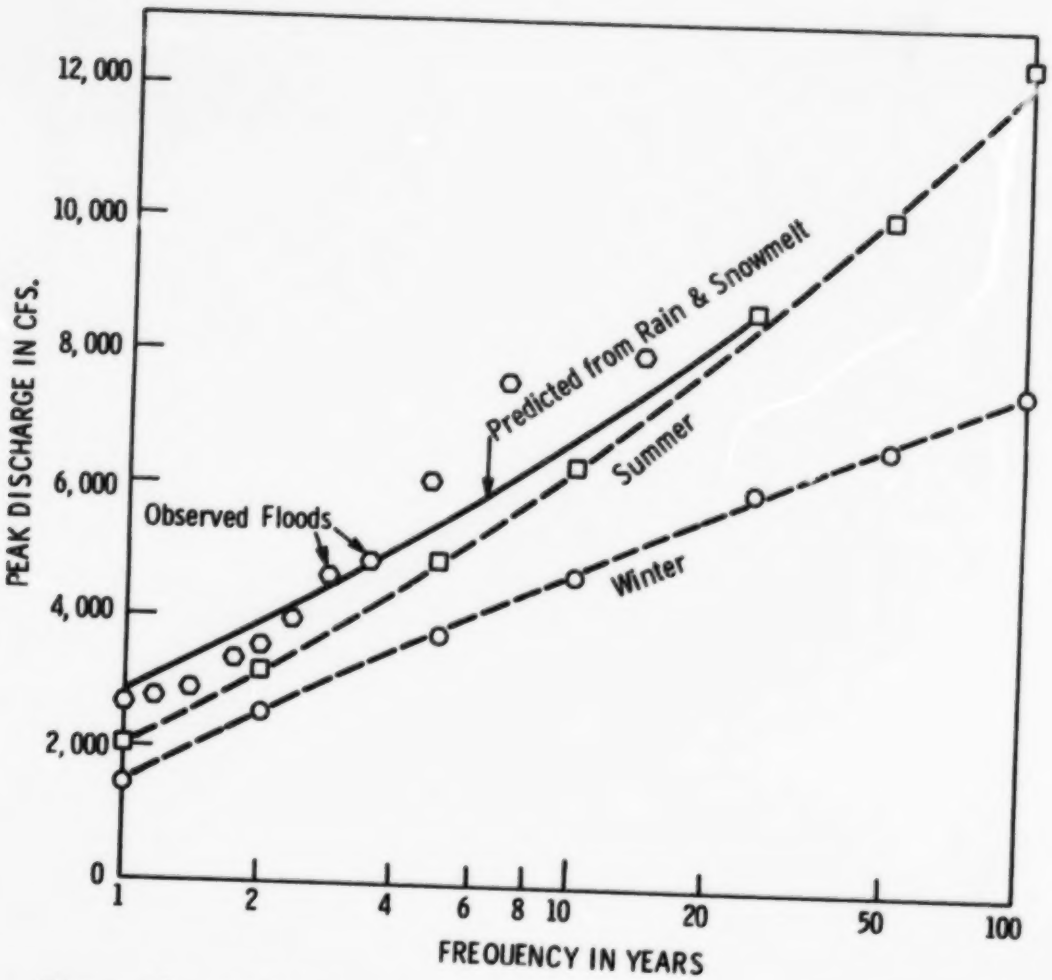

Figure 36. Predicted and observed flood frequencies for Red Run.

The frequency curve for Red Run computed from Eq. (53) is shown in Figure 36. Also plotted on this figure are the observed frequencies from 14 yr of records for Red Run. The higher values of frequency in this series are not reliable due to the shortness of the period of records but the lower values should be reasonably correct and serve as a check with lower portion of the total frequency curve derived from precipitation and snowmelt. Such remarkable agreement cannot always be expected. It stems in part from the fact that the unit hydrograph characteristics of Red Run fall near to the average lines for high population densities in Figures 14, 17, and 20. However, the close agreement serves to verify the concept that rainfall frequency can be used to predict flood frequency if a sound hydrological approach is used in computing runoff from rain and snowmelt.

SECTION XIII

REFERENCES

1. Horton, R. E., "Surface Runoff Phenomena," Publ. 101, Edwards Bros., Ann Arbor, Michigan, 1935.

2. Horton, R. E., "An Approach Toward a Physical Interpretation on Infiltration Capacity," Soil Sci. Soc. Proc., 1940.

3. Swartzendruber, D. and M. R. Huberty, "Use of Infiltration Equation Parameters to Evaluate Infiltration Differences in the Field," Trans. Am. Geophys. Union, v. 39, February 1958, p. 84.

4. Betson, R. P., "What is Runoff?," J. Geophys. Res., v. 69, April 15, 1964, p. 1541.

5. Thames, J. L. and S. J. Ursic, "Runoff as a Function of Moisture-Storage Capacity, J. Geophys. Res., v. 65, February 1960, p. 651.

6. Horner, W. W. and C. Leonard Lloyd, "Infiltration-Capacity Values as Determined from a Study of an Eighteen-Month Record at Edwardsville, Ill., Trans. Am. Geophys. Union, Part II, 1940, pp. 522-541.

7. Wisler, C. O. and E. F. Brater, "Report on Floods on the Rouge River," Report to Wayne County Board of Road Commissioners, August 1957.

8. Brater, E. F. and J. D. Sherrill, "Prediction of Magnitudes and Frequencies of Floods in Michigan," Report to Michigan Department of State Highways and U.S. Bureau of Public Roads, 1971.

9. Wisler, C. O. and E. F. Brater, "Hydrology," John Wiley & Sons, Inc., New York, 2nd Ed., 1959.

10. Ursic, S. J. and J. L. Thames, "Effect of Cover Types and Soils on Runoff in Northern Mississippi," J. Geophys. Res., v. 65, February 1960, p. 663.

11. Kueligan, G. H., "Spatially Variable Discharge Over a Sloping Plane," Trans. Am. Geophys. Union, Part VI, 1944.

12. Izzard, C. F., "The Surface Profile of Overland Flow," Trans. Am. Geophys. Union, Part VI, 1944.

13. Woo, D. C. and E. F. Brater, "Spatially Varied Flow from Controlled Rainfall," J. Hydraulics Div., ASCE, v. 88, November 1962, p. 31.

14. Woolhiser, D. A. and J. A. Liggett, "Unsteady One-Dimensional Flow Over a Plane—The Rising Hydrograph," Water Resources Research, v. 3, no. 3, 1967.

15. Lin, P. N., "Numerical Analysis of Unsteady Flow in Open Channels," Trans. Am. Geophys. Union, v. 33, April 1952, p. 226.

16. Lin, P. N. and Ching Seng Fang, "Streamflow Routing with Application to North Carolina Rivers," Report No. 17, University of North Carolina, Chapel Hill (January 1969).

17. Sangal, S., "The Surface Runoff Provess During Intense Storms," Doctoral Dissertation, Department of Civil Engineering, The University of Michigan, 1970.

18. Tholin, A. L. and C. J. Keller, "Hydrology of Urban Runoff," Trans. ASCE, v. 125, 1960, p. 1308.

19. Holtan, H. N. and D. E. Overton, "Storage-Flow Hysteresis in Hydrograph Synthesis," J. Hydrology, v. II, No. 4, April 1965, pp. 309-323.

20. Crawford, Norman H. and Ray K. Kinsley, "Digital Simulation in Hydrology: Stanford Watershed Model IV," Technical Report No. 39, Department of Civil Engineering, Stanford University, 1966.

21. Laurenson, E. M., "A Catchment Storage Model for Runoff Routing," J. Hydrology. v. II, 1964, p. 141.

22. Sherman, L. K., "Stream Flow from Rainfill by the Unit Hydrograph Method," Eng. News-Record, v. 108, 1932, p. 501.

23. Bernard, Merrill M., "An Approach to Determinate Stream Flow," Trans. ASCE, v. 100, 1935. p. 347.

24. Brater, E. F., "The Unit Hydrograph Principle Applied to Small Water-Sheds," Trans. ASCE, v. 105, 1940, p. 1154.

25. Snyder, Franklin F. "Synthetic Unit-Graphs," Trans. Am. Geophys. Union, Part I, 1938, p. 447.

26. Taylor, A. B. and H. E. Schwartz, "Unit Hydrograph Lag and Peak Flow Related to Basin Characteristics," Trans. Am. Geophys. Union, v. 33, no. 2, 1952, p. 235.

27. O'Kelley, J. J. "The Employment of Unit Hydrographs to Determine the Plans of Irish Arterial Drainage Channels," Proc. Inst. Civil Engrs., v. 4, Part III, 1955, p. 365.

28. O'Kelley, J. J., "A Unit Hydrograph Study with Particular Reference to British Catchments," Proc. Inst. Civil Engrs., v. 17, 1960, p. 249.

29. Gray, Don M., "Synthetic Unit Hydrographs for Small Watersheds," J. Hydraulics Div., ASCE, July 1961, pp. 35-54.

30. Eagleson, Peter S., "Unit Hydrograph Chacteristics for Sewered Areas," J. Hydraulics Div., ASCE, Marcy 1962, pp. 1-25.

31. Wu, I. Pai, "Design Hydrographs for Small Watersheds in Indiana," J. Hydraulics Div., ASCE, November 1963, p. 35.

32. Espey, William H., Jr., Carl W. Morgan, and Frank D. Masch, "A Study of Some Effects of Urbanization on Storm Runoff from a Small Watershed," Center for Research in Water Resources, Department of Civil Engineering, The University of Texas (1965).

33. Brater, E. F., "Steps Toward a Better Understanding of Urban Runoff Processes," Water Resources Research, v. 4, no. 2, April 1968, pp. 335-347.

34. Brater, E. F. and S. Sangal, "Effects of Urbanization on Peak Flows," University of Texas, Water Research Symposium on the Effects of Watershed Changes on Streamflow, University of Texas Press, Austin, 1969.

35. Viessman, W., Jr., "The Hydrology of Small Impervious Areas," Water Resources Research, v. 2, no. 3, 1966, p. 405.

36. Horton, R. E., "The Role of Infiltration in the Hydrological Cycle," Trans. Am. Geophys. Union, v. 14, 1933, p. 446.

37. Betson, R. P., "What is Runoff?," J. Geophys. Res. v. 69, April 15, 1964, p. 1541.

38. Brater, E. F., S. Sangal, and J. D. Sherrill, "Seasonal Effects on Flood Synthesis," Water Resources Research, A.G.U., v. 10, no. 3, June 1974.

39. U.S. Weather Bureau, "Rainfall Frequency Atlas of the United States for Durations from 30 Minutes to 24 Hours and Return Periods from 1 to 100 Years," Technical Paper No. 40, Washington, D.C., May 1961.